ANALYTICAL STUDY ON SOLUTE TRANSPORT IN STREAMS WITH TRANSIENT STORAGE AND HYPORHEIC ZONES

Akhilesh Kumar

DEPARTMENT OF MATHEMATICS
INDIAN INSTITUTE OF TECHNOLOGY GUWAHATI

ANALYTICAL STUDY ON SOLUTE TRANSPORT IN STREAMS WITH TRANSIENT STORAGE AND HYPORHEIC ZONES

A Thesis Submitted

for the Award of the Degree of

DOCTOR OF PHILOSOPHY

by

Akhilesh Kumar

(Roll Number: 04612305)

to the

DEPARTMENT OF MATHEMATICS

INDIAN INSTITUTE OF TECHNOLOGY GUWAHATI

June, 2009

CERTIFICATE

It is certified that the work contained in the thesis titled **"Analytical study on solute transport in streams with transient storage and hyporheic zones"** by **Akhilesh Kumar**, a student in the Department of Mathematics, Indian Institute of Technology Guwahati for the award of the degree of Doctor of Philosophy has been carried out under my supervision and this work has not been submitted elsewhere for a degree.

June, 2009

Prof. Durga Charan Dalal
Department of Mathematics
Indian Institute of Technology Guwahati

Dedicated to my Parents.

Acknowledgement

This section of nostalgia, I hold dear to my heart because it gives me an opportunity to recollect and recognize the effects of many people whose assistance I almost took for granted during the period of my research.

First and foremost, I express my heartfelt gratitude to **Prof. Durga Charan Dalal** who magnanimous enough to bear the responsibility of guiding me. I am deeply indebted to him for his invaluable guidance, immense patience, utmost care and constant encouragement through out this work. It is always a pleasure getting into argument with him and making me feel free to express my views. Without his help the work could not have been accomplished.

I owe my thanks to my doctoral committee members Dr. R. K. Sinha, Dr. S.N. Bora and Dr. S. Dutta for their valuable suggestions during the progress of my research that helped me to improve the quality of my research work. I am conveying my gratitude to Prof. A. Baruah, Dr. Robert L. Runkel and Prof. P.M. Röwinski to solve my innumerable queries and doubts. I would also like to thank to Dr. B.H. Schmid and Dr. S.P. Chakrabarty to provide me research papers. I express my sincere thanks to our lab assistance Mr. Shantanu Mazumdar for technical support. Mr. Sridhar Sasmal and Mr. Manoj Boro of Mathematics Department, IIT Guwahati deserve special thanks for their assistance in all official matters. I am highly grateful to my colleagues and friends for their co-operation and pleasant company during my research tenure.

I would like to thank my parents and family members for letting me work without too many commitments. They given me the freedom to work for Ph.D. and tolerated my long absence from my sweet home shouldering the family responsibilities during the entire duration of my stay at this institute. They have always encouraged me and supported me and most importantly they always believed in me.

Finally, I am very much thankful to Ministry of Human Resources Department

(MHRD) to provide me the financial support during my research at Indian Institute of Technology Guwahati (IITG).

June, 2009 **(Akhilesh Kumar)**

Abstract

This thesis presents the derivation of general analytical solutions of the transient storage model and also of the diffusive transfer model for the longitudinal solute transport in streams with transient storage and hyporheic zones for conservative and reactive solutes. These general analytical solutions are derived by means of Laplace transform. The transient storage model deals with the first order mass transfer between the main channel of stream and the storage zone, and the diffusive transfer model deals with the diffusive mass transfer of solute between the main channel of stream and the hyporheic zone. Parameters of the transient storage model and also of the diffusive transfer model are estimated for the Uvas Creek tracer experiment by using the large scale Newton reflexive method. The analytical results of these models for conservative solutes are compared with the observed data of the Uvas Creek tracer experiment for chloride concentration. Sensitivity analysis is performed in order to identify the critical parameters on solute concentrations. Effects of different parameters that represent physical, chemical and hydrological processes involved in the transport of solutes in streams are studied for hypothetical situations. Results are presented for conservative solutes considering step concentration-time profile as the upstream boundary condition whereas in the case of reactive solutes, an instantaneous release of the solute is considered to be the upstream boundary condition.

Contents

List of Figures

List of Tables

Chapter 1

Introduction

1.1 Introduction

Analysis of solute transport with the effects of transient storage and hyporheic zones has been an active research area since 1966's (first described by Hays et al. (1966)). It is a common practice to discharge waste materials into the water systems from different type of sources e.g. domestic sources, chemical plants, industrial or agricultural effluents, accidental release of pollutants. These waste materials are discharged into the main flow of stream undergo stages of mixing while being transported downstream. Some part of the waste materials normally goes into storage zone or hyporheic zone. Due to exchange of water between the main flow of stream and storage zone or hyporheic zone, a part of waste materials releases back into the main flow of stream (which can be seen from Figure 1.1).

It is well-established from the field studies of river contamination that the storage zone and hyporheic zone play an important role in the transport of contaminants in river systems. It is important to understand the transport properties of water and solutes through the storage and hyporheic zones in order to elucidate the mechanisms of instantaneous and continuous injection of solute in the main stream of the river as well as in the storage zone or in the hyporheic zone. Accidental and continuous pollutant spills can influence the water quality of rivers up to several hundred kilometers due to the rapid interaction of water between the surface and subsurface zones.

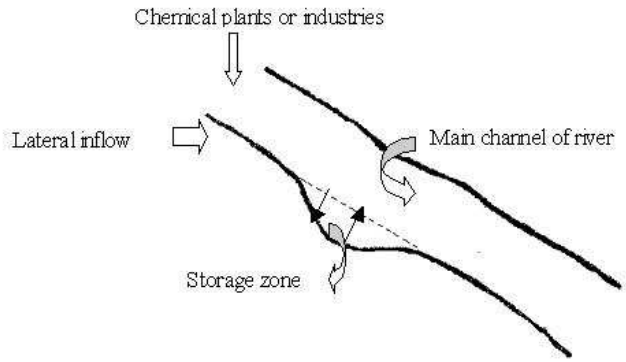

Figure 1.1: *Schematic physical system for stream and storage zone hydrologic process.*

Therefore, the calculation of transport of solute in such a large domain is restricted to one dimensional approach. Transport of solutes through the water systems is also affected by several physical, chemical and hydrological processes. These processes are difficult to understand clearly from the field experiments. In order to improve the prediction ability of these processes in the main channel and in the hyporheic zone, several modeling and tracer experiment approaches are developed (e.g. Bencala and Walters [2], Bencala [3], Bencala et al. [4], Broshears et al. [5], Gooseff et al. [16], Harvey et al. [18], Hays et al. [19], Holley and Jirka [20], Jackman et al. [21], Keefe et al. [24], Runkel [30], Rutherford [32], Wagner and Harvey [39], Wörman [40]).

The most commonly used solute transport model is the advective-dispersive equation (ADE) (Fischer et al. [14]). This equation is based on solute transport in a homogeneous and isotropic medium with constant and uniform flow. Analytical solutions of these solute transport equations are available in the literature. The solution of the ADE due to instantaneous injection of solute produces asymmetric shape of concentration-time curve in comparison with the Gaussian shape. But in the tracer experiments, the asymmetric nature in the shape of the concentration-time curves further increases. The asymmetric shape of the concentration-time curve reveals short rising limbs and long tails in the concentration-time curves. Due to the slow release of the solute particles from the storage zone into the main channel of the stream, it

is observed that some part of the solute particles returns only after the main portion of the solute cloud has passed the sampling location (e.g. Fischer et al. [14]) and this process is responsible for the appearance of long tail. The ADE model is incapable of reproducing the asymmetric shape of the observed concentration-time curves obtained in the tracer experiments.

To address this problem, Hays et al. [19] described the dead zone model (DZM) in the form of two coupled partial differential equations, one for the main channel of stream and the second one for the storage zone. They have not solved these coupled partial differential equations analytically but found approximate solutions only. They showed that the approximate solutions of these equations could describe the natural behavior of longitudinal concentration distribution more accurately than the solution of classical advection-dispersion equation. They also stated that two additional parameters due to the transient storage (i.e. exchange coefficient and the dead zone ratio, which is the ratio between cross-sectional areas of the dead zone and of the main channel), were difficult to predict with the help of bulk hydraulic or geometrical parameters.

Thackston and Schnelle [38] used the similar approximate solution as obtained by Hays et al. [19], which is in the transformed (Laplace) domain. The approximate solution is a function of four parameters: mean residence time, Péclet number or dimensionless dispersion coefficient, fraction of stream volume which is dead zone and mean residence time in a dead zone. Thackston and Schnelle [38] estimated these parameters with the help of field data. In their analysis, they assumed the exchange co-efficient to be constant and the dead zone volume to be a function of the friction factor.

Later, several models were proposed to describe the physical, chemical, hydrological and geochemical processes in streams. Two types of models are mostly used to describe the solute exchange between the main channel of the stream and the tran-

sient storage/hyporheic zone for conservative as well as for reactive solute. The first model is based on the classical advection-dispersion phenomenon with the first order mass exchange between the main channel of the stream and the transient storage. This model is known as transient storage model (TSM) (Bencala and Walters [2], Bencala [3], Runkel and Chapra [30], Wagner and Harvey [39]). The second one is based on the classical advection-dispersion equation with diffusive transfer between the main channel of the stream and the hyporheic zone (De Smedt [13], Jackman et al. [21], Wörman [40]).

Several physical and chemical processes are responsible for contaminant transport in stream with transient storage and hyporheic zones. The physical processes affecting the solute concentrations include advection, dispersion, lateral inflow, lateral outflow and transient storage. The chemical processes affecting the solute concentrations include sorption to the stream bed and decay. Some of the important terminologies related to contaminant transport in streams with transient storage and hyporheic zone are listed below:

- Solute

  Solute can be any substance or entity that is transported downstream by the flowing water. Under this definition, solutes could be waste materials, such as pesticides and hydrocarbons, or naturally occurring substances such as dissolved gases, nutrients, and trace elements.

- Storage zone

  Storage zone is a stagnant water zone which is stationary relative to the main flow of the stream. e.g. pools, side arms of the stream or adjacent wetland areas. Waste materials are usually temporarily trapped in the storage zones and slowly released back into the main channel.

- Hyporheic zone

  Hyporheic zone is a porous area that connects surface water and subsurface water and exchange of water takes place through this zone. e.g. porous areas and bed sediments under and near the stream.

- Advection

  Advection is the process by which the mass of solute is transported due to the movement of the surrounding medium and the direction is determined by a flow field.

  Mathematically, advection is represented by the scalar product $u_m^\star . \triangle c_m^\star$, which is the magnitude of $u_m^\star$ times the component of $\triangle c_m^\star$ in the direction of $u_m^\star$. Here $\triangle c_m^\star$ is the concentration gradient and $u_m^\star$ is the advective velocity.

- Diffusion

  Diffusion is the process by which the mass of solute is transported from one part of the system to another as a result of random movement of the surrounding medium which forces mass to spread out in any direction.

  Mathematically, diffusion can be described by using Fick's law. It states that the mass flux of a solute is proportional to the gradient of concentration of the solute. Thus, $q_x^\star = -D^\star . \bigtriangledown c_m^\star$, where $q_x^\star$ is the mass flux of the solute and $D^\star$ is the diffusion coefficient of the solute.

- Dispersion

  Dispersion is the spreading of the mass of a solute by the combined effects of velocity distribution and diffusion.

- Lateral inflow

  Lateral inflow is a flow of water that is added to the stream due to ground water inflow, overland flow and small springs. The main channel solute concentration

gets diluted or concentrated depending on the concentration coming through the lateral inflow is less or more compared to the main channel solute concentration.

- Lateral outflow

  Lateral outflow is a flow of water that is discharged from the main flow of the stream to the surrounding watershed.

- Partition coefficient

  Partition coefficient is a proportionality constant in an equilibrium adsorption isotherm. It is the ratio of adsorbed content to the concentration in an aqueous solution for the linear equilibrium isotherm.

1.2 Transient storage models due to first order mass exchange

Transient storage model for conservative solute due to first order exchange is described by dividing the domain (streams) into two distinct zones. The first zone represents the main channel of the stream. The advection and dispersion processes in the stream is described by one dimensional advection dispersion equation. The second zone represents the storage zone. The exchange of solute between the main channel of the stream with storage zones is represented by a first order exchange term (i.e. $\alpha^\star(c_m^\star - c_s^\star)$, where $\alpha^\star$ is the exchange coefficient, $c_m^\star$ is the solute concentration in the main channel of streams, $c_s^\star$ is the solute concentration in the storage zone). The advection-dispersion equation in the main channel of the stream is linked to the storage zone equation through the exchange term. This model is mostly used as a predictive tools and also to simulate the observe concentrations of the solutes of different tracer experiments (e.g. Sodium chloride(NaCl), Uvas Creek, [1]; Lithium chloride (LiCl), Potassium bromide (KBr), St. Kevin Gulch, [25]).

Bencala and Walters [2] described the physical TSM to characterize the different

behavior of solute transport for conservative solute (i.e. chloride) in a mountain pool-and-riffle stream under low flow condition. The storage zone concept is introduced to characterize the smaller peaks and longer tails in the mountain streams. Bencala and Walters [2] applied the model to a tracer experiment conducted in the Uvas Creek and emphasized the importance of the transient storage mechanism to describe the behavior of solutes in the Uvas Creek. They were estimated the parameters of the TSM by the trial and error approach for the best fit of the observed solute concentration curve of the Uvas Creek tracer experiment to the numerical solution of the TSM. However, Bencala and Walters [2] found that the effects of lateral inflow was negligible in the simulation procedure.

Bencala et al. [4] simulated the observed concentrations of conservative solute (i.e. Lithium) in the Snake river. They considered the lateral inflow as distributed inflows and estimated the parameters of the TSM. It was found that the estimated cross-sectional area of the stream channel and the estimated volumetric inflow rate varied by a factor of 3.

Runkel and Chapra [29] presented numerical solution of the coupled transient storage equations by using the Crank-Nicolson numerical scheme. They reduced the computational costs by decoupling the transient storage equations and using the Thomas algorithm. This is the basis to describe "One-dimensional Transport with Inflow and Storage (OTIS)". It also includes the numerical solution for reactive solute transient storage model.

Hart [17] presented a stochastic model for solute transport in streams with transient storage zones. He found a semi-analytical solution in the form of a rapidly converging infinite series for the model without considering the effects of lateral inflow.

Wagner and Harvey [39] analyzed the field experiments through parameter sensitivity, where it is assumed that informative periods are those time steps during which

the model outputs show a high sensitivity to the changes in the model parameters.

Davis et al. [10] found an analytical solution for instantaneous injection of conservative solute (i.e. Rhodamine WT dye). The solution was successfully applied to interpret the physical mechanisms of transport of solutes in the tracer experiments conducted in river Severn.

Rowiński et al. [28] presented numerical solution of the TSM. They used an upwind scheme for the advection term, Crank-Nicolson scheme for the dispersion term and Runge-Kutta method for the storage zone equations. The solution was applied to the observed data of conservative solute (i.e. fluorescent red dye) obtained from the Wkra River tracer experiment. The parameter estimation was accomplished using the control random search method.

De Smedt et al. [11] found analytical solutions of the TSM described by Bencala and Walters [2] without considering the lateral inflow for instantaneous injection of solute in a river with constant and uniform flow. De Smedt et al. [11] evaluated the parameters of the TSM for the five tracer experiments conducted in the Chillán river, Chile. In all experiments, the exchange of solute between the main channel and transient storage zones is markedly present. Later, De Smedt [12] obtained analytical solutions of the TSM for decaying solutes only, without considering the effects of lateral inflow and background concentrations. However, in all these analytical solutions the volumetric flow rate is constant throughout the study reach. Effects of the background concentrations and the lateral inflow solute concentration can be observed through the analytical solution of De Smedt [12] only when these concentrations are equal and constant.

Transient storage model for reactive solute is described by including the effects of decay and sorption in the transport equations of conservative solute. Both the zones include decay and sorption. There is a first order kinetic mass transfer between the stream water and stream bed sediment. It is represented by the difference between

the solute concentration on the streambed sediment and its potential equilibrium concentration in the main channel. Also, a first order kinetic reaction is considered in the storage zone. It is described by the difference between the storage concentration and equilibrium concentration. This model is used to simulate the observed concentrations obtained in different tracer experiments (e.g. Strontium chloride hexahydroxide ($SrCl_26H_2O$), Uvas Creek, [1, 3]).

Bencala [3] proposed the reactive solute transport model (RSTM), in which decay is absent in both the zones, for small pool-and-riffle mountain streams. Usually in these streams, the flow rate is low and that allows solutes to have repeated opportunities to be in contact with the relatively immobile bed materials. If a solute (e.g. strontium) can sorb onto bed materials, then both hydrodynamic and chemical processes control solute transport. Parameters of the RSTM are evaluated for the best fit to the observed solute concentration curve obtained in the Uvas Creek tracer experiment by using the numerical solution to the differential equations. The effects of lateral inflow were found to be negligible in this study.

Schmid [33] developed a semi-analytical solution to the transient storage equations accounting for different decay rates in main channel and the storage zone. He considered the physical mechanisms of the transient storage as a stochastic process.

Runkel [31] extended the OTIS with the nonlinear least squares method to optimize the parameters. This extended OTIS is known as OTIS-P. This is extensively used to estimate the transient storage behavior of streams through tracer experiments (e.g. Choi et al. [7], Fernald et al. [15]).

1.3 Transient storage models due to diffusive exchange

Transient storage model for conservative solute due to diffusive exchange is described by dividing streams into two distinct zones. The first zone represents the main channel

of the stream. The advection and dispersion processes in the streams are described by one dimensional advection-dispersion equation in the main channel of the stream. The second zone represents the hyporheic zone. The one dimensional diffusion equation is used to describe the diffusion process in the hyporheic zone. It is assumed that the solute concentration at the interface (i.e. $z^\star = 0$) of the two zones is equal. The exchange of solute between the main channel of the stream and the hyporheic zone is represented by a diffusive exchange term (i.e. $D_h^\star \frac{\partial c_m^\star}{\partial z^\star}\big|_{z^\star=0}$, where $c_m^\star$ is the solute concentration in the main channel, $z^\star$ is the lateral co-ordinate, $D_h^\star$ is the diffusive exchange coefficient). The advection-dispersion equation in the main channel of the stream is linked to the diffusive exchange term.

Jackman et al. [21] described three different conceptual models to represent the transient storage of solute in the streambed: (1) the exchange model, (2) the diffusion model, and (3) the underflow model. The exchange model is based on the classical advection-dispersion equations with the exchange of mass due to the concentration gradient between the main channel and its bed sediment. The diffusion model is based on the classical advection-dispersion equations with the exchange of mass due to the lateral diffusive transfer of solutes. The underflow model assumes a convective channel in one portion of the bed through which stream water flows by entering at one location and returning to the stream at another location, and the exchange model is used to describe storage throughout the rest of the bed. Jackman et al. [21] found that the diffusion model is more complex compared to the TSM but the diffusion model predicts the observed concentration profiles better than the TSM.

Transient storage model for reactive solute due to the diffusive exchange is described by considering the effects of sorption in the stream water and in the hyporheic zone in both the adsorbed and dissolved phases of solute. The kinetic reaction in the stream water as well as in the hyporheic zone is represented by the difference in concentrations of adsorbed and dissolved phases of solute at the equilibrium [23].

Maloszewski and Zuber [26] presented similar transport equations as considered by Jackman et al. [21] but they considered the chemical transport in a single fissure in a porous matrix. Maloszewski and Zuber [26] derived analytical solution for the transport equations by considering instantaneous injection as the upstream boundary condition.

Wörman [40] developed a model for the solute transport that includes the effects of hyporheic exchange, sorption and first order reaction. He derived an analytical solution for this model which describes the stream concentration as a function of distance along the stream, depth of the storage zone and time. However, he found that the effects due to dispersion in the stream was negligible. He applied the solution to several tracer experiments.

Wörman et al. [41] described the exchange mechanisms of the dissolved and adsorbed phases of a sorbing solute between the stream water and the hyporheic zones of the stream retaining the solute. They did the analysis for Chromium solute based on the Lanna Brook tracer experiment data.

In another work, Wörman [42] compared three models for transient storage of solutes in small stream, which are (1) first order mass transfer model (FOT model), (2) impermeable surface model (IS model) and (3) water infiltration model (WI). In the FOT model, the exchange term is based on the assumption that the mixing in the storage zone is instantaneous and the exchange is taking place only in the dissolved form of solute. The IS model is based on the similar concept as described by Jackman et al. [21] and Wörman [40] for diffusion model. The WI model includes both the advection and diffusion processes in the storage zone also. Wörman [42] found that these models yield similar representations of the first three temporal moments due to instantaneous input at the upstream boundary. In all these models, dispersion in the stream was not taken into account.

De Smedt [13] extended the approach of Wörman [40] to include the dispersion

in the main channel. De Smedt [13] presented an analytical solution for the case of instantaneous injection of solute assuming the flow to be constant and uniform. Solutions were applied to the five tracer experiments conducted in the Chillán river, Chile.

Jonsson et al. [23] introduced a diffusive transfer model for reactive solutes. Parameters of the proposed model were evaluated for the best fit of the observed solute concentration data obtained from the Säva stream tracer experiment to the approximate analytical solution of the model. They did the analysis of a conservative as well as a reactive solute. They found that a first-order kinetic description of the sorption process could acceptably describe the concentration-time curves in both the stream water and the bed sediment. However, no complete analytical solution of this model is available in the literature.

1.4 Objectives

Solute transport in streams is a complex phenomenon that involves physical, chemical and hydrological processes and has not yet been fully explored. Though many different models are available in the literature, but their complete analytical solutions are not yet known. An overall objective of this thesis is to improve the fundamental understanding of the solute transport in streams with transient storage and hyporheic zones. This thesis focuses on deriving complete analytical solutions for the contaminant transport problems in streams with storage zone and hyporheic zone. Sensitivity analysis is performed for transient storage models, in order to find the critical parameters on solute concentrations. Effects of different parameters, which represent physical, chemical and hydrological processes involved in the transport of the solutes in streams, are also studied.

In the first problem, general analytical solutions of the TSM are derived considering initial concentrations and lateral inflow concentration are non-constant. Analyt-

ical results for the main channel of streams are compared with the observed chloride concentrations of the Uvas Creek tracer experiment. Step concentration-time profile is considered as upstream boundary condition. Effects of lateral inflow rate and exchange Damköhler number on concentration distribution are studied.

In the second problem, we derive analytical solutions of the RSTM with decay, sorption and lateral inflow. These solutions are derived for a general situation, in which initial concentrations, lateral inflow concentration and equilibrium storage zone concentration are considered to be non-constant like previous study. Analytical solutions are presented for instantaneous release of solute. Effects of decay Damköhler numbers, reaction Damköhler numbers and lateral inflow are presented as well.

In the third problem also, we derive general analytical solutions of the diffusive transfer model for conservative solute for variable initial concentrations. Analytical solution for the main channel is compared with the observed data of the Uvas Creek tracer experiment for conservative (Chloride) solute. Effects of dilution factor, Péclet number and porosity in the hyporheic zone on the concentration-time curves are studied. A step concentration-time profile is considered as upstream boundary condition in this study as well.

In the fourth problem, we derive analytical solutions of the diffusive transfer model for reactive solute with sorption in the hyporheic zone. These solutions are also for a general situation, like previous studies. An instantaneous injection of solute is taken as an upstream boundary condition to show the effects of dilution factor, Péclet number in the hyporheic zone, porosity in the hyporheic zone and sorption Damköhler number.

Chapter 2

An analytical study on solute transport in streams with transient storage and lateral inflow: Conservative solute

This chapter deals with the derivation of analytical solutions for solute transport in a stream in the presence of storage zone where the exchange of solute between the main channel and the storage zone is dominated by a first order mass exchange. In this study, we follow the model proposed by Bencala and Walters [2] for conservative solute. This model is based on mass balance approach.

2.1 Introduction

Over the last few decades, the analysis of solute transport in streams with the effects of transient storage has become an active research area. Several models are proposed to describe the solute transport in streams with transient storage (e.g. Bencala and Walters [2], Harvey et al. [18], Hays et al. [19], Runkel [29], Wagner and Harvey [39], Wörman [40]). A commonly referenced model known as transient storage model (TSM) or dead zone model (DZM) is based on the classical advection-dispersion phenomenon with the exchange of solute between the main channel of a stream and the stagnant water zones such as pools, side arms of the river or adjacent wetland

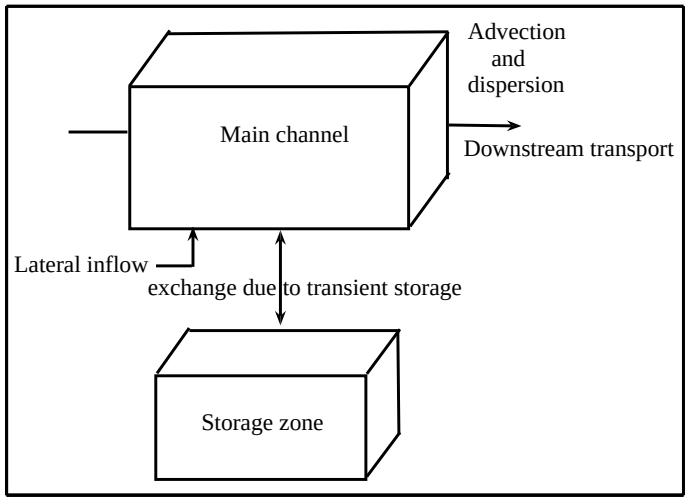

Figure 2.1: *Conceptual model describe the stream and storage zone hydrologic process for conservative solute.*

areas (Bencala and Walters [2], Runkel and Chapra [30], Wagner and Harvey [39]).

Generally, streams are divided into two distinct zones in the TSM for conservative solute. The first zone represents the main flow region that includes the process of advection, dispersion and lateral inflow. The second one represents the storage zone area, which is stagnant relative to the main channel flow of a river. Both the zones are linked by the mass exchange process (which can be seen from Fig. 2.1).

Both semi-analytical and analytical solutions are available for the model. Hays et al. [19] found the approximate solution of the transient storage model by means of Laplace transform. They found that the dead zone parameters (i.e. exchange coefficient and dead zone ratio) were difficult to predict with the help of field data. Thackston and Schnelle [38] evaluated the dead zone parameters using similar approximate solution given by Hays et al. [19] with the help of field data. In their analysis, they assumed the exchange co-efficient to be constant and the dead zone volume to be

a function of the friction factor. In 1995, Hart developed a semi-analytical solution for conservative solutes whereas Schmid [33] developed it for decaying solutes. Both of them considered the physical mechanisms of transient storage as stochastic processes and they did not consider the effects of lateral inflow in their studies. Later, Bencala and Walters [2] included the term due to the lateral inflow in the dead zone model proposed by Hays et al. [19]. Parameters for the TSM were evaluated for the best fit to the observed solute concentration curve by using the numerical solution of the TSM. Bencala and Walters [2] found that the effect of lateral inflow was negligible. Runkel [30] explained the TSM by using the mass balance approach. Subsequently, several experimental studies are made to characterize the physical transport properties and hydrological processes in streams (e.g. Harvey et al. [18], Scott et al. [35]). The effects of transient storage on solute transport in streams with lateral inflow were among the main issues discussed in these experimental studies. Harvey et al. [18] and Wagner and Harvey [39] presented sensitivity analysis in order to improve the understanding of different parameters reliability to stream tracer approach.

Runkel and Chapra [29] presented a numerical solution of the TSM by using the Crank-Nicolson numerical scheme. This is the basis to describe "One-dimensional Transport with Inflow and Storage (OTIS)". It also includes the numerical solution of the transient storage model for reactive solute. OTIS was extended by Runkel [31] with the nonlinear least squares method to optimize the parameters. This extended OTIS is known as OTIS-P. This is extensively used to estimate the transient storage behavior of streams through tracer experiments (Choi et al. [7], Fernald et al. [15]).

Davis et al. [10], De Smedt et al. [11] and De Smedt [12] found analytical solutions of the TSM for instantaneous solute release without considering the effects of lateral inflow and background concentration. They all assumed that the flow was constant and uniform in their studies.

In the present chapter, we derive general analytical solutions for the main channel

solute concentration as well as for the storage zone solute concentration for conservative solute transport. In this study, the initial solute concentrations are considered to be the function of space and the lateral inflow concentration to be the function of both time and space. Present analytical solutions also consider that the flow of the stream varies linearly with the longitudinal distance between the injection location and the downstream sampling location. Analytical solution in the absence of storage zone can easily be obtained from the present analytical solution. The present analytical results for the main channel are compared with the observed concentrations of the Uvas Creek tracer experiment. A sensitivity analysis is presented in order to identify the critical parameters for solute concentration. A hypothetical situation is considered to study the effects of exchange Damköhler number and lateral inflow rate on the concentration-time curves. Step concentration-time profile is considered as an upstream boundary condition for the analytical solutions.

2.2 Governing equations

The present problem is intended to study the solute transport in a stream in the presence of a storage zone where the exchange of solute between the main channel and the storage zone is considered as a first order mass transfer. In order to obtain the governing equations, the following assumptions are made.

2.2.1 Assumptions for the model

1. Medium is isotropic and homogeneous in both the zones.

2. Physical transport processes (advection, dispersion and lateral inflow) are affecting the solute concentration in the main channel.

3. Advection, dispersion and lateral inflow don't occur in the storage zone. Transient storage is the only process affecting solute concentrations in the storage zone.

4. Lateral inflow enters directly into the main channel bypassing the storage zone.

5. The exchange of solute between the main channel and the storage zone is considered to be first-order mass exchange. It is represented by the difference in concentrations between the main channel and the storage zone.

6. The volume of the storage zone is considered to be constant with time.

7. Solute concentrations in the main channel and in the storage zone vary only in the longitudinal direction.

8. Usually in conservative tracer experiments, the distance and time interval are short. So, all the parameters may be assumed to be constant throughout the study reach [11]. In our study, we assume all the parameters to be constant except the volumetric flow rate $Q_x^\star$ which vary linearly with the longitudinal distance between the injection and the downstream sampling location.

Based on these assumptions and following the work of Bencala and Walters [2], the governing equations can be written as:

$$\frac{\partial c_m^\star}{\partial t^\star} + u_m^\star \frac{\partial c_m^\star}{\partial x^\star} = D_m^\star \frac{\partial^2 c_m^\star}{\partial x^{\star 2}} + \alpha^\star (c_s^\star - c_m^\star) + \frac{q_L^\star}{A_m^\star}(c_L^\star - c_m^\star) \tag{2.1}$$

$$\frac{\partial c_s^\star}{\partial t^\star} = \frac{\alpha^\star A_m^\star}{A_s^\star}(c_m^\star - c_s^\star) \tag{2.2}$$

where $c_m^\star$ is the solute concentration in the main flow direction of the stream, $c_s^\star$ is the solute concentration in the storage zone, $c_L^\star$ is the solute concentration in lateral inflow, $u_m^\star$ is the cross-sectional average velocity, $x^\star$ is the longitudinal distance, $t^\star$ is time, $D_m^\star$ is the longitudinal dispersion coefficient in the main flow, $A_m^\star$ is the cross-sectional area of the main channel of stream, $A_s^\star$ is the cross-sectional area of the storage zone, $\alpha^\star$ is the stream storage exchange coefficient, $q_L^\star$ is the lateral inflow rate into the stream per unit stream length.

Eq. (2.1) is obtained by linking the one-dimensional classical advection-dispersion equation with a first order mass exchange term between the main channel and the storage zone (the second term on the right hand side), and a term for lateral inflow that enters directly into the main channel bypassing the storage zone (the last term on the right hand side). Eq. (2.2) represents that the rate of change of solute concentration in the storage zone is proportional to the difference in the solute concentrations between the main channel and the storage zone.

2.2.2 General boundary and initial conditions

Generally, in tracer experiments, a known amount of solute is injected at a constant rate at the injection location over a certain interval of time and then the solute concentrations are measured at different sampling locations (Bencala and Walters [2], Schmid [34]). So, the upstream boundary condition can be expressed as

$$c_m^\star(x^\star = x_0^\star, t^\star) = c_u^\star(t^\star) \text{ for } t^\star > 0. \tag{2.3}$$

where $x_0^\star$ is the upstream boundary location and $c_u^\star(t^\star)$ is the upstream concentration at the location $x_0^\star$ and time $t^\star$. It is assumed that Laplace transform of $c_u^\star(t^\star)$ exists and is bounded.

The other boundary condition at far downstream location is taken as:

$$c_m^\star(x^\star \to \infty, t^\star) = 0 \text{ for all } t^\star, \tag{2.4}$$

The initial conditions for the main channel and the transient storage are

$$c_m^\star(x^\star, t^\star = 0) = c_{minit}^\star(x^\star), \tag{2.5}$$

$$c_s^\star(x^\star, t^\star = 0) = c_{sinit}^\star(x^\star), \tag{2.6}$$

where $c_{minit}^\star(x^\star)$ and $c_{sinit}^\star(x^\star)$ are the initial concentrations in the main channel and in the storage zone respectively.

2.2.3 Dimensionless forms of governing equations, general boundary and initial conditions

The dimensionless forms of the governing equations, general boundary and initial conditions given in (2.1)-(2.6) are written as

$$\frac{\partial c_m}{\partial t} + \frac{\partial c_m}{\partial x} = \frac{1}{Pe_m}\frac{\partial^2 c_m}{\partial x^2} + Da_{em}(c_s - c_m) + q_L(c_L - c_m) \tag{2.7}$$

$$\frac{\partial c_s}{\partial t} = \frac{Da_{em}}{k_r}(c_m - c_s) \tag{2.8}$$

$$c_m(x_0, t) = c_u(t) \text{ for } t > 0. \tag{2.9}$$

$$c_m(x \to \infty, t) = 0 \text{ for all } t, \tag{2.10}$$

$$c_m(x, t = 0) = c_{minit}(x), \tag{2.11}$$

$$c_s(x, t = 0) = c_{sinit}(x), \tag{2.12}$$

where $x(= \frac{x^\star}{l^\star})$ is the distance in the longitudinal direction, $l^\star(\approx \sqrt{2.5A_m^\star})$ is the characteristic length, $t(= \frac{u_m^\star t^\star}{l^\star})$ is the dimensionless time, $u_m^\star$ is a constant quantity, $c_m(= \frac{c_m^\star}{c_0^\star})$ is the concentration in the main channel of the stream, $c_0^\star$ is the plateau concentration at the head of the tracer experiment, $c_s(= \frac{c_s^\star}{c_0^\star})$ is the concentration in the storage zone, $c_L(= \frac{c_L^\star}{c_0^\star})$ is the concentration in the lateral inflow, $c_{minit}(x)(= \frac{c_{minit}^\star(x^\star)}{c_0^\star})$ is the initial concentration in the main channel, $c_{sinit}(x)(= \frac{c_{sinit}^\star(x^\star)}{c_0^\star})$ is the initial concentration in the storage zone, $c_u(t)(= \frac{c_u^\star(t)}{c_0^\star})$ is the upstream concentration, $Pe_m(= \frac{u_m^\star l^\star}{D_m^\star})$ is the Péclet number in the main channel of the stream, $Da_{em}(= \frac{\alpha^\star l^\star}{u_m^\star})$ is the exchange Damköhler number in the main channel, $k_r(= \frac{A_s^\star}{A_m^\star})$ is the ratio of cross-sectional area of storage zone and the cross-sectional area of the main channel, and $q_L(= \frac{q_L^\star l^\star}{A_m^\star u_m^\star})$ is the lateral inflow rate.

2.2.4 Calculation of the cross-sectional average velocity ($u_m^\star$):

Both of the equations (2.1) and (2.2) are based on the theory of conservation of mass. The conservation of mass of water can be written, following Yan and Boufadel [43],

as $\frac{dQ_x^\star}{dx^\star} = q_L^\star - q_{Lout}^\star$, where $q_{Lout}^\star$ is the lateral outflow per unit stream length. In our study, we assume that the water does not leave the main channel throughout the study reach, which means $q_{Lout}^\star$ is zero. So, the volumetric flow rate at the downstream river reach ($Q_1^\star$) can be obtained, integrating the resulting equation over $[x_0^\star, x_1^\star]$, as $Q_1^\star = Q_0^\star + q_L^\star(x_1^\star - x_0^\star)$, where subscripts 0 and 1 represent the injection location and the downstream location respectively. We consider the averaged value of the volumetric flow rate ($Q^\star$), which is a constant quantity throughout the study reach, as $Q^\star = (Q_0^\star + Q_1^\star)/2$ to calculate the cross-sectional average velocity $u_m^\star (= Q^\star/A_m^\star)$, which is also a constant quantity throughout the study reach.

2.3 Analytical solution for conservative solutes with storage zone

The solution of the initial-boundary value problem (2.7)-(2.12) is obtained by means of Laplace transform.

Laplace transform of a function $f(t)$ is defined as

$$\overline{f}(s) = L\{f(t); t \to s\} = \int_0^\infty f(t)e^{-st}dt, \tag{2.13}$$

where s is the Laplace variable, which is a complex number.

By using the initial condition (2.12) in the Laplace transform of Eq.(2.8), we get

$$\overline{c}_s = \frac{c_{sinit}(x) + \frac{Da_{em}}{k_r}\overline{c}_m}{(s + \frac{Da_{em}}{k_r})}, \tag{2.14}$$

where $\overline{c}_m$ and $\overline{c}_s$ are Laplace transforms of c_m and c_s respectively.

Applying Laplace transform to Eq. (2.7) and using Eq. (2.14), we obtain a linear nonhomogeneous differential equation as,

$$\frac{1}{Pe_m}\frac{d^2\overline{c}_m}{dx^2} - \frac{d\overline{c}_m}{dx} - R\,\overline{c}_m = -c_{minit}(x) - \frac{Da_{em}c_{sinit}(x)}{(s + \frac{Da_{em}}{k_r})} - q_L\,\overline{c}_L(x,s), \tag{2.15}$$

where $\overline{c}_L(x,s)$ is the Laplace transform of $c_L(x,t)$ and

$$R = \left(s + q_L + Da_{em} - \frac{Da_{em}^2}{k_r(s + \frac{Da_{em}}{k_r})}\right).$$

Using the boundary conditions (2.9) and (2.10) in the solution of Eq. (2.15), we obtain

$$\begin{aligned}
\bar{c}_m(x,s) &= \bar{c}_u(s)e^{m_1 x} \\
&- \frac{Pe_m e^{m_1 x}}{(m_2-m_1)}\int_0^{+\infty}\left[c_{minit}(x^{'}) + \frac{Da_{em}c_{sinit}(x^{'})}{(s+\frac{Da_{em}}{k_r})} + q_L\bar{c}_L(x^{'},s)\right]e^{-m_2 x^{'}}dx^{'} \\
&+ \frac{Pe_m e^{m_1 x}}{(m_2-m_1)}\int_0^{x}\left[c_{minit}(x^{'}) + \frac{Da_{em}c_{sinit}(x^{'})}{(s+\frac{Da_{em}}{k_r})} + q_L\bar{c}_L(x^{'},s)\right]e^{-m_1 x^{'}}dx^{'} \\
&+ \frac{Pe_m e^{m_2 x}}{(m_2-m_1)}\int_x^{+\infty}\left[c_{minit}(x^{'}) + \frac{Da_{em}c_{sinit}(x^{'})}{(s+\frac{Da_{em}}{k_r})} + q_L\bar{c}_L(x^{'},s)\right]e^{-m_2 x^{'}}dx^{'},
\end{aligned} \tag{2.16}$$

where where $\bar{c}_u(s)$ is the Laplace transform of $c_u(t)$ and $m_{1,2} = \frac{Pe_m}{2} \mp \sqrt{Pe_m}\sqrt{\frac{Pe_m}{4}+R}$.

With the help of the convolution theorem (details are given in Appendix A), inverse Laplace transform of Eq. (2.16) gives,

$$\begin{aligned}
c_m(x,t) &= \int_0^t c_u(\eta)f_1(x,t-\eta)d\eta \\
&+ \int_0^{+\infty}\Big[c_{minit}(x^{'})(f_2(x-x^{'},-1,t) - e^{Pe_m x}f_2(x+x^{'},+1,t)) \\
&+ Da_{em}c_{sinit}(x^{'})(f_3(x-x^{'},-1,t) - e^{Pe_m x}f_3(x+x^{'},+1,t)) \\
&+ q_L\int_0^t\{c_L(x^{'},\eta)(f_2(x-x^{'},-1,t-\eta) - e^{Pe_m x}f_2(x+x^{'},+1,t-\eta))\}d\eta\Big]dx^{'},
\end{aligned} \tag{2.17}$$

where

$$a = Da_{em}\eta, \quad b = \frac{Da_{em}}{k_r}(t-\eta), \quad a_1 = Da_{em}\gamma, \quad b_1 = \frac{Da_{em}}{k_r}(t-\gamma-\eta),$$

$$f_1(x,t-\eta) = c_0(x,t-\eta)e^{-Da_{em}(t-\eta)} + \frac{Da_{em}}{k_r}\int_0^{t-\eta} c_0(x,\gamma)e^{-a_1-b_1}\sqrt{\frac{a_1}{b_1}}I_1(2\sqrt{a_1 b_1})d\gamma, \tag{2.18}$$

$$f_2(x,si,t) = c_1(x,si,t)\exp(-Da_{em}t) + \frac{Da_{em}}{k_r}\int_0^t c_1(x,si,\gamma)\exp(-(a+b))\sqrt{\frac{a}{b}}I_1(2\sqrt{ab})d\gamma, \tag{2.19}$$

$$f_3(x,si,t) = \int_0^t c_1(x,si,\gamma)\exp(-(a+b))I_0(2\sqrt{ab})d\gamma, \tag{2.20}$$

I_0 and I_1 are the modified Bessel function of first kind, and of order zero and one respectively,

$$c_0(x,t) = \frac{x\sqrt{Pe_m}}{2\sqrt{\pi t^3}} \exp\left(- \frac{Pe_m(x-t)^2}{4t} - q_L t \right), \tag{2.21}$$

$$c_1(x,si,t) = \frac{\sqrt{Pe_m}}{2\sqrt{\pi t}} \exp\left(- \frac{Pe_m(x+si\ t)^2}{4t} - q_L t \right). \tag{2.22}$$

The analytical solution for the storage zone is obtained by substituting Eq. (2.16) into Eq. (2.14) and taking inverse Laplace transform, we get

$$\begin{aligned} c_s(x,t) &= c_{sinit}(x) e^{-\frac{Da_{em}}{k_r}t} + \frac{Da_{em}}{k_r}\int_0^t c_u(\eta) f_4(x,t-\eta)d\eta \\ &+ \int_0^{+\infty} \Bigg[\frac{Da_{em}}{k_r} c_{minit}(x^{'})(f_3(x-x^{'},-1,t) - e^{Pe_m x} f_3(x+x^{'},+1,t)) \\ &+ Da_{em} c_{sinit}(x^{'})(f_5(x-x^{'},-1,t) - e^{Pe_m x} f_5(x+x^{'},+1,t)) \\ &+ q_L \int_0^t \{c_L(x^{'},\eta)(f_3(x-x^{'},-1,t-\eta) - e^{Pe_m x} f_3(x+x^{'},+1,t-\eta))\} d\eta \Bigg] dx^{'}, \end{aligned} \tag{2.23}$$

$$f_4(x,t-\eta) = \int_0^{t-\eta} c_0(x,\gamma) \exp(-(a_1+b_1)) I_0(2\sqrt{a_1 b_1}) d\gamma, \tag{2.24}$$

$$f_5(x,si,t) = \int_0^t c_1(x,si,\gamma) \exp(-(a+b)) \sqrt{\frac{b}{a}} I_0(2\sqrt{ab}) d\gamma, \tag{2.25}$$

It is verified that Eqs. (2.17) and (2.23) are satisfying the initial-boundary problem (2.7)-(2.12). This assures the analytical expressions given in Eqs. (2.17) and (2.23) are the exact analytical solutions of the TSM [i.e. Eqs. (2.7) and (2.8)] with lateral inflow for conservative solutes.

It is easy to see that the analytical solution presented in Eq. (2.17) reduces to the analytical solution of the classical advection-dispersion equation with lateral inflow when $Da_{em} = 0$ (i.e. the exchange of mass between the storage zone and the main channel is absent).

2.4 Results and Discussion

In order to compare the present analytical solutions with the existing experimental data [1, 2], parameters are estimated for the Uvas Creek tracer experiment. A sen-

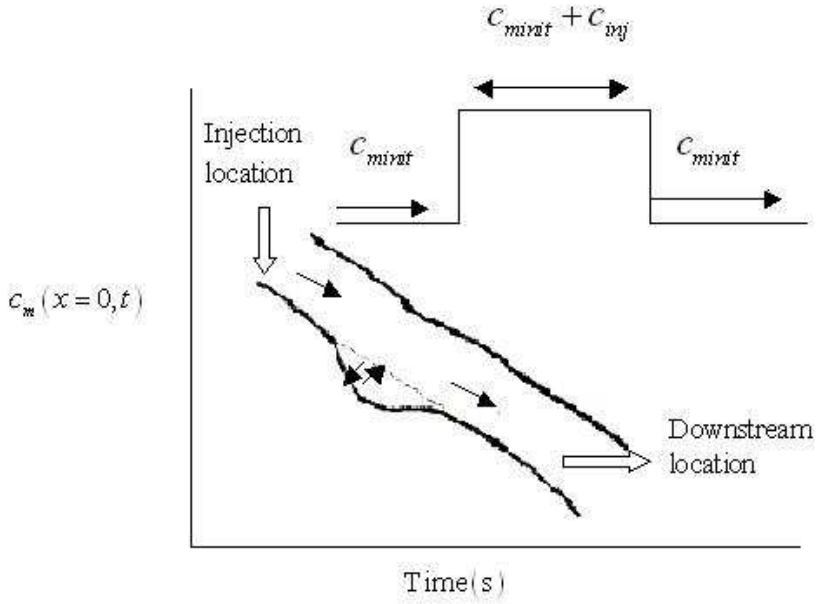

Figure 2.2: *Schematic diagram of the solution domain with step-concentration profile as upstream boundary condition.*

sitivity analysis is presented in order to identify the critical parameters for solute concentration. Effects of lateral inflow rate and exchange Damköhler number on solute concentrations are studied for a hypothetical situation. Integrations appearing in the different analytical expressions are evaluated by the Simpson's rule. The modified Bessel functions I_0 and I_1 are approximated by the polynomials

$$I_0(2\sqrt{ab}) = \sum_{n=0}^{n=\infty} \frac{a^n}{n!}\frac{b^n}{n!}$$

and

$$I_1(2\sqrt{ab}) = \sum_{n=0}^{n=\infty} \frac{a^{n+1}}{n+1!}\frac{b^n}{n!}$$

as given in Carslaw and Jaeger [6].

The upstream boundary condition is chosen to be a step-concentration profile as shown in Fig. 2.2.

$x^\star$	$A_m^\star$	$Q^\star$	$D_m^\star$	$q_L^\star(\times 10^{-6})$	$A_s^\star$	$\alpha^\star(\times 10^{-6})$	Pe_m
m	m^2	m^3/s	m^2/s	$m^3/s.m$	m^2	$1/s$	–
38	0.3496	0.0125	0.015785	1.64	0	0	2.26
105	0.3880	0.0126	0.08295	1.5	0	0	0.39
281	0.3771	0.0136	0.1217	8.3	0.0689	7.5	0.29
433	0.4201	0.0141	0.181	7.556	0.0999	8.1667	0.18
619	0.4897	0.0154	0.1798	9.34	0.3822	0.14	0.17

Table 2.1: *Estimated values of parameters for the transient storage model for the observed chloride concentrations of the Uvas Creek tracer experiment.*

2.4.1 Application to tracer experiment

In the Uvas Creek tracer experiment (Avanzino et al. [1]), a concentrated solution of dissolved sodium chloride was added to the stream at a rate of 50 ml/min for 3 hours. The conservative solute (chloride) concentration was 11.4 mg/l at the injection location and the background concentration was 3.7 mg/l. The concentration-time curves were measured at different downstream locations (i.e. $x^\star$ = 38, 105, 281, 433 and 619 m) from the injection location. The solute concentration profile at upstream boundary location ($x_0^\star = 0$) is chosen to be a step-concentration profile to simulate the observed concentration profiles at each downstream location by the analytical solution given in Eq. (2.17). The parameter estimation was accomplished using the Matlab Optimization Toolbox (The MathWorks, 2003). Parameters are estimated by minimizing the sum of the squared differences between the observed and theoretical results. In order to solve the nonlinear parameter estimation problem, a subspace trust region method algorithm based on the interior-reflective Newton method [8, 9] was used. Dimensional estimated values of parameters are presented in Table 2.1.

The estimated value of the lateral inflow ($q_L^\star$) gradually increases with slight oscillation and also the averaged volumetric flow rate ($Q^\star$) increases along the downstream as given in Table 2.1. This ensures that the conservation of mass is obeyed by the predicted values of $q_L^\star$ and $Q^\star$. Consequently, the increase in the value of volumetric flow rate often dilutes solute concentrations. The Péclet number gradually decreases

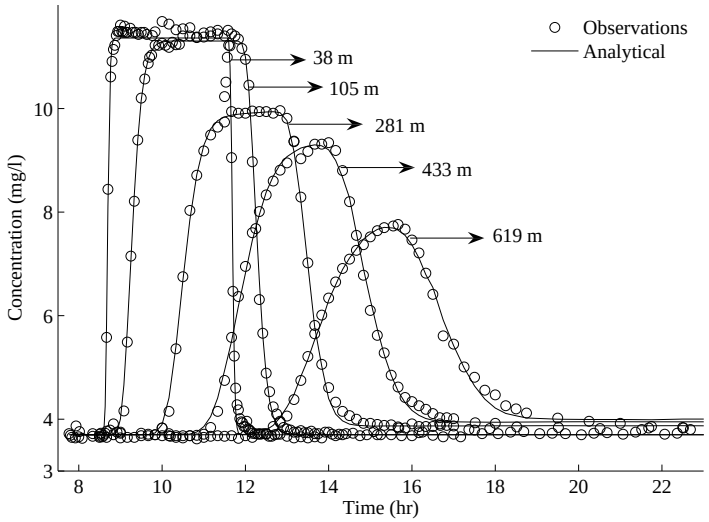

Figure 2.3: *Comparison of concentration profiles of the analytical solution given by Eq.* (2.17) *(solid lines), and observed concentration profiles (open dots) of the Uvas Creek tracer experiment for the TSM.*

along the longitudinal direction of the stream, which implies that the spread of solute increases along the downstream locations. Similar observation can be noticed in the observed data (which can also be verified from Fig. 2.3). The exchange Damköhler number found to be maximum at the sampling location 433 m and the ratio of cross-sectional areas found to be maximum at the last sampling location. All parameters are found to be nearly constant or in the same order of magnitude along the downstream direction of the stream, which confirm the validity of the assumption made for the mathematical models. Values of the parameters also follow the similar trend as presented in the work of Bencala and Walters [2]. Using the estimated values of the parameters, results are calculated by Eq. (2.17) in dimensionless form and presented in dimensional form in Fig. 2.3 to compare with the observed data. It is found that the concentration-time curves of the analytical solution agree well with the observed concentration-time curves of the Uvas Creek tracer experiment.

p_j	dc_{min}	dc_{max}	$dc_{max} - dc_{min}$
Pe_m	-0.59	0.59	1.18
Da_{em}	-252.95	126.35	379.30
q_L	-310.43	0.0	310.43
k_r	-0.31	0.0	0.31

Table 2.2: *TSM: minimum (dc_{min}) and maximum (dc_{max}) values of sensitivity of solute concentration in the main channel to the parameter p_j.*

Sensitivity Analysis

A sensitivity analysis is performed in order to identify the critical parameters for the present situation. Sensitivity is the partial derivative of the simulated stream tracer concentration with respect to a change in the value of a parameter (Wagner and Harvey [39]),

$$s_{ij} = \frac{\partial c_{m_i}}{\partial p_j}, \tag{2.26}$$

where s_{ij} is the sensitivity of simulated stream tracer concentration c_{m_i} to the parameter p_j. Sensitivities of Péclet number (Pe_m), exchange Damköhler number in the main channel (Da_{em}), ratio of cross-sectional areas (k_r) and lateral inflow rate (q_L) are calculated at 433 m. Results are presented in Table 2.2 and in Figs. 2.4 and 2.5. From the table and figures, it is clear that the Da_{em} and q_L are much more sensitive compared to the Pe_m and k_r. However, Da_{em} is the most sensitive and k_r is the least sensitive among all these parameters. It reveals that the change in main channel concentration is maximum due to the exchange of solute between the main channel and storage zone.

2.4.2 Hypothetical Experiment

In order to study the effects of lateral inflow rate and exchange Damköhler number, a hypothetical situation is considered on taking the values of the parameters same as given in Table 2.3. It is assumed that 25 unit of conservative solute is injected at the injection location $x_0 = 0$ with a constant rate over a time interval of 252 unit.

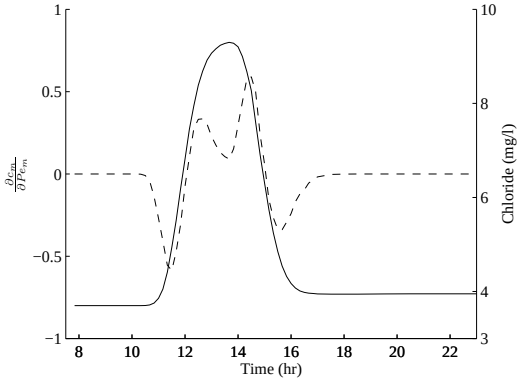

(a) *sensitivity (dashed line) to Péclet number*

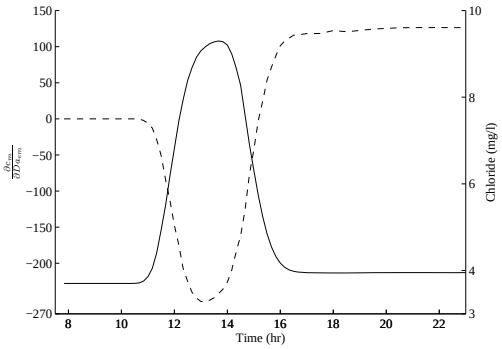

(b) *sensitivity (dashed line) to exchange Damköhler number in the main channel*

Figure 2.4: *Sensitivity of Péclet number and exchange Damköhler number on the concentration-time curve (solid line) calculated with the analytical solution given by Eq.* (2.17) *at* 433 m.

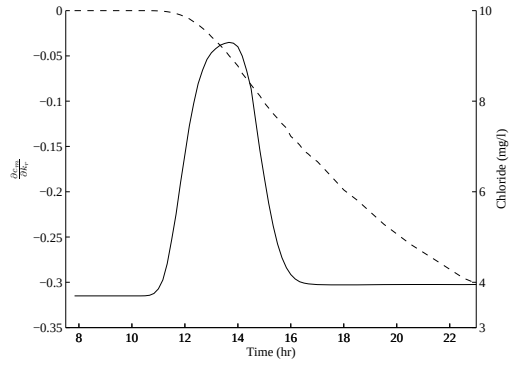

(a) *sensitivity (dashed line) to ratio of cross-sectional area*

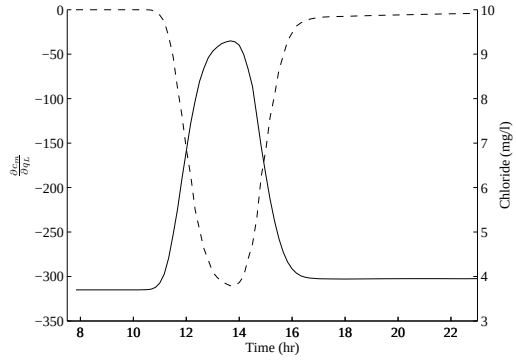

(b) *sensitivity (dashed line) to lateral inflow rate*

Figure 2.5: *Sensitivity of ratio of cross-sectional area and lateral inflow rate on the concentration-time curve (solid line) calculated with the analytical solution given by Eq.* (2.17) *at* 433 m.

Results are obtained at a distance of 1000 unit from the injection location along the downstream direction and presented in the dimensionless form.

Effect of lateral inflow rate and exchange rate

In order to discuss the effects of lateral inflow rate and exchange Damöhler number, the initial concentrations and lateral inflow concentration are considered to be equal

c_{inj}	x	$Q_0^\star$	Pe_m	Da_{em}	k_r	q_L
25	1000	10	0.21	9.5238×10^{-4}	0.2	4.7619×10^{-5}

Table 2.3: *Parameter values for the analysis of results of conservative solute.*

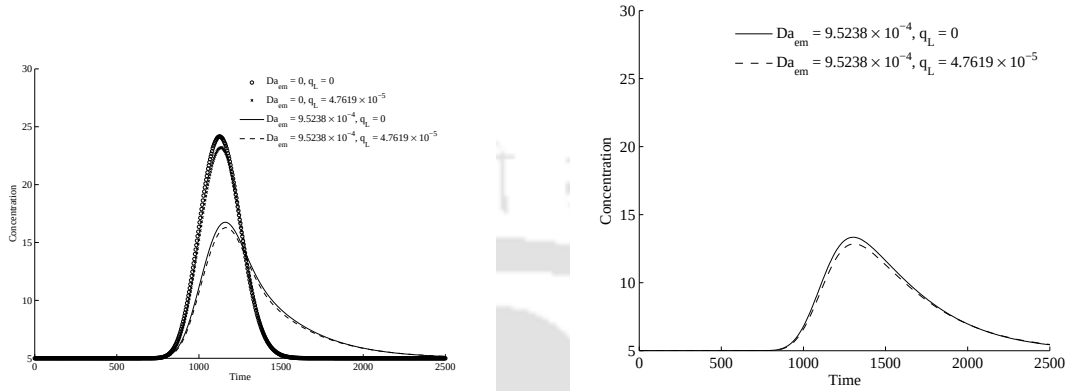

(a) *Main channel solute concentration* (b) *Storage zone solute concentration*

Figure 2.6: *Effects of lateral inflow rate and exchange Damköhler number on the concentration-time profiles of the analytical solution given by* (a) *Eq.* (2.17) *and* (b) *Eq.* (2.23) *at* 1000 *unit downstream from the injection location.*

to 5 unit. The concentration-time curves are presented in Fig. 2.6. If the lateral inflow solute enters into the main channel of a stream, then the solute mass increases in the main channel of the stream and the solute concentration gets diluted throughout the study reach compared to the case of no lateral inflow. When a solute is injected into the main channel of a stream, a portion of it initially enters into the storage zone and slowly releases back into the main channel of the stream over a period of time. This exchange of mass is the main cause of reduction in the solute mass and also forms a long tail in the downstream edge of the solute concentration profiles in the main channel at a downstream location compared to the case in which the storage zone is absent. Fig. 2.6 also shows that the effects of lateral inflow are not influenced by the presence of storage zone.

2.5 Conclusions

Analytical solutions for conservative solute concentrations in rivers with lateral inflow and transient storage are found and are presented in this chapter. The already existing analytical solutions for the case of no transient storage can easily be obtained from the present analytical solution on assuming $Da_{em} = 0$. The solution for concentration in the main channel of the stream is applied to the analysis of the Uvas Creek tracer experiment. A sensitivity analysis for this case is also carried out in order to study the sensitivity of predicted concentrations to controlling parameters. Finally, a hypothetical case is considered to investigate the effect of lateral inflow rate and exchange Damköhler number.

The analytical results are found to be in good agreement with the observed data of the Uvas Creek tracer experiment. Sensitivity analysis shows that the exchange Damköhler number in the main channel (Da_{em}) and lateral inflow rate (q_L) are much more sensitive compared to the Péclet number in the main channel (Pe_m) and ratio of cross-sectional areas (k_r).

Due to the lateral inflow rate, it is noticed that the solute mass gets diluted at the downstream locations. Due to the exchange Damköhler number, the solute mass gets reduced and the long tail appears in the downstream edge of the concentration profile. Present analytical solutions clearly reveal the effects of lateral inflow rate and the exchange Damköhler number. The solutions are presented for step concentration-time profile. It can be concluded that the present solutions can be reliably used for the analysis of solute transport in tracer experiments.

Chapter 3

An analytical study on solute transport in streams with transient storage and lateral inflow: Reactive solute

In this chapter, analytical solutions are derived for the transport of reactive solute in a stream in the presence of storage zone where the exchange of solute between the main channel and the storage zone is due to the first order mass exchange. The first order reaction and the decay are considered in the main channel as well as in the storage zone. In this study, we follow the model proposed by Bencala [3] for reactive solute. This model is based on mass balance approach.

3.1 Introduction

Reactive solute transport models (RSTM) are frequently used for the analysis of tracer experiments for reactive solute. The transient storage model (TSM) of Bencala and Waters [2] was extended by Bencala [3] for reactive solute by incorporating the effects of sorption in the main channel as well as in the storage zone. This extended model is commonly known as RSTM. Two distinct zones are usually considered in RSTM also like in transient storage model (TSM) for conservative solute. The first zone represents the main flow region that includes the processes of advection, dispersion

and lateral inflow. The second zone represents the storage zone that is stagnant relative to the main flow of stream such as pools, gravel beds, side arms of the stream or adjacent wetland areas. These two zones are linked by the mass exchange process (Bencala and Walters [2], Runkel and Chapra [29], Wagner and Harvey [39]). In the case of reactive solute, kinetic submodels are considered in both the zones (Bencala [2]). In the main channel, the kinetic submodel relates the first order mass transfer reaction between the main channel of stream and the streambed sediment, whereas in the storage zone, the kinetic submodel relates the first order kinetic reaction by the concentration difference between the storage concentration and its equilibrium concentration. Both the zones include the first order decay (Runkel [31]).

There are two kinds of RSTM available in the literature. The first model deals with the decay in the main channel as well as in the transient storage (De Smedt [12], Schmid [33]) whereas the second one deals with the sorption on streambed sediments with lateral inflow [3]. Both the models are considered in the present study (which can be seen from Fig. 3.1).

Bencala [3] described the RSTM, without taking the effects of decay into account. Parameters of this RSTM are evaluated for the best fit of the observed solute concentration curve by using the numerical solution of the proposed model. In his study, Bencala [3] found that the effect of lateral inflow was negligible. Later, a number of experimental studies are conducted to characterize the physical transport properties and hydrological processes in streams (e.g. Gooseff et al. [16], Scott et al. [35]). The effects of transient storage on solute transport in streams with lateral inflow are discussed in these studies. Runkel [31] developed OTIS-P for the RSTM, with the nonlinear least squares method to optimize the parameters, by using the Crank-Nicolson scheme. OTIS-P is extensively used to estimate the transient storage behavior of streams through tracer experiments (Choi et al. [7], Fernald et al. [15]).

Schmid [33] found semi-analytical solution of the RSTM, including the effects

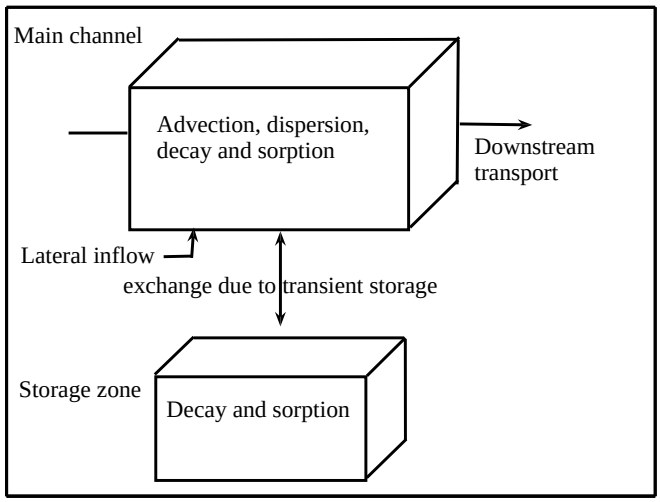

Figure 3.1: *Conceptual model describe the stream and storage zone hydrologic process for reactive solute.*

of decay in both the zones. He treated the physical mechanisms of the RSTM, as stochastic processes. De Smedt [12] obtained analytical solutions for decaying solutes without taking the effects of lateral inflow and sorption into consideration. In chapter 2, we have derived analytical solutions of the TSM for conservative solute without including the effects of decay and sorption.

In this chapter, we derive analytical solutions of the RSTM for a general situation (i.e. including the effects of sorption and decay). Analytical solutions are derived for the main channel, the storage zone and the stream sediment bed solute concentrations. The initial concentrations are considered to be the function of longitudinal distance whereas lateral inflow concentration and equilibrium solute concentration in the storage zone are assumed to be the functions of both space and time. Analytical solutions are presented for instantaneous release of the solute for a hypothetical situation. Sensitivity analysis is presented in order to identify the critical parameters for

reactive solute. Effects of decay Damköhler numbers, reaction Damköhler numbers and lateral inflow are presented as well.

3.2 Governing equations

The governing equations presented in the previous chapter is valid only for the transport of a conservative solute. Often in practice, reaction of a solute can occur due to various chemical and biogeochemical processes (Broshears et al. [5], Choi et al. [7], Keefe et al. [24], Stream Solute Workshop [37]). Generally, first order decay and reaction processes are considered to study the transport of reactive solute. In the present problem, the exchange of solute mass between the main channel and the storage zone is due to both the first order mass transfer and the kinetic transfer of solute. In this study, we follow the model proposed by Bencala [3], which is based on mass balance approach. Along with the assumptions already made in the case of conservative solute in the previous chapter, the following points are also included for reactive solutes.

3.2.1 Assumptions for the model

1. Chemical reaction and decay affect the solute concentration in the main channel as well as in the storage zone.

2. First order kinetic reaction due to sorption is assumed to take place between the main channel of stream and its sediment bed.

3. In the transient storage, it is assumed that the solute (e.g. strontium) that enters the storage zone is rapidly and permanently lost from the water in the storage zone. Since the solute resides for relatively longer period of time in the storage zone in comparison to the time scale of the stream transport, the solute in the storage zone is assumed to be in equilibrium. The sorption in the storage zone is represented by first order mass transfer reaction (Bencala [3]).

4. Solute which enters into the storage zone has the opportunity for essentially continual contact with the stagnant bed materials.

5. The combined time for transport into a storage zone, sorption, desorption and transport back into stream channel is very long compared to the time for passage of the solute pulse.

6. Like the previous chapter, all parameters except $Q_x^\star$ are assumed to be constant.

The physical transient storage model developed by Bencala [3] and also presented by Runkel [31], can be written under the above assumptions as:

$$\frac{\partial c_m^\star}{\partial t^\star}+u_m^\star\frac{\partial c_m^\star}{\partial x^\star}=D_m^\star\frac{\partial^2 c_m^\star}{\partial x^{\star 2}}+\alpha^\star(c_s^\star-c_m^\star)+\frac{q_L^\star}{A_m^\star}(c_L^\star-c_m^\star)+\rho\hat{\lambda}_m^\star(c_{sed}^\star-k_d c_m^\star)-\lambda_m^\star c_m^\star, \quad (3.1)$$

$$\frac{\partial c_s^\star}{\partial t^\star}=\frac{\alpha^\star A_m^\star}{A_s^\star}(c_m^\star-c_s^\star)+\hat{\lambda}_s^\star(\hat{c}_s^\star-c_s^\star)-\lambda_s^\star c_s^\star, \quad (3.2)$$

$$\frac{\partial c_{sed}^\star}{\partial t^\star}=\hat{\lambda}_m^\star(k_d c_m^\star-c_{sed}^\star), \quad (3.3)$$

where $c_m^\star$ is the solute concentration in the main flow direction of stream, $c_s^\star$ is the solute concentration in the storage zone, $\hat{c}_s^\star$ is the equilibrium solute concentration in the storage zone, $c_{sed}^\star$ is the sorbate concentration on the streambed sediment, $c_L^\star$ is the solute concentration in lateral inflow, $u_m^\star$ is the cross-sectional average velocity in the main channel, $x^\star$ is the longitudinal distance, $t^\star$ is time, $D_m^\star$ is the longitudinal dispersion coefficient in the main flow, $A_m^\star$ is the cross-sectional area of the main channel of stream, $A_s^\star$ is the cross-sectional area of the storage zone, $\alpha^\star$ is the rate by which mass exchanges from the main channel to storage zone, $q_L^\star$ is the lateral inflow rate into the stream per unit stream length, ρ is the mass of accessible sediment per volume of stream water, $\hat{\lambda}_m^\star$ is the first order sorption rate coefficient in the main channel, k_d is the distribution coefficient, $\hat{\lambda}_s^\star$ is the first order sorption rate coefficient in the storage zone, $\lambda_m^\star$ is the first order decay coefficient in the main channel and $\lambda_s^\star$ is the first order decay coefficient in the storage zone.

Governing Eqs. (3.1) and (3.2) of this study are obtained by adding the terms for the first order mass transfer reaction and also for the first order decay in the main channel as well as in the storage zone to the Eqs. (2.1) and (2.2) of the transient storage model (TSM) for conservative solute (described in chapter 2). Eq. (3.3) represents that the rate of change of concentration of the sorbing element on the bed sediment is proportional to the difference between the solute concentration on the streambed sediment and its potential equilibrium concentration in the main channel.

3.2.2 General boundary and initial conditions

The boundary condition due to the continuous injection of solutes is given by

$$c_m^\star(x^\star = x_0^\star, t^\star) = c_u^\star(t^\star) \text{ for } t^\star > 0. \tag{3.4}$$

where $x_0^\star$ is the upstream boundary location and $c_u^\star(t^\star)$ is the upstream concentration at the location $x_0^\star$ and time $t^\star$. It is assumed that Laplace transform of $c_u^\star(t^\star)$ exists and is bounded.

The other boundary condition at far downstream location is taken as:

$$c_m^\star(x^\star \to \infty, t^\star) = 0 \text{ for all } t^\star. \tag{3.5}$$

The initial conditions for the main channel, storage zone and sediment bed are

$$c_m^\star = c_{minit}^\star(x^\star) \text{ at } t^\star = 0, \tag{3.6}$$

$$c_s^\star = c_{sinit}^\star(x^\star) \text{ at } t^\star = 0, \tag{3.7}$$

$$c_{sed}^\star = c_{sedinit}^\star(x^\star) \text{ at } t^\star = 0, \tag{3.8}$$

where $c_{minit}^\star(x^\star)$, $c_{sinit}^\star(x^\star)$ and $c_{sedinit}^\star(x^\star)$ are initial concentrations in the main channel, in the storage zone and in the stream sediment bed respectively.

3.2.3 Dimensionless forms of governing equations, general boundary and initial conditions

The dimensionless forms of the the governing equations, boundary and initial conditions (3.1)-(3.8) are given as

$$\frac{\partial c_m}{\partial t}+\frac{\partial c_m}{\partial x}=\frac{1}{Pe_m}\frac{\partial^2 c_m}{\partial x^2}+Da_{em}(c_s-c_m)+q_L(c_L-c_m)+\rho Da_{rm}(c_{sed}-k_d c_m)-Da_{dm}c_m, \tag{3.9}$$

$$\frac{\partial c_s}{\partial t}=\frac{Da_{em}}{k_r}(c_m-c_s)+Da_{rs}(\hat{c}_s-c_s)-Da_{ds}c_s, \tag{3.10}$$

$$\frac{\partial c_{sed}}{\partial t}=Da_{rm}(k_d c_m-c_{sed}), \tag{3.11}$$

$$c_m(x_0,t)=c_u(t) \text{ for } t>0, \tag{3.12}$$

$$c_m(x\to\infty,t)=0 \text{ for all } t, \tag{3.13}$$

$$c_m(x,t=0)=c_{minit}(x), \tag{3.14}$$

$$c_s(x,t=0)=c_{sinit}(x), \tag{3.15}$$

$$c_{sed}(x,t=0)=c_{sedinit}(x), \tag{3.16}$$

where $x\left(=\frac{x^\star}{l^\star}\right)$ is the distance in the longitudinal direction, $l^\star(\approx\sqrt{0.05A_m^\star})$ is the characteristic length, $t\left(=\frac{u_m^\star t^\star}{l^\star}\right)$ is the time, $u_m^\star$ is a constant quantity, $c_m\left(=\frac{c_m^\star}{c_0^\star}\right)$ is the concentration in the main channel of the stream, $c_0^\star$ is the plateau concentration at the head of the tracer experiment, $c_s\left(=\frac{c_s^\star}{c_0^\star}\right)$ is the concentration in the storage zone, $c_L\left(=\frac{c_L^\star}{c_0^\star}\right)$ is the concentration in the lateral inflow, $c_{sed}\left(=\frac{c_{sed}^\star}{c_0^\star}\right)$ is the sorbate concentration on the streambed sediment, $c_{minit}(x)\left(=\frac{c_{minit}^\star(x^\star)}{c_0^\star}\right)$ is the initial concentration in the main channel, $c_{sinit}(x)\left(=\frac{c_{sinit}^\star(x^\star)}{c_0^\star}\right)$ is the initial concentration in the storage zone, $c_{sedinit}(x)\left(=\frac{c_{sedinit}^\star(x^\star)}{c_0^\star}\right)$ is the initial concentration in the stream sediment bed, $c_u(t)\left(=\frac{c_u^\star(t)}{c_0^\star}\right)$ is the upstream concentration, $Pe_m\left(=\frac{u_m^\star l^\star}{D_m^\star}\right)$ is the Péclet number in the main channel, $Da_{em}\left(=\frac{\alpha^\star l^\star}{u_m^\star}\right)$ is the exchange Damköhler number in the main channel, $k_r\left(=\frac{A_s^\star}{A_m^\star}\right)$ is the ratio of cross-sectional areas, $Da_{dm}\left(=\frac{\lambda_m^\star l^\star}{u_m^\star}\right)$

is the decay Damköhler number in the main channel, $Da_{ds}\left(=\frac{\lambda_s^\star l^\star}{u_m^\star}\right)$ is the decay Damköhler number in the storage zone, $Da_{rm}\left(=\frac{\hat{\lambda}_m^\star l^\star}{u_m^\star}\right)$ is the reaction Damköhler number in the main channel, $Da_{rs}\left(=\frac{\hat{\lambda}_s^\star l^\star}{u_m^\star}\right)$ is the reaction Damköhler number in the storage zone and $q_L(=\frac{q_L^\star l^\star}{A_m^\star u_m^\star})$ is the lateral inflow rate.

3.3 Analytical solution for kinetic transport of reactive solutes with storage zone

The analytical solutions of (3.9)-(3.16) are obtained by using Laplace transform.

By using the initial conditions (3.15) and (3.16) in the Laplace transform of Eqs. (3.10) and (3.11) respectively, we obtain

$$\overline{c}_s = \frac{c_{sinit}(x) + \frac{Da_{em}}{k_r}\overline{c}_m + Da_{rs}\overline{\hat{c}}_s(x,s)}{s + \frac{Da_{em}}{k_r} + Da_{rs} + Da_{ds}}, \tag{3.17}$$

$$\overline{c}_{sed} = \frac{c_{sedinit}(x) + Da_{rm}k_d\overline{c}_m}{s + Da_{rm}}, \tag{3.18}$$

where $\overline{c}_m$, $\overline{c}_s$, $\overline{\hat{c}}_s(x,s)$ and $\overline{c}_{sed}$ are the Laplace transforms of c_m, c_s, $\hat{c}_s(x,t)$ and c_{sed} respectively.

On applying Laplace transform to Eq. (3.9), using Eqs. (3.17) and (3.18), we obtain a non-homogeneous ordinary differential equation as,

$$\frac{1}{Pe_m}\frac{d^2\overline{c}_m}{dx^2} - \frac{d\overline{c}_m}{dx} - R_1\overline{c}_m = -R_2(x), \tag{3.19}$$

where

$$R_1 = \left(s + q_L + Da_{dm} + Da_{em} + \rho k_d Da_{rm} - \frac{Da_{em}^2}{k_r\left(s + \frac{Da_{em}}{k_r} + Da_{rs} + Da_{ds}\right)} - \frac{\rho k_d Da_{rm}^2}{s + Da_{rm}}\right)$$

and

$$R_2(x) = c_{minit}(x) + \frac{Da_{em}(c_{sinit}(x) + Da_{rs}\overline{\hat{c}}_s(x,s))}{s + \frac{Da_{em}}{k_r} + Da_{rs} + Da_{ds}} + \frac{\rho Da_{rm}c_{sedinit}(x)}{s + Da_{rm}} + q_L\overline{c}_L(x,s);$$

$\overline{c}_L(x,s)$ is the Laplace transform of $c_L(x,t)$.

Using the boundary conditions (3.12) and (3.13) in the solution of Eq. (3.19), we obtain

$$\begin{aligned}\overline{c}_m(x,s) &= \overline{c}_u(s)e^{m_1 x} - \frac{Pe_m e^{m_1 x}}{(m_2-m_1)}\int_0^{+\infty} R_2(x^{'})e^{-m_2 x^{'}}dx^{'} \\ &+ \frac{Pe_m e^{m_1 x}}{(m_2-m_1)}\int_0^{x} R_2(x^{'})e^{-m_1 x^{'}}dx^{'} + \frac{Pe_m e^{m_2 x}}{(m_2-m_1)}\int_x^{+\infty} R_2(x^{'})e^{-m_2 x^{'}}dx^{'},\end{aligned} \tag{3.20}$$

where $\overline{c}_u(s)$ is the Laplace transform of $c_u(t)$ and $m_{1,2} = \frac{Pe_m}{2} \mp \sqrt{Pe_m}\sqrt{\frac{Pe_m}{4}+R_1}$.

With the help of convolution theorem (given in Prudnikov et al. [27], Sneddon [36]), inverse Laplace transform of Eq. (3.20) gives,

$$\begin{aligned}c_m(x,t) &= \int_0^t c_u(\eta)f_1(x,t-\eta)d\eta \\ &+ \int_0^{+\infty}\Big[c_{minit}(x^{'})(f_2(x-x^{'},-1,t) - e^{Pe_m x}f_2(x+x^{'},+1,t)) \\ &+ Da_{em}c_{sinit}(x^{'})(f_3(x-x^{'},-1,t) - e^{Pe_m x}f_3(x+x^{'},+1,t)) \\ &+ \rho Da_{rm}c_{sedinit}(x^{'})(f_4(x-x^{'},-1,t) - e^{Pe_m x}f_4(x+x^{'},+1,t)) \\ &+ \int_0^t\{q_L c_L(x^{'},\eta)(f_2(x-x^{'},-1,t-\eta) - e^{Pe_m x}f_2(x+x^{'},+1,t-\eta)) \\ &+ Da_{em}Da_{rs}\hat{c}_s(x^{'},t)(f_3(x-x^{'},-1,t-\eta) - e^{Pe_m x} \\ &\times f_3(x+x^{'},+1,t-\eta))\}d\eta\Big]dx^{'},\end{aligned} \tag{3.21}$$

where

$$\begin{aligned}f_1(x,t) &= c_0(x,t)e^{-(Da_{em}+\rho k_d Da_{rm})t} \\ &+ \frac{Da_{em}}{k_r}\int_0^t c_0(x,\gamma)e^{-a-b-p-r}\sqrt{\frac{a}{b}}\ I_1(2\sqrt{ab})d\gamma \\ &+ Da_{rm}\int_0^t c_0(x,\gamma)e^{-a-p-q}\sqrt{\frac{p}{q}}\ I_1(2\sqrt{pq})d\gamma \\ &+ \frac{Da_{em}Da_{rm}}{k_r}\int_0^t c_0(x,\gamma)\int_0^{t-\gamma} e^{-a-b_1-p-q_1-r_1}\sqrt{\frac{ap}{b_1 q_1}}I_1(2\sqrt{ab_1}) \\ &\times I_1(2\sqrt{pq_1})d\mu d\gamma,\end{aligned} \tag{3.22}$$

$$
\begin{aligned}
f_2(x,si,t) &= c_1(x,si,t)e^{-(Da_{em}+\rho k_d Da_{rm})t} \\
&+ \frac{Da_{em}}{k_r}\int_0^t c_1(x,si,\gamma)e^{-a-b-p-r}\sqrt{\frac{a}{b}}\ I_1(2\sqrt{ab})d\gamma \\
&+ Da_{rm}\int_0^t c_1(x,si,\gamma)e^{-a-p-q}\sqrt{\frac{p}{q}}\ I_1(2\sqrt{pq})d\gamma \\
&+ \frac{Da_{em}Da_{rm}}{k_r}\int_0^t c_1(x,si,\gamma)\int_0^{t-\gamma} e^{-a-b_1-p-q_1-r_1}\sqrt{\frac{ap}{b_1q_1}}I_1(2\sqrt{ab_1}) \\
&\times I_1(2\sqrt{pq_1})d\mu d\gamma, \qquad (3.23)
\end{aligned}
$$

$$
\begin{aligned}
f_3(x,si,t) &= \int_0^t c_1(x,si,\gamma)e^{-a-b-p-r}\ I_0(2\sqrt{ab})d\gamma \\
&+ Da_{rm}\int_0^t c_1(x,si,\gamma)\int_0^{t-\gamma} e^{-a-b_1-p-q_1-r_1}\sqrt{\frac{p}{q_1}}I_0(2\sqrt{ab_1}) \\
&\times I_1(2\sqrt{pq_1})d\mu d\gamma, \qquad (3.24)
\end{aligned}
$$

$$
\begin{aligned}
f_4(x,si,t) &= \int_0^t c_1(x,si,\gamma)e^{-a-p-q}\ I_0(2\sqrt{pq})d\gamma \\
&+ \frac{Da_{em}}{k_r}\int_0^t c_1(x,si,\gamma)\int_0^{t-\gamma} e^{-a-b_1-p-q_1-r_1}\sqrt{\frac{a}{b_1}}I_1(2\sqrt{ab_1}) \\
&\times I_0(2\sqrt{pq_1})d\mu d\gamma, \qquad (3.25)
\end{aligned}
$$

where

$$
a = Da_{em}\gamma, \quad b = \frac{Da_{em}}{k_r}(t-\gamma), \quad p = \rho k_d Da_{rm}\gamma, \quad q = Da_{rm}(t-\gamma),
$$

$$
r = (Da_{ds}+Da_{rs})(t-\gamma), \quad b_1 = \frac{Da_{em}}{k_r}\mu, \quad r_1 = (Da_{ds}+Da_{rs})\mu, \quad q_1 = Da_{rm}(t-\gamma-\mu),
$$

$$
c_0(x,t) = \frac{x\sqrt{Pe_m}}{2\sqrt{\pi t^3}}e^{-\frac{Pe_m(x-t)^2}{4t}-(Da_{dm}+q_L)t}, \qquad (3.26)
$$

and

$$
c_1(x,si,t) = \frac{\sqrt{Pe_m}}{2\sqrt{\pi t}}\exp\left(-\frac{Pe_m(x+si\ t)^2}{4t}-(q_L+Da_{dm})t\right), \qquad (3.27)
$$

The analytical solution for the storage zone is obtained by substituting Eq. (3.20) into Eq. (3.17) and applying inverse Laplace transform as,

$$\begin{aligned} c_s(x,t) &= c_{sinit}(x)e^{-p_1 t} + \frac{Da_{rs}\hat{c}_s(x,t)}{p_1}(1-e^{-p_1 t}) + \frac{Da_{em}}{k_r}\int_0^t c_u(\eta) f_5(x,t-\eta)d\eta \\ &+ \int_0^{+\infty}\Big[c_{minit}(x^{'})(f_3(x-x^{'},-1,t) - e^{Pe_m x} f_3(x+x^{'},+1,t)) \\ &+ k_r c_{sinit}(x^{'})(f_6(x-x^{'},-1,t) - e^{Pe_m x} f_6(x+x^{'},+1,t)) \\ &+ \rho Da_{rm} c_{sedinit}(x^{'})(f_7(x-x^{'},-1,t) - e^{Pe_m x} f_7(x+x^{'},+1,t)) \\ &+ \int_0^t \{q_L c_L(x^{'},\eta)(f_3(x-x^{'},-1,t-\eta) - e^{Pe_m x} f_3(x+x^{'},+1,t-\eta)) \\ &+ Da_{rs} k_r \hat{c}_s(x^{'},\eta)(f_6(x-x^{'},-1,t-\eta) - e^{Pe_m x} f_6(x+x^{'},+1,t-\eta))\}d\eta\Big]dx^{'}, \end{aligned} \tag{3.28}$$

where $p_1 = \frac{Da_{em}}{k_r} + Da_{ds} + Da_{rs}$,

$$\begin{aligned} f_5(x,t) &= \int_0^t c_0(x,\gamma)e^{-a-b-p-r}\, I_0(2\sqrt{ab})d\gamma \\ &+ Da_{rm}\int_0^t c_0(x,\gamma)\int_0^{t-\gamma} e^{-a-b_1-p-q_1-r_1}\sqrt{\frac{p}{q_1}} I_0(2\sqrt{ab_1}) \\ &\times I_1(2\sqrt{pq_1})d\mu d\gamma, \end{aligned} \tag{3.29}$$

$$\begin{aligned} f_6(x,si,t) &= \int_0^t c_1(x,si,\gamma)e^{-a-b-p-r}\sqrt{\frac{b}{a}}\, I_1(2\sqrt{ab})d\gamma \\ &+ Da_{rm}\int_0^t c_1(x,si,\gamma)\int_0^{t-\gamma} e^{-a-b_1-p-q_1-r_1}\sqrt{\frac{b_1 p}{a q_1}}\, I_1(2\sqrt{ab_1}) \\ &\times I_1(2\sqrt{pq_1})d\mu d\gamma, \end{aligned} \tag{3.30}$$

$$f_7(x,si,t) = \int_0^t c_1(x,si,\gamma)\int_0^{t-\gamma} e^{-a-b_1-p-q_1-r_1} I_0(2\sqrt{ab_1}) I_0(2\sqrt{pq_1})d\mu d\gamma, \tag{3.31}$$

The analytical solution for the stream sediment bed is also obtained by substituting Eq. (3.20) into Eq. (3.18) and applying inverse Laplace transform as,

$$
\begin{aligned}
c_{sed}(x,t) &= c_{sedinit}(x)e^{-Da_{rm}t} + Da_{rm}k_d\int_0^t c_u(\eta)f_8(x,t-\eta)d\eta \\
&+ \int_0^{+\infty}\Bigg[Da_{rm}k_d c_{minit}(x^{'})(f_9(x-x^{'},-1,t) - e^{Pe_m x}f_9(x+x^{'},+1,t)) \\
&+ k_d\Bigg\{\frac{Da_{em}Da_{rm}}{k_r}c_{sinit}(x^{'})(f_7(x-x^{'},-1,t) - e^{Pe_m x}f_7(x+x^{'},+1,t)) \\
&+ \rho Da_{rm}c_{sedinit}(x^{'})(f_{10}(x-x^{'},-1,t) - e^{Pe_m x}f_{10}(x+x^{'},+1,t)) \\
&+ \int_0^t\{q_L c_L(x^{'},\eta)(f_9(x-x^{'},-1,t-\eta) - e^{Pe_m x}f_9(x+x^{'},+1,t-\eta)) \\
&+ \frac{Da_{em}Da_{rs}}{k_r}\hat{c}_s(x^{'},\eta)(f_7(x-x^{'},-1,t-\eta) - e^{Pe_m x}f_7(x+x^{'},+1,t-\eta))\} \\
&\times d\eta\Bigg\}\Bigg]dx^{'}, \qquad (3.32)
\end{aligned}
$$

where

$$
\begin{aligned}
f_8(x,t) &= \int_0^t c_0(x,\gamma)e^{-a-p-q}\, I_0(2\sqrt{pq})d\gamma \\
&+ \frac{Da_{em}}{k_r}\int_0^t c_0(x,\gamma)\int_0^{t-\gamma} e^{-a-b_1-p-q_1-r_1}\sqrt{\frac{a}{b_1}}I_1(2\sqrt{ab_1}) \\
&\times I_0(2\sqrt{pq_1})d\mu d\gamma, \qquad (3.33)
\end{aligned}
$$

$$
\begin{aligned}
f_9(x,si,,t) &= \int_0^t c_1(x,si,\gamma)e^{-a-p-q}\, I_0(2\sqrt{pq})d\gamma \\
&+ \frac{Da_{em}}{k_r}\int_0^t c_1(x,si,\gamma)\int_0^{t-\gamma} e^{-a-b_1-p-q_1-r_1}\sqrt{\frac{a}{b_1}}\, I_1(2\sqrt{ab_1}) \\
&\times I_0(2\sqrt{pq_1})d\mu d\gamma, \qquad (3.34)
\end{aligned}
$$

$$
\begin{aligned}
f_{10}(x,si,,t) &= \int_0^t c_1(x,si,\gamma)e^{-a-p-q}\sqrt{\frac{q}{p}}\, I_1(2\sqrt{pq})d\gamma \\
&+ \frac{Da_{em}}{k_r}\int_0^t c_1(x,si,\gamma)\int_0^{t-\gamma} e^{-a-b_1-p-q_1-r_1}\sqrt{\frac{aq_1}{b_1 p}}\, I_1(2\sqrt{ab_1}) \\
&\times I_1(2\sqrt{pq_1})d\mu d\gamma, \qquad (3.35)
\end{aligned}
$$

It is verified that Eqs. (3.21), (3.28) and (3.32) satisfy the initial-boundary problem (3.9)-(3.16). This assures the analytical expressions given in Eqs. (3.21), (3.28) and (3.32) are the exact analytical solutions of the RSTM [i.e. Eqs. (3.9)-(3.11)].

M	x	$Q_0^\star$	Pe_m	Da_{em}	k_r	Da_{dm}	Da_{ds}	Da_{rm}	Da_{rs}	k_d	ρ
500	2000	20	4×10^{-2}	5×10^{-4}	0.25	10^{-4}	10^{-3}	5×10^{-3}	10^{-3}	9×10^{-5}	750

Table 3.1: *Parameter values for the analysis of results of reactive solute.*

3.4 Results and Discussion

Effects of decay Damköhler numbers, reaction Damköhler numbers and lateral inflow rate, are studied through a hypothetical situation. A sensitivity analysis is presented in order to obtain the critical parameters. $u_m^\star$ is calculated in similar way as described in the section 2.2.4.

3.4.1 Hypothetical Experiment

In order to discuss the effects of decay Damköhler numbers (Da_{dm}, Da_{ds}), reaction Damköhler numbers (Da_{rm}, Da_{rs}) and lateral inflow rate (q_L), a hypothetical situation is considered based on the parameters values given in Table 3.1.

An instantaneous injection ($\frac{M^\star}{Q_0^\star}\delta(t^\star)$) serves as the upstream boundary at the injection location, so the upstream boundary condition in the dimensionless form will be (shown in Fig. 3.2),

$$c_m(x_0 = 0, t) = c_u(t) = M\delta(t). \tag{3.36}$$

where $M\left(= \frac{M^\star u_m^\star}{Q_0^\star l^\star c_0^\star}\right)$ is the dimensionless mass, $M^\star$ is the injected mass and $Q_0^\star$ is the volumetric flow rate at the injection location.

The analytical solutions for the main channel, the storage zone and the stream sediment bed are obtained from the Eqs. (3.21), (3.28) and (3.32) respectively (assuming initial concentrations, lateral inflow concentration and equilibrium solute concentration are zero), using the upstream boundary condition given in Eq. (3.36), as

$$c_m(x,t) = Mf_1(x,t), \tag{3.37}$$

$$c_s(x,t) = \frac{MDa_{em}}{k_r} f_5(x,t), \tag{3.38}$$

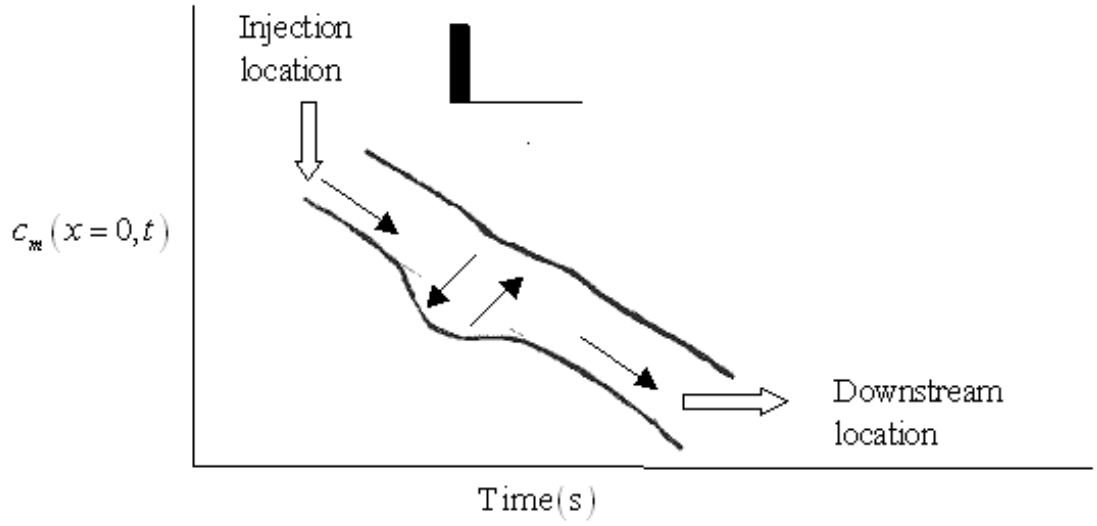

Figure 3.2: *Schematic diagram of the solution domain with an instantaneous injection of solute as upstream boundary condition.*

and

$$c_{sed}(x,t) = MDa_{rm}k_d f_8(x,t), \tag{3.39}$$

where f_1, f_5, f_8 are given by Eqs. (3.22), (3.29) and (3.33) respectively. The analytical expressions given in Eqs. (3.37)-(3.39) are evaluated in the similar way as described in the previous chapter.

The solute concentration profiles for the main channel, the storage zone and the stream sediment bed are calculated at 2000 unit downstream from the injection location $x_0 = 0$ using the time step $\Delta t = 2$ unit.

RSTM without sorption and lateral inflow

Effects of decay Damköhler numbers

In order to study the effects of decay Damköhler numbers, solutions of the RSTM are considered on assuming the parameters related to reaction Damköhler number and lateral inflow are zero. The resulting concentration-time curves are shown in Fig. 3.3. In all these figures, three situations (1. decay in main channel, 2. decay in storage

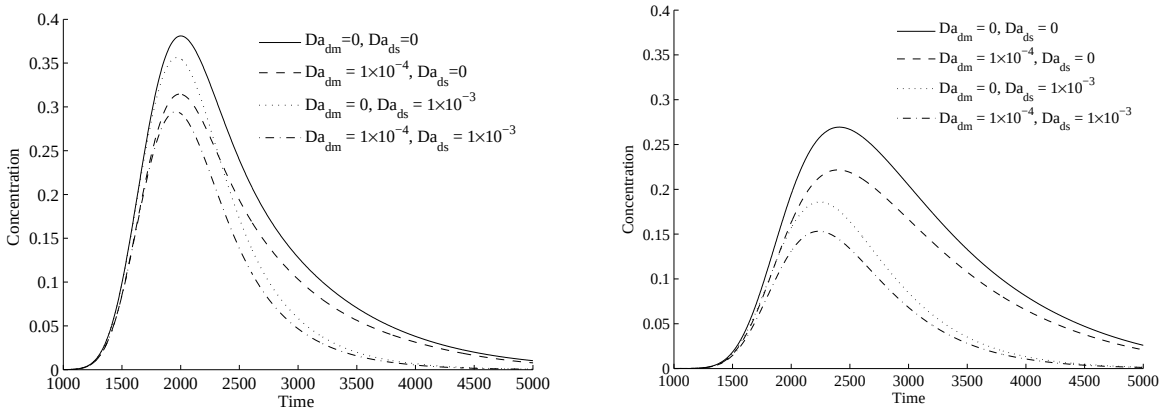

(a) *Main channel solute concentration* (b) *Storage zone solute concentration*

Figure 3.3: *Effects of decay Damköhler numbers on the concentration-time profiles of the analytical solution given by* (a) *Eq.* (3.37) (b) *Eq.* (3.38)*, at* 2000 *unit downstream from the injection location.*

zone and 3. decay in both the zones) are discussed and they are compared with the no decay case.

Fig. 3.3(a) shows the effects of the decay Damköhler numbers on main channel solute concentration. From the graph it is clear that the solute concentration decreases due to the presence of decay effects in both the zones. When decay takes place only in the main channel ($Da_{dm} = 10^{-4}, Da_{ds} = 0$), the reduction in concentration value is more compared to the case of decay taking place only in the storage zone ($Da_{dm} = 0, Da_{ds} = 10^{-3}$) but as time elapses the situation becomes slowly reverse which can be seen from the figure. If decay takes place in the storage zone only, the return of solute from the storage zone is very less and this could be the reason that main channel concentration is less affected compared to the case when decay takes place in the main channel only. However, maximum reduction is noticed when decay takes place in both the zones.

Fig. 3.3(b) shows the effects of decay Damköhler numbers on the storage zone concentration-time curves. The effects are slightly different from the previous case (Fig. 3.3 (a)). Reduction in storage zone solute concentration value is more when

decay takes place in the storage zone instead of in the main channel and this is true for all time.

RSTM without decay

In the case of RSTM without decay, the effects of background concentrations can be realized by simply adding the background concentration to the results of Eqs. (3.37)-(3.39). The background concentration is taken to be 5 unit in the present study. Bencala [3] estimated the parameters of the model by taking the equilibrium solute concentration in the storage zone is equal to the stream's background concentration. In the present situation we also follow the similar consideration for the equilibrium solute concentration in the storage zone. Its value is taken as 5 unit.

Effects of reaction Damköhler numbers

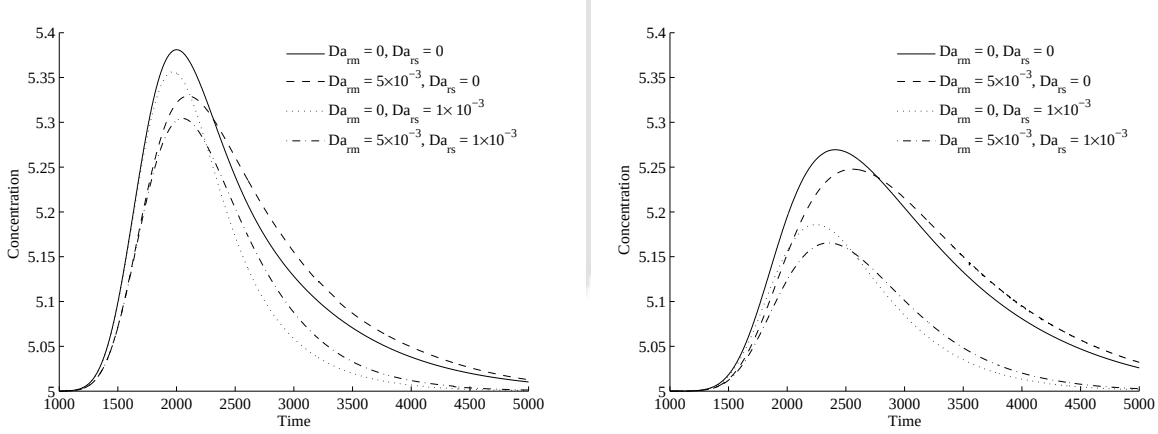

(a) *main channel solute concentration* (b) *storage zone solute concentration*

Figure 3.4: *Effects of reaction Damköhler numbers on the concentration-time profiles of the analytical solution given by* (a) *Eq.* (3.37) (b) *Eq.* (3.38) *at* 2000 *unit downstream from the injection location.*

In order to discuss the effects of reaction Damköhler numbers (Da_{rm}, Da_{rs}), the effects of decay and lateral inflow are not considered in the solutions of the RSTM given by Eqs. (3.37)-(3.39). The solute concentrations in the main channel, in the storage zone and in the stream sediment bed are calculated. The resulting concentration-time

curves based on the analytical solutions of the above situation are presented in Figs. 3.4 and 3.5. When the solute mass is injected in the main channel of the stream, a portion of solute mass goes into the storage zone due to exchange between the main channel and storage zone and some amount goes into the stream sediment bed due to adsorption. As solute mass moves along the longitudinal direction of the channel, some amount of solute mass returns into the main channel of the stream with time due to desorption from the stream bed. Consequently, the resulting concentration-time curve gradually shifts to the right and the peak concentration become less compared to the solute concentration profile for the case of no reaction. This indicates that the solute moves faster when reaction does not take place compared to the case with reaction. If the reaction Damköhler number in the main channel (Da_{rm}) is zero (i.e. the stream bed is absent), the solute mass does not return to the main channel from the sediment bed and the storage zone reaction Damköhler number acts as a sink. As a result, the difference between the two solute concentration profiles (without and with reaction Damköhler number in the storage zone) increases. This can be clearly observed from the Fig. 3.4. If we choose the value of Da_{rs} as 53 (as given in Bencala [3], Scott et al. sco03), the effects of Da_{rs} is found to be negligible on the analytical concentration-time curve. Similar observations of Da_{rs} are noticed by Scott et al. [35] for the observed concentrations. The value of Da_{rs} used in the present hypothetical situation agree well with the estimated value in the work of Jonsson et al. [23] for Chromium solute. Due to increase in the value of Da_{rm}, the kinetic transfer of solute between the main channel and its sediment bed increases. As a result, more solute particles enter into the sediment bed due to adsorption. Consequently, the solute concentrations in the stream sediment bed are increased at downstream locations (which can be seen from Fig. 3.5). It is observed that the concentration-time curves show similar effects of Da_{rs} in the main channel and its sediment bed.

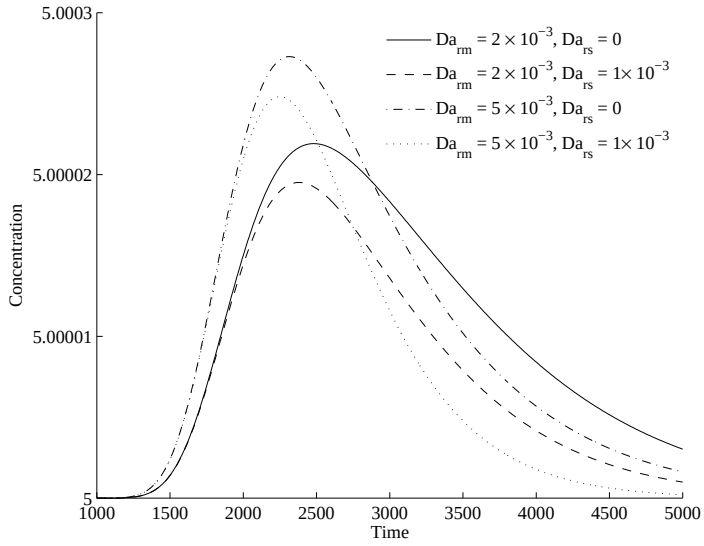

Figure 3.5: *Effects of reaction Damköhler numbers on the concentration-time profiles of the analytical solution given by Eq.* (3.39) *at* 2000 *unit downstream from the injection location for the stream sediment bed .*

Effects of lateral inflow

The effects of lateral inflow rate can be studied through the results of Eq. (3.37) without taking the decay term into consideration. The concentration profiles of the main channel are presented in Fig. 3.6. With the increase in the lateral inflow rate, the solute mass decreases. This can be seen from Fig. 3.6. It is observed that the breakthrough curves show the similar effects in the storage area also. However, the maximum reduction in the solute mass occurs when sorption takes place in both the zones and the lateral inflow is present in the main channel (the innermost curve in the Fig. 3.6 represents this case).

Sensitivity Analysis

A sensitivity analysis is performed for the parameters: decay Damköhler number in the main channel (Da_{dm}), decay Damköhler number in the storage zone (Da_{ds}), reaction Damköhler number in the main channel (Da_{rm}) and reaction Damköhler number

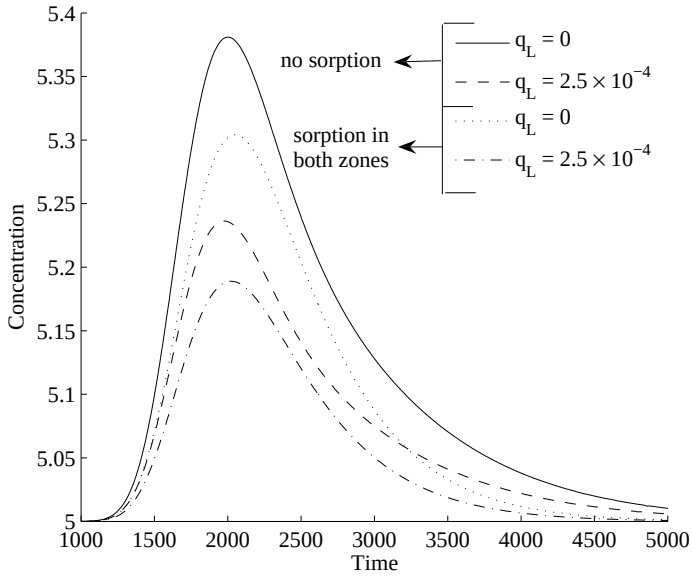

Figure 3.6: *Effects of lateral inflow in the main channel solute concentration profiles at* 2000 *unit downstream from the injection location through the analytical solution presented in Eq.* (3.37).

p_j	dc_{min}	dc_{max}	$dc_{max} - dc_{min}$
Da_{dm}	-456.41	0.0	456.41
Da_{ds}	-41.69	0.0	41.69

Table 3.2: *RSTM without sorption and lateral inflow: minimum (dc_{min}) and maximum (dc_{max}) values of sensitivity of solute concentration in the main channel to the parameter p_j respectively.*

in the storage zone (Da_{rs}). Results for the sensitivities of the solute concentration to different parameters are presented in the forms of Tables 3.2-3.3 and Figs. 3.7-3.8. In the case of RSTM without sorption and lateral inflow, it is observed that decay Damköhler number in the main channel (Da_{dm}) is approximately 10 times more sensitive compared to that in the storage zone (Da_{ds}), and the reaction Damköhler number in the storage zone (Da_{rs}) is approximately 4.5 times more sensitive compared to that in the main channel (Da_{rm}) in the case of RSTM without decay and lateral inflow.

p_j	dc_{min}	dc_{max}	$dc_{max} - dc_{min}$
Da_{rm}	-5.44	4.87	10.32
Da_{rs}	-46.61	0.0	46.61

Table 3.3: *RSTM without decay: minimum (dc_{min}) and maximum (dc_{max}) values of sensitivity of solute concentration in the main channel to the parameter p_j respectively.*

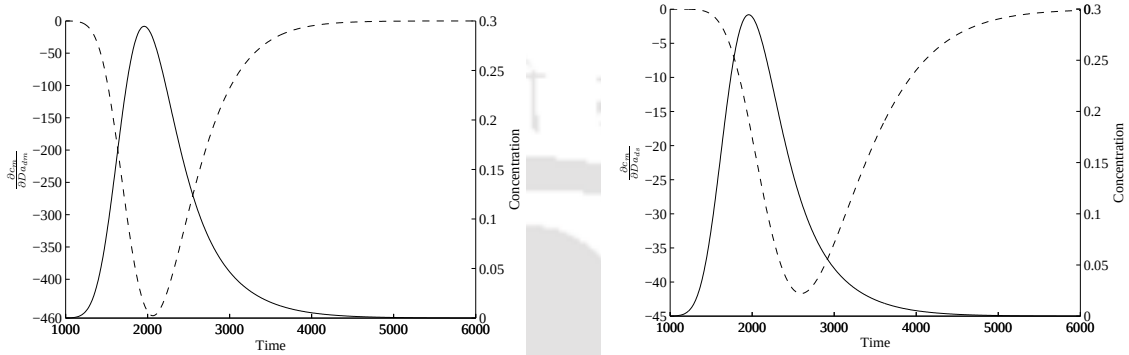

(a) *sensitivity (dashed line) to decay Damköhler number in main channel*

(b) *sensitivity (dashed line) to decay Damköhler number in the storage zone*

Figure 3.7: *Sensitivity of decay Damköhler numbers on the concentration-time curve (solid line) calculated with the analytical solution given by Eq.* (3.37) *at* 2000 *unit downstream from the injection location.*

3.5 Conclusions

In this chapter, analytical solutions are presented for reactive solutes in streams with the lateral inflow and the transient storage and for a general situation in which initial concentrations are the functions of space and lateral inflow concentration and the storage zone equilibrium concentration are the functions of space and time. In order to discuss results, instantaneous release of solute and a hypothetical situation are considered. A sensitivity analysis is presented in order to identify the critical parameters. Effects of background concentration can be observed through the solutions for the case of RSTM without decay, by simply adding the background concentration.

The peak values of the breakthrough curves decrease due to the effects of decay Damköhler numbers. Delaying of the solute concentrations due to the reaction

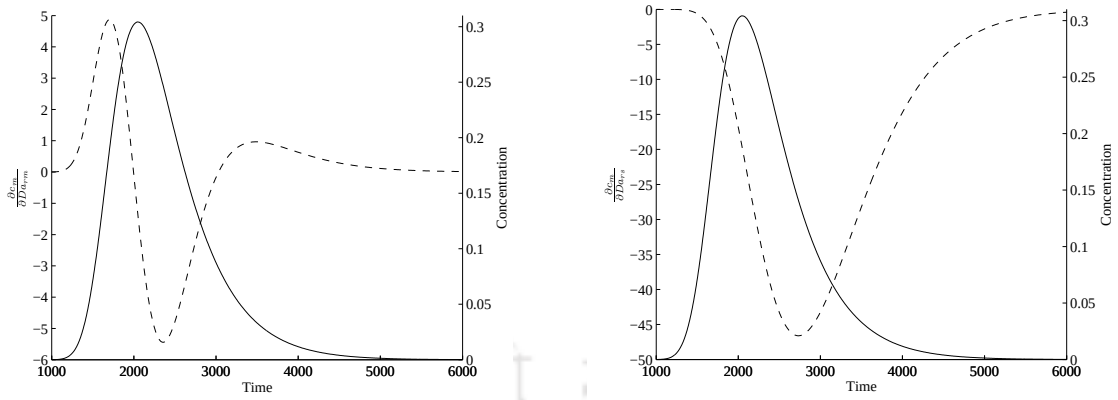

(a) *sensitivity (dashed line) to the reaction Damköhler number in the main channel*

(b) *sensitivity (dashed line) to the reaction Damköhler number in the storage zone*

Figure 3.8: *Sensitivity of reaction Damköhler numbers on the concentration-time curve (solid line) calculated with the analytical solution given by Eq.* (3.37) *at* 2000 *unit downstream from the injection location.*

Damköhler number in the main channel is also noticed by our analytical solutions. The dilution of solute concentration takes place when the effect of lateral inflow is included. Present analytical solutions clearly reveal the effects of decay, reaction and lateral inflow. Sensitivity analysis shows that the decay Damköhler number in the main channel is more sensitive compared to that in the storage zone in the case of RSTM without sorption and lateral inflow, whereas in the case of RSTM without decay and lateral inflow, reaction Damköhler number in the storage zone is more sensitive compared to that in the main channel. It can be concluded that our analytical solutions for reactive solute transport in streams can be reliably applied for the analysis of tracer experiments and transport characteristics in streams with mass exchange in transient storage. The analytical solutions can also be used for the verification of more complex models.

Chapter 4

Analytical solution and analysis for conservative solute transport in streams with diffusive transfer in the hyporheic zone

This chapter deals with the derivation of analytical solutions for the solute transport in a stream in the presence of hyporheic zone where exchange of solute between the main channel and the hyporheic zone is dominated by the diffusive exchange. In this study we follow the model proposed by Jonsson et al. [23], for conservative solute, which is based on mass balance approach.

4.1 Introduction

Several modelling approaches are developed to describe the solute transport in streams with hyporheic zone. The most commonly used solute transport model is the transient storage model (TSM) (e.g. Bencala and Walters [2], Harvey et al. [18], Hays et al. [19], Runkel [29], Wagner and Harvey [39], Wörman [40]). The model described in chapters 2 and 3 is based on the idea of first order mass exchange between the main channel and the stagnant zone whereas in the present chapter the exchange of mass between the main channel and the hyporheic zone is considered to be diffusive exchange. The Diffusive transfer model for conservative solute was introduced by

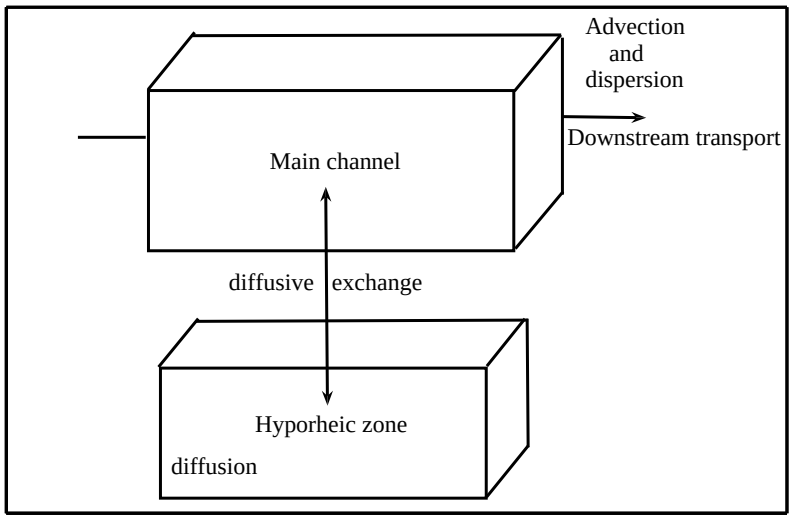

Figure 4.1: *Conceptual model describe the stream and hyporheic zone hydrologic process for conservative solute.*

Jackman et al. [21]. Like the model of Bencala and Walters [2], Jackman et al. [21] also considered two distinct zones to describe the diffusive transfer model. The first zone represents the main flow region, where advection and dispersion processes take place. The second one represents the hyporheic zone area, where only diffusion takes place. Both the zones are linked by the diffusive exchange process between them (which can be seen from Fig. 4.1).

The model described by Jackman et al. [21] is based on the classical advection-dispersion equations with the exchange of mass due to the lateral diffusive transfer of solutes. Jackman et al. [21] found that the diffusion model is more complex compared to the TSM but the diffusion model predicts the concentration profiles better than the TSM. Maloszewski and Zuber [26] have presented similar transport equations as described by Jackman et al. [21] but they considered the chemical transport in a single fissure in a porous matrix. Maloszewski and Zuber [26] presented

analytical solutions of the transport equations considering instantaneous injection as the upstream boundary condition. In 1998, Wörman [40] found an analytical solution of the diffusive transfer model without considering the effects of dispersion. In 2000, he compared the diffusive transfer model with the TSM and water infiltration model. Wörman [42] found that these three models yield similar representations of the first three temporal moments due to instantaneous input at the upstream boundary. De Smedt [13] considered the dispersion in the main channel to extend the work of Wörman [40]. De Smedt [13] presented an analytical solution of the model in the case of instantaneous injection of conservative solute for constant and uniform flow. Jonsson and his group (2001; 2003) described the diffusive transfer model for conservative as well as for reactive solute. However, the analytical solutions, available in the literature, of this model are restricted to the instantaneous injection of a solute only.

The purpose of the present study is to derive analytical solutions of the model described by Jonsson et al. [23], for the continuous injection of a conservative solute. The solutions are derived for a very general situation, in which the initial concentrations are not constant. The present analytical results for the main channel are compared with the observed data of the Uvas Creek tracer experiment for chloride concentration. A hypothetical situation is considered to study the effects of dilution factor, Péclet number and porosity in the hyporheic zone on the breakthrough curves. Step concentration-time profile is considered as upstream boundary condition.

4.2 Governing equations

The present problem describes the solute transport in streams with hyporheic zone due to diffusive transfer between the two zones. In this study, we derive the analytical solutions of the model proposed by Jonsson and his group [22, 23] for conservative solutes. The model is mainly based on the mass balance approach. The following

assumptions are also considered in order to obtain analytical solutions.

4.2.1 Assumptions for the model

1. The medium is isotropic and homogeneous in both the zones.

2. Advection and dispersion processes are affecting the solute concentration in the main channel.

3. Advection don't occur in the hyporheic zone and only diffusion affects the solute concentration in this zone.

4. Solute concentration in stream water can vary only in the longitudinal direction while the solute concentration in the hyporheic zone can vary in the longitudinal as well as in the lateral direction.

5. Exchange of solute between the main channel and the hyporheic zone is represented by a diffusive exchange term. It is assumed that only the diffusive exchange is occurred between the main channel and the hyporheic zone and is driven by the concentration gradient at the interface of the stream water and the hyporheic zone [21].

6. All parameters are assumed to be constant except the volumetric flow rate ($Q_x^\star$), which varies exponentially along the downstream between the injection location and the downstream sampling location.

7. Porosity in the hyporheic zone is assumed to be independent of depth.

8. There is no sorption in both the zones.

The governing equations based on the above assumptions can be written following Jonsson [23] as:

$$\frac{\partial c_m^\star}{\partial t^\star} + \frac{1}{A_m^\star(1+k_r)}\left(c_m^\star \frac{\partial Q_x^\star}{\partial x^\star} + Q_x^\star \frac{\partial c_m^\star}{\partial x^\star}\right) = \frac{D_m^\star}{1+k_r}\frac{\partial^2 c_m^\star}{\partial x^{\star 2}} + \frac{D_h^\star \epsilon}{A_m^\star}\frac{\partial c_h^\star/\epsilon}{\partial z^\star}\Big|_{z^\star=0}, \tag{4.1}$$

$$\frac{\partial c_h^\star}{\partial t^\star} = D_h^\star \frac{\partial^2 c_h^\star}{\partial z^{\star 2}}, \tag{4.2}$$

where, $c_m^\star$ is the solute concentration in the main channel of stream, $c_h^\star$ is the solute concentration in the hyporheic zone, $A_m^\star$ is the cross-sectional area of the main channel, $Q_x^\star$ is the in-stream volumetric flow rate, $u_m^\star$ is the cross-sectional average velocity in the main channel, $x^\star$ is the longitudinal distance, $t^\star$ is time, $z^\star$ is the lateral co-ordinate, $D_m^\star$ is the dispersion coefficient in the main channel, $D_h^\star$ exchange diffusion coefficient in the hyporheic zone, ϵ is the porosity in the hyporheic zone (-), k_r is the ratio of the cross-sectional area of the hyporheic zone and the cross-sectional area of the main channel (-), $P^\star$ is the wetted perimeter of the main channel and $R_h^\star (= \frac{A_m^\star}{P^\star})$ is the hyraulic radius.

Eq. (4.1) is obtained by linking the one-dimensional classical advection-dispersion equation with a diffusive exchange between the main channel of the stream and the hyporheic zone. Eq. (4.2) represents the one dimensional diffusion equation for the hyporheic zone.

4.2.2 General boundary and initial conditions

The upstream boundary condition due to the continuous injection of solutes in the main channel is given by

$$c_m^\star(x^\star = x_0^\star, t^\star) = c_u^\star(t^\star), \tag{4.3}$$

where $x_0^\star$ is the upstream boundary location, $c_u^\star(t^\star)$ is the solute concentration in the main channel of stream at $x_0^\star$ at time $t^\star$. It is also assumed that Laplace transform of $c_u^\star(t^\star)$ exists and is bounded.

The other boundary condition at the downstream location is given as,

$$c_m^\star(x^\star \to \infty, t^\star) = 0 \text{ for all } t^\star, \tag{4.4}$$

Apart from this, the concentrations in the main channel and in the hyporheic zone are equal at the interface,

$$c_h^\star(x^\star, z^\star = 0, t^\star) = \epsilon\, c_m^\star(x^\star, t^\star), \tag{4.5}$$

and the other boundary condition in the hyporheic zone is taken as,

$$c_h^\star(x^\star, z^\star \to \infty, t^\star) = 0 \text{ for } t^\star > 0, \tag{4.6}$$

The initial conditions in the main channel and in the hyporheic zone are

$$c_m^\star(x^\star, t^\star = 0) = c_{minit}^\star(x^\star), \tag{4.7}$$

$$c_h^\star(x^\star, z^\star, t^\star = 0) = c_{hinit}^\star(x^\star, z^\star). \tag{4.8}$$

where $c_{minit}^\star(x^\star)$ and $c_{hinit}^\star(x^\star, z^\star)$ are initial concentrations in the main channel and in the hyporheic zone respectively.

4.2.3 Dimensionless forms of governing equations, general boundary and initial conditions

The dimensionless forms of the governing equations, boundary and initial conditions (4.1)-(4.8) are given as

$$\frac{\partial c_m}{\partial t} + \frac{\phi}{(1+k_r)} c_m + \frac{1}{(1+k_r)} \frac{\partial c_m}{\partial x} = \frac{1}{Pe_m(1+k_r)} \frac{\partial^2 c_m}{\partial x^2} + \frac{\epsilon}{R_h Pe_h} \frac{\partial (c_h/\epsilon)}{\partial z}\bigg|_{z=0}, \tag{4.9}$$

$$\frac{\partial c_h}{\partial t} = \frac{1}{Pe_h} \frac{\partial^2 c_h}{\partial z^2}, \tag{4.10}$$

$$c_m(x_0, t) = c_u(t), \tag{4.11}$$

$$c_m(x \to \infty, t) = 0 \text{ for all } t, \tag{4.12}$$

$$c_h(x, z = 0, t) = \epsilon\ c_m(x, t), \tag{4.13}$$

$$c_h(x, z \to \infty, t) = 0 \text{ for } t > 0, \tag{4.14}$$

$$c_m(x, t = 0) = c_{minit}(x), \tag{4.15}$$

$$c_h(x, z, t = 0) = c_{hinit}(x, z) \tag{4.16}$$

where $x \left(= \frac{x^\star}{l^\star}\right)$ is distance in the longitudinal direction, $l^\star (\approx \sqrt{2.5 A_m^\star})$ is the characteristic length, $t \left(= \frac{u_m^\star t^\star}{l^\star}\right)$ is time, $u_m^\star (= \frac{Q_1^\star}{A_m^\star})$ is a constant quantity, $Q_1^\star$ is the volumetric flow rate at the sampling location, $c_m \left(= \frac{c_m^\star}{c_0^\star}\right)$ is concentration in the main channel of the stream, $c_0^\star$ is the plateau concentration at the head of the tracer experiment, $c_h \left(= \frac{c_{h_d}^\star}{c_0^\star}\right)$ is concentration in the hyporheic zone, $c_{minit}(x) \left(= \frac{c_{minit}^\star(x^\star)}{c_0^\star}\right)$ is initial concentration in the main channel, $c_{hinit}(x, z) \left(= \frac{c_{hinit}^\star(x^\star, z^\star)}{c_0^\star}\right)$ is initial concentration in the hyporheic zone, $c_u(t) \left(= \frac{c_u^\star(t)}{c_0^\star}\right)$ is upstream concentration, $Pe_m \left(= \frac{u_m^\star l^\star}{D_m^\star}\right)$ is Péclet number in the main channel, $Pe_h \left(= \frac{u_m^\star l^\star}{D_h^\star}\right)$ is Péclet number in the hyporheic zone, $\phi \left(= \frac{l^\star}{u_m^\star A_m^\star} \frac{dQ_x^\star}{dx^\star}\right)$ is the dilution factor and $R_h \left(= \frac{R_h^\star}{l^\star}\right)$ is the hyraulic radius.

It is easy to see that Eq. (4.9), in the absence of dilution factor, becomes the classical advection-dispersion equation when $Pe_h \to \infty$ (i.e. the tracer particles do not enter into the hyporheic zone).

4.3 Analytical solution for diffusive transfer of conservative solutes with hyporheic zone

The analytical solutions of (4.9)-(4.16) are obtained by using Laplace transform.

By using the initial conditions (4.16) in the transformed form of Eq. (4.10), we obtain

$$\frac{1}{Pe_h}\frac{d^2\overline{c}_h}{dz^2} - s\overline{c}_h = -c_{hinit}(x,z), \tag{4.17}$$

Applying the boundary conditions (4.13) and (4.14) in the solution of Eq. (4.17), we obtain

$$\begin{aligned}\overline{c}_h(x,z,s) &= e^{-z\sqrt{Pe_h s}}\left[\epsilon\overline{c}_m + \frac{\sqrt{Pe_h}}{2\sqrt{s}}\left\{\int_0^{+\infty} -c_{hinit}(x,z^{'})e^{-z^{'}\sqrt{Pe_h s}}dz^{'}\right.\right.\\ &+ \left.\left.\int_0^{z} c_{hinit}(x,z^{'})e^{z^{'}\sqrt{Pe_h s}}dz^{'}\right\}\right] + \frac{\sqrt{Pe_h}\ e^{z\sqrt{Pe_h s}}}{2\sqrt{s}}\int_z^{+\infty} c_{hinit}(x,z^{'})\\ &\times\ e^{-z^{'}\sqrt{Pe_h s}}dz^{'},\end{aligned} \tag{4.18}$$

where $\overline{c}_m$ and $\overline{c}_h$ are Laplace transforms of c_m and c_h respectively.

Applying Laplace transform to Eq. (4.9) and using Eqs. (4.15) and (4.18), we obtain a linear nonhomogeneous differential equation as,

$$\begin{aligned}\frac{1}{Pe_m(1+k_r)}\frac{d^2\overline{c}_m}{dx^2} - \frac{1}{1+k_r}\frac{d\overline{c}_m}{dx} &- \left(s + \frac{\phi}{1+k_r} + a_1\sqrt{s}\right)\overline{c}_m = -c_{minit}(x)\\ &- \frac{1}{R_h}\int_0^{+\infty} c_{hinit}(x,z^{'})e^{-z^{'}\sqrt{Pe_h s}}dz^{'},\end{aligned} \tag{4.19}$$

where $a_1 = \frac{\epsilon}{R_h\sqrt{Pe_h}}$.

Using the boundary conditions (4.11) and (4.12) in the solution of Eq. (4.19), we obtain

$$
\begin{aligned}
\bar{c}_m(x,s) &= \bar{c}_u(s)e^{m_1 x} \\
&- \frac{Pe_m(1+k_r)}{(m_2-m_1)}e^{m_1 x}\int_0^{+\infty}\left[c_{minit}(x^{'})+\int_0^{+\infty}\frac{c_{hinit}(x^{'},z^{'})}{R_h}e^{-z^{'}\sqrt{Pe_h s}}dz^{'}\right]e^{-m_2 x^{'}}dx^{'} \\
&+ \frac{Pe_m(1+k_r)}{(m_2-m_1)}e^{m_1 x}\int_0^{x}\left[c_{minit}(x^{'})+\int_0^{+\infty}\frac{c_{hinit}(x^{'},z^{'})}{R_h}e^{-z^{'}\sqrt{Pe_h s}}dz^{'}\right]e^{-m_1 x^{'}}dx^{'} \\
&+ \frac{Pe_m(1+k_r)}{(m_2-m_1)}e^{m_2 x}\int_x^{+\infty}\left[c_{minit}(x^{'})+\int_0^{+\infty}\frac{c_{hinit}(x^{'},z^{'})}{R_h}e^{-z^{'}\sqrt{Pe_h s}}dz^{'}\right]e^{-m_2 x^{'}}dx^{'}
\end{aligned}
\tag{4.20}
$$

where $\bar{c}_u(s)$ is the Laplace transform of $c_u(t)$ and $m_{1,2} = \frac{Pe_m}{2} \mp \sqrt{Pe_m(1+k_r)}\sqrt{\frac{Pe_m}{4(1+k_r)}+A_1}$ and $A_1 = \left(s+\frac{\phi}{1+k_r}+a_1\sqrt{s}\right)$.

With the help of convolution theorem (given in Prudnikov et al. [27], Sneddon [36]), inverse Laplace transform of Eq. (4.20) gives,

$$
\begin{aligned}
c_m(x,t) &= \int_0^t c_u(\eta)f_1(x,t-\eta)d\eta \\
&+ \int_0^{+\infty} c_{minit}(x^{'})\Big(f_2(x-x^{'},-1,t)-e^{Pe_m x}f_2(x+x^{'},+1,t)\Big)dx^{'} \\
&+ \frac{1}{R_h}\int_0^{+\infty}\int_0^{+\infty} c_{hinit}(x^{'},z^{'})\Big(f_3(x-x^{'},-1,t)-e^{Pe_m x}f_3(x+x^{'},+1,t)\Big) \\
&\times\ dz^{'}dx^{'},
\end{aligned}
\tag{4.21}
$$

$$
f_1(x,t) = \int_0^t c_0(x,\gamma)c_1(a_1\gamma,t-\gamma)d\gamma, \tag{4.22}
$$

$$
f_2(x,si,t) = \int_0^t c_2(x,si,\gamma)c_1(a_1\gamma,t-\gamma)d\gamma, \tag{4.23}
$$

$$
f_3(x,si,t) = \int_0^t c_2(x,si,\gamma)c_1(a_1\gamma+z^{'}\sqrt{Pe_h},t-\gamma)d\gamma, \tag{4.24}
$$

where

$$
c_0(x,t) = \frac{x\sqrt{Pe_m(1+k_r)}}{2\sqrt{\pi t^3}}\exp\left(-\frac{Pe_m(x(1+k_r)-t)^2}{4(1+k_r)t}-\frac{\phi t}{1+k_r}\right), \tag{4.25}
$$

$$c_1(a_1\tau_1,\tau_2)=\frac{a_1\tau_1}{2\sqrt{\pi{\tau_2}^3}}\exp\left(-\frac{(a_1\tau_1)^2}{4\tau_2}\right), \tag{4.26}$$

$$c_2(x,si,t)=\frac{\sqrt{Pe_m(1+k_r)}}{2\sqrt{\pi t}}\exp\left(-\frac{Pe_m(x(1+k_r)+si\ t)^2}{4(1+k_r)t}-\frac{\phi t}{1+k_r}\right), \tag{4.27}$$

The analytical solution for the hyporheic zone solute concentration is obtained by substituting Eq. (4.20) into Eq. (4.18) and applying inverse Laplace transform as,

$$\begin{aligned} c_h(x,z,t) &= \epsilon\Bigg[\int_0^t c_u(\eta)f_4(x,t-\eta)d\eta \\ &+ \int_0^{+\infty} c_{minit}(x^{'})\Big(f_5(x-x^{'},-1,t)-e^{Pe_m x}f_5(x+x^{'},+1,t)\Big)dx^{'} \\ &+ \frac{1}{R_h}\int_0^{+\infty}\int_0^{+\infty} c_{hinit}(x^{'},z^{'})\Big(f_6(x-x^{'},-1,t)-e^{Pe_m x}f_6(x+x^{'},+1,t)\Big) \\ &\times dx^{'}dz^{'}\Bigg]+\int_0^{+\infty} c_{hinit}(x,z^{'})(c_3(z+z^{'},t)-c_3(z-z^{'},t))dz^{'}, \end{aligned} \tag{4.28}$$

$$f_4(x,t)=\int_0^t c_0(x,\gamma)c_1(a_1\gamma+z\sqrt{Pe_h},t-\gamma)d\gamma, \tag{4.29}$$

$$f_5(x,si,t)=\int_0^t c_2(x,si,\gamma)c_1(a_1\gamma+z\sqrt{Pe_h},t-\gamma)d\gamma, \tag{4.30}$$

$$f_6(x,si,t)=\int_0^t c_2(x,si,\gamma)c_1(a_1\gamma+(z+z^{'})\sqrt{Pe_h},t-\gamma)d\gamma, \tag{4.31}$$

$$c_3(z,t)=\frac{\sqrt{Pe_h}e^{-\frac{z^2Pe_h}{4t}}}{2\sqrt{\pi t}}, \tag{4.32}$$

It is verified that Eqs. (4.21) and (4.28) are satisfying the initial-boundary problem (4.9)-(4.16). This assures the analytical expressions given in Eqs. (4.21) and (4.28) are the exact analytical solutions of Eqs. (4.9) and (4.10).

$x^\star$	$A_m^\star$	$Q_1^\star$	$D_m^\star$	k_r	$D_h^\star(10^{-5})$	$R_h^\star$	ϵ	$\phi(10^{-4})$	Pe_m
m	m^2	m^3/s	m/s	–	m^2/s	m	–	m	–
38	0.3599	0.0127	0.0183	–	–	–	–	4.888	1.93
105	0.3977	0.0128	0.0918	–	–	–	–	2.5742	0.35
281	0.3189	0.0134	0.0808	0.0539	2.5815	1.4772	0.8213	2.4417	0.52
433	0.3403	0.0135	0.1030	0.0449	2.7146	1.5424	0.8805	1.7508	0.39
619	0.3563	0.0143	0.0985	0.0936	3.8	1.3717	0.8432	2.2109	0.42

Table 4.1: *Estimated values of parameters for the diffusive transfer model for the observed chloride concentrations of the Uvas Creek tracer experiment.*

4.4 Results and Discussion

The present analytical solution, given in Eq. (4.21), is compared with the observed data of the Uvas Creek tracer experiment for conservative solute (chloride) as described in chapter 2. Parameters of the model are estimated for the Uvas Creek tracer experiment by using the large scale algorithm. A sensitivity analysis is performed in order to identify the critical parameters for the present situation. Effects of dilution factor (ϕ), Péclet number in the hyporheic zone (Pe_h) and porosity in the hyporheic zone (ϵ) on solute concentration are studied for a hypothetical situation.

We use $Q_1^\star = Q_0^\star\ e^{\phi x^\star}$ to calculate the cross-sectional average velocity $u_m^\star = Q_1^\star/A_m^\star$, where subscript 0 represents the injection location.

4.4.1 Application to tracer experiment

Uvas Creek tracer experiment for conservative solute (chloride) is used in the present study. The parameters of the present model is estimated using the similar procedure as described in chapter 2 and presented in Table 4.1. Breakthrough solute concentrations are measured at different sampling points (i.e. $x^\star$ = 38, 105, 281, 433 and 619 m respectively). In order to simulate the observed concentration profiles at each downstream locations by the analytical solution given in Eq. (4.21), the solute concentration profile at upstream boundary location ($x_0^\star = 0$) is chosen as a step-concentration profile.

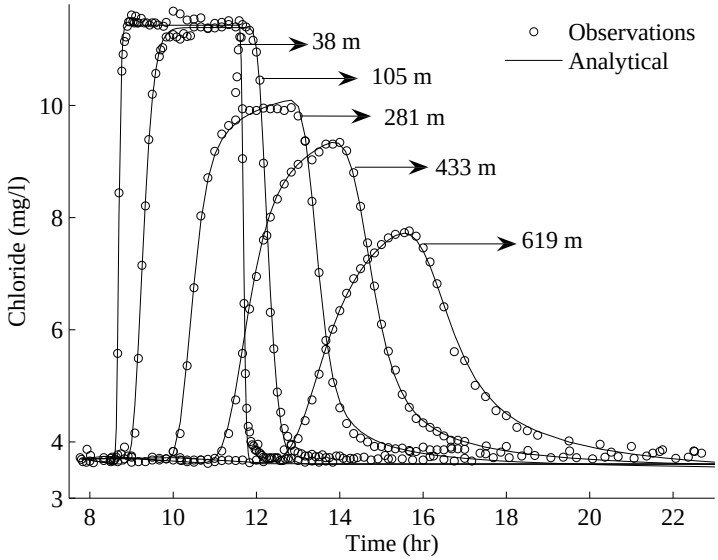

Figure 4.2: *Comparison of concentration profiles of the analytical solution given by Eq.* (4.21) *(solid lines), and observed concentration profiles (open dots) of the Uvas Creek tracer experiment for the diffusive transfer model.*

Table 4.1 shows that the value of volumetric flow rate increases along the longitudinal direction of the stream. Due to increase in the value of volumetric flow rate, solute concentration gets diluted (which can be noticed from Fig. 4.2). The estimated value of the Péclet number in the main channel gradually decreases with slight oscillation along the downstream as given in Table 4.1, which implies that the dispersion of solute dominates over the advection of solute. The diffusive exchange coefficient ($D_h^\star$) increases from the sampling location 281 m to the downstream sampling locations, which indicates that the exchange between the two zones increases along the downstream direction of the stream. This implies that there is more interaction between the main channel and the hyporheic zone. The estimated values of all other parameters (i.e. hydraulic radius, porosity and ratio of cross-sectional areas) are found to be nearly constant along the downstream direction of the stream, which confirm the validity of the assumption of constant parameters values made for the mathematical models. Using the estimated values of parameters, results are

calculated from Eq. (4.21) in the dimensionless form and presented in dimensional form in Fig. 4.2. It shows that the simulated concentration-time curves agree well with the observed concentration-time curves of the Uvas Creek tracer experiment.

Fig. 2.3, which is based on the TSM, shows a good agreement between the analytical and the observed concentration-time curves except at the long tails of the curves obtained at large downstream distances. So, the TSM fails to produce accurate results when comparisons are made with the experimental data obtained at far downstream distances from the injection point (e.g. 619 m) at larger time. On the other hand, Fig.4.2 shows that the diffusive transfer model is free from the above drawbacks of the TSM and produces more accurate results. Also, the diffusive transfer model is computationally more efficient than the TSM.

Sensitivity Analysis

Sensitivity analysis is performed to characterize the sensitivities of the parameters of the diffusive transfer model. Sensitivities of different parameters (i.e. Péclet numbers, (Pe_m, Pe_h); ratio of cross-sectional areas, (k_r) ; hydraulic radius, (R_h) ; porosity, (ϵ)) are calculated at a downstream location 433 m. Results for the sensitivities of the solute concentration to different parameters are presented in Figs. 4.3-4.5 and Table 4.2. From the table and figures, it is clear that the k_r is much more sensitive compared to the Pe_m, Pe_h, R_h and ϵ. It is also noticed that though Pe_m, R_h and ϵ are of the same order of magnitude, Pe_h is the least sensitive parameter.

4.4.2 Hypothetical Experiment

In order to study the effects of dilution factor (ϕ), Péclet number in hyporheic zone (Pe_h) and porosity in the hyporheic zone (ϵ), a hypothetical situation is considered and the values of the parameters are used from the Table 4.3. It is assumed that 25 g/m^3 of conservative solute is injected at the injection location $x_0^\star = 0$ with a constant rate for 5 hours. The initial concentrations in the main channel and in the hyporheic

p_j	dc_{min}	dc_{max}	$dc_{max} - dc_{min}$
Pe_m	-1.48	1.51	2.99
k_r	-15.67	14.61	29.78
Pe_h	-3.62 $\times 10^{-4}$	0.0028	0.0032
ϵ	-3.81	0.76	4.57
R_h	-0.45	2.23	2.68

Table 4.2: *Diffusive transfer model for conservative solute: minimum (dc_{min}) and maximum (dc_{max}) values of sensitivity of solute concentration in the main channel to the parameter p_j respectively.*

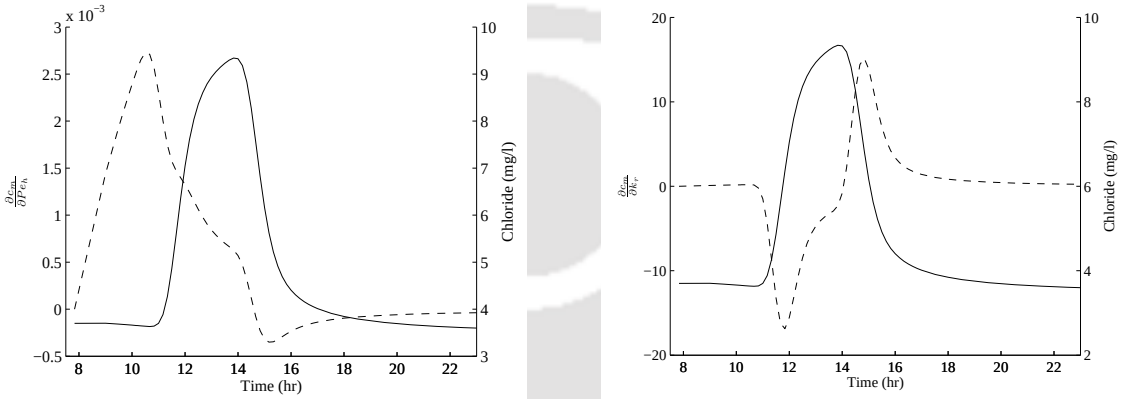

(a) *sensitivity (dashed line) to Péclet number in the hyporheic zone*

(b) *sensitivity (dashed line) to ratio of cross-sectional areas*

Figure 4.3: *Sensitivity of Péclet number in the hyporheic zone and ratio of cross-sectional areas on the concentration-time curve (solid line) calculated with the analytical solution given by Eq.* (4.21) *at* 433 m.

zone are considered to be constant and are assumed to be equal to 5 g/m^3. Results are obtained at a 1000 unit downstream distance from the injection location.

Effects of dilution factor (ϕ)

In order to discuss the effects of dilution factor, the concentration-time curves are presented in Fig. 4.6. The increase in the dilution factor is the main cause of reduction in the solute mass in the main channel at the downstream locations.

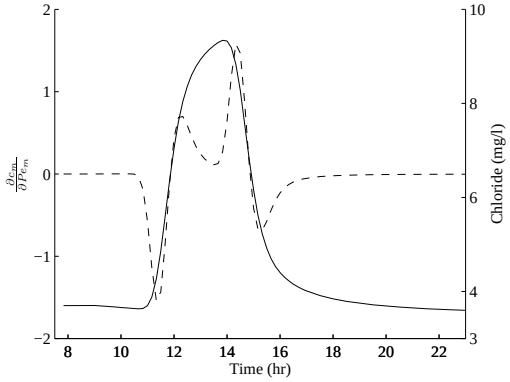

(a) *sensitivity (dashed line) to Péclet number in the main channel*

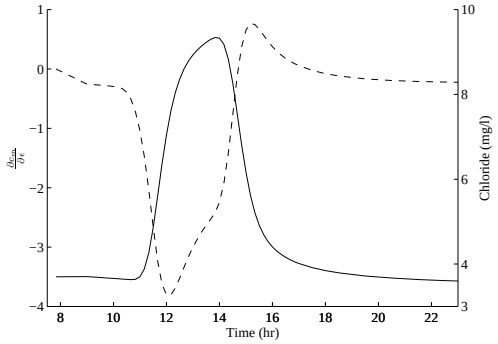

(b) *sensitivity (dashed line) to porosity*

Figure 4.4: *Sensitivity of Péclet number in the main channel and porosity on the concentration-time curve (solid line) calculated with the analytical solution given by Eq.* (4.21) *at* 433 m.

c_{inj}	x	Pe_m	Pe_h	k_r	ϵ	ϕ	R_h
25	1000	0.4773	1.2×10^3	0.112	0.6761	2.2×10^{-4}	1.3341

Table 4.3: *Parameter values for the analysis of results of conservative solute for diffusive transfer model.*

Effects of Péclet number in hyporheic zone (Pe_h)

Results are calculated for at a 1000 unit downstream distance from the injection point for different values of $Pe_h(= 1.6\times10^3,\ 1.2\times10^3$ and $0.7\times10^3)$ and the concentration-time curves are presented in Fig. 4.7. It shows that with the decrease in the value of Pe_h, the concentration-time curve becomes more asymmetric. Fig. 4.7 also depicts that the peak concentration value of the curve decreases and the long tail gradually becomes more prominent with the decrease in the value of Pe_h. The main cause for these effects on the concentration-time curves could be the diffusive exchange between the main channel and the hyporheic zone.

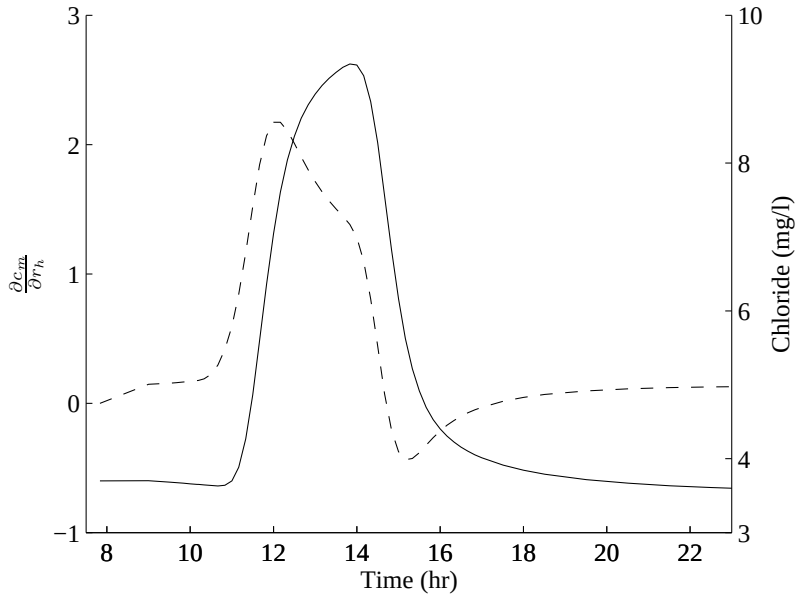

Figure 4.5: *Sensitivity (dashed line) to hyraulic radius on the concentration-time curve (solid line) calculated with the analytical solution given by Eq.* (4.21) *at* 433 m.

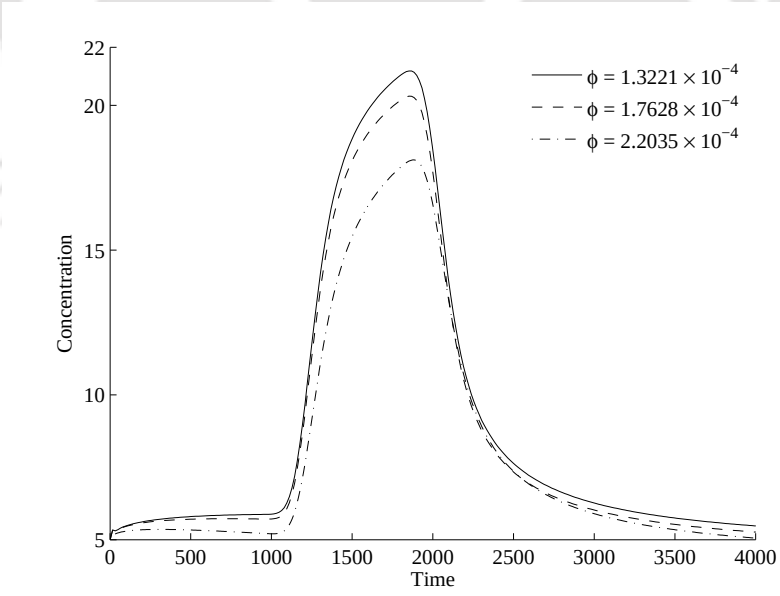

Figure 4.6: *Effects of dilution factor on concentration-time curve at* 1000 *unit downstream from the injection location.*

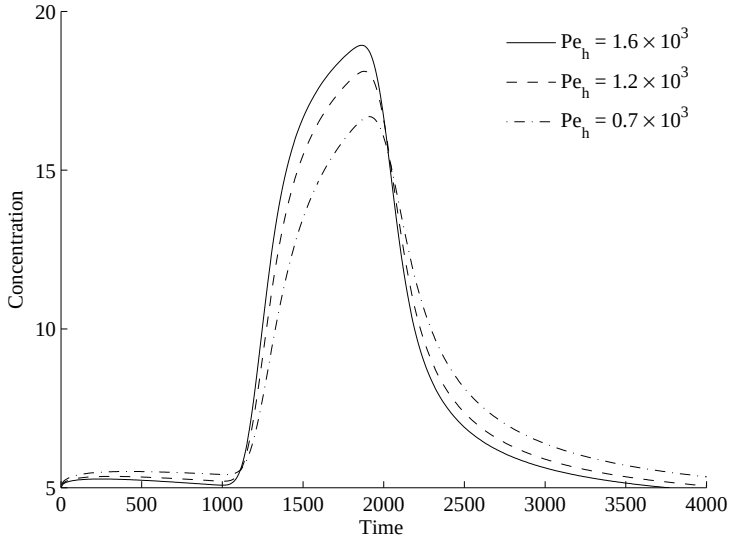

Figure 4.7: *Effects of Péclet number in hyporheic zone on concentration-time curve at* 1000 *unit downstream from the injection location.*

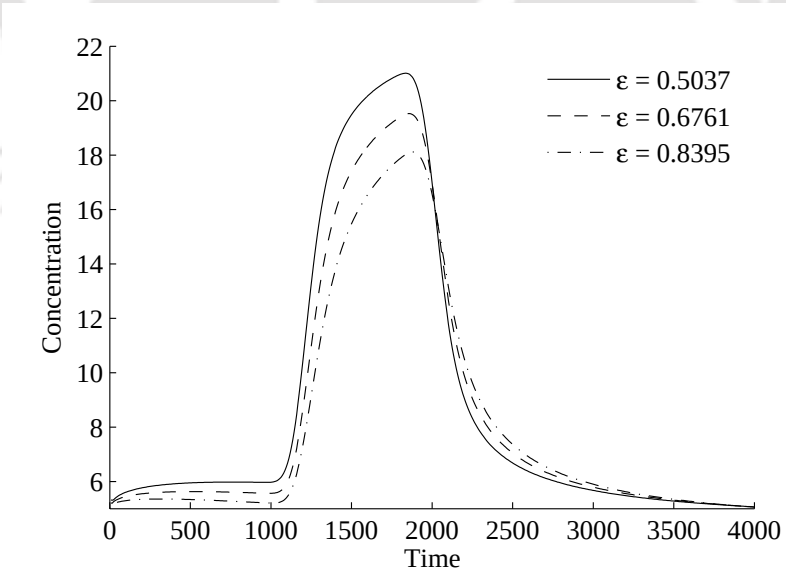

Figure 4.8: *Effects of porosity on concentration-time curve at* 1000 *unit downstream from the injection location.*

Effects of porosity in the hyporheic zone (ϵ)

In order to study the effects of porosity (ϵ) on the concentration-time curves in the main channel of the stream, different values of ϵ are chosen and results are presented in Fig. 4.8. It shows that the peak concentration decreases with the increase in the value of ϵ. It also accounts for the clipping of the shoulders of the leading edges. These effects are mainly because of more solute particles enter into the hyporheic zone but reside there for the lesser period of time.

4.5 Conclusions

In this study, general analytical solutions for the continuous injection of solute are derived. The analytical solution of the classical advection-dispersion equation can easily be obtained from the general analytical solution of the main channel, when the Péclet number in the hyporheic zone tends to infinity and the dilution factor becomes zero. The analytical results of the main channel are compared with the observed data of the Uvas Creek tracer experiment. Parameters are estimated by using the large scale algorithm. A sensitivity analysis is performed in order to identify the critical parameters in the present situation. Apart from this, the effects of dilution factor; Péclet number in the hyporheic zone and porosity in the hyporheic zone are also studied.

The analytical results for the main channel are found to be in excellent agreement with the observed data of the Uvas Creek tracer experiment. It is observed in the present analysis that the diffusive transfer model is computationally more efficient and realistic compared to the TSM. Sensitivity analysis shows that the k_r is much more sensitive compared to the other parameters Pe_m, Pe_h, R_h and ϵ. Present analytical solutions reveal that the solute concentration gets diluted because of dilution factor, which is similar to the expected results. Results depict that the long tail gradually becomes more prominent with the decrease in the Péclet number in the hyporheic

zone. Increased porosity accounts for decrease in the peak concentration and also for clipping of the shoulders of the leading edges at downstream locations in the main channel. It can be concluded that the analytical solutions are reliable and usefully applied for the analysis of tracer experiments.

Chapter 5

Analytical solution and analysis for reactive solute transport in streams with diffusive transfer in the hyporheic zone

This chapter deals with the derivation of analytical solutions for the reactive solute in presence of the hyporheic zone where exchange of solute between the main channel and the hyporheic zone is dominated by the diffusive exchange in the dissolved phase of solute. In this study, we follow the model proposed by Jonsson et al. [23], which is based on mass balance approach, for reactive solute.

5.1 Introduction

Two types of models are commonly used to describe the solute exchange between the main channel and the storage/hyporheic zone. The first type is the transient storage model (TSM), in which streams are divided into two distinct zones. The first zone represents the main flow region that includes the process of advection, dispersion and lateral inflow and the second zone includes the storage zone area. These two zones are linked by mass exchange process between them (Bencala and Walters [2], Runkel and Chapra [29], Wagner and Harvey [39]). Bencala [3] included kinetic submodels in the transport equations of the TSM for conservative solute. But in these

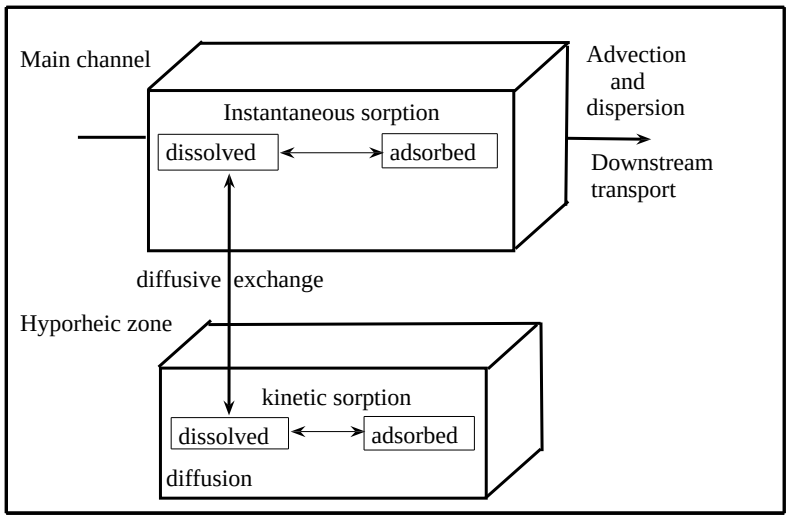

Figure 5.1: *Conceptual model describe the stream and hyporheic zone hydrologic process for reactive solute.*

submodels, there is no distinct representation of the sorption process for the adsorbed and dissolved phases of solute within the sediment. The second type of model is based on the hypothesis of diffusive hyporheic exchange, which relates the classical advection-dispersion equation with diffusive transfer between the main channel of the stream and the hyporheic zone in the dissolved phase of solute (Jackman et al. [21], Wörman [40]). Jonsson et al. [23] described that sorption on the particulate matter is instantaneous in the stream water whereas sorption in the hyporheic zone is not so. They considered the sorption in the hyporheic zone as a kinetic first order reaction between the adsorbed and dissolved phases of solute in their model (which can be seen from Fig. 5.1). The detailed study is already described in 4.1.

Jonsson [22] and Jonsson et al. [23] considered the dispersion in the main channel and the kinetic reaction due to sorption in both the zones. They did the analysis of conservative as well as for reactive solute, based on the Säva stream tracer experiment

data, using the semi-analytical solution of the model.

The purpose of the present study is to derive complete analytical solution of the model described by Jonsson [22] and Jonsson et al. [23] in the case of continuous injection of reactive solutes. The solutions are derived for a general situation, in which the initial concentrations are not constant. A hypothetical situation is considered to study the effects of dilution factor (ϕ), Péclet number (Pe_h), porosity (ϵ), sorption Damköhler number (Da_{sh}) and equilibrium distribution coefficient (k_h) on the concentration-time curves in the main channel. A sensitivity analysis is presented in order to find the critical parameters on the main channel solute concentration. An instantaneous injection of solute is adopted as upstream boundary condition.

5.2 Governing equations

The governing equations presented in the chapter 4 is for the conservative solute transport. The present chapter is intended to study the transport of reactive solute. In the present problem, the exchange of solute mass between the main channel and the hyporheic zone is due to diffusive transfer of solute. There is kinetic transfer of solute in the hyporheic zone which takes place between the adsorbed and dissolved phases of solute. In this study, the transport equations presented by Jonsson [22] and Jonsson et al. [23] are followed. The model described in the chapter 4 does not consider two distinct phases of solute concentration in any of these zones. In the present chapter, due to reactive nature of the solute and distinct phase of solute concentration, the following points can be included in the list of assumptions already considered in the chapter 4.

5.2.1 Assumptions for the model

1. The exchange between the main channel and hyporheic zone is represented by a diffusive exchange term. It is assumed that the diffusive exchange is occurred

only in the dissolve phase of solute and is driven by the concentration gradient at the interface of the stream water and the hyporheic zone [23].

2. In the stream water, sorption on the particulate matter attains its equilibrium instantaneously, and the sorption in the hyporheic zone is described as a kinetic first order reaction.

The governing equations for the model, based on the above assumptions, can be written as (Jonsson [22], Jonsson et al. [23]):

$$\frac{\partial c_m^\star}{\partial t^\star} + \frac{1}{A_m^\star(1+k_r)}\left(c_m^\star \frac{\partial Q_x^\star}{\partial x^\star} + Q_x^\star \frac{\partial c_m^\star}{\partial x^\star}\right) = \frac{D_m^\star}{1+k_r}\frac{\partial^2 c_m^\star}{\partial x^{\star 2}} + \frac{P^\star \epsilon D_h^\star}{A_m^\star}\frac{\partial c_{h_d}^\star/\epsilon}{\partial z^\star}\bigg|_{z^\star=0}, \quad (5.1)$$

$$\frac{\partial c_{h_d}^\star}{\partial t^\star} = D_h^\star \frac{\partial^2 c_{h_d}^\star}{\partial z^{\star 2}} - \hat{\lambda}_h^\star(k_h c_{h_d}^\star - c_{h_a}^\star), \quad (5.2)$$

$$\frac{\partial c_{h_a}^\star}{\partial t^\star} = \hat{\lambda}_h^\star(k_h c_{h_d}^\star - c_{h_a}^\star), \quad (5.3)$$

where $c_m^\star (= c_{m_a}^\star + c_{m_d}^\star)$ is the total solute concentration in the stream water, $c_{m_a}^\star$ is the adsorbed solute concentration in the stream water, $c_{m_d}^\star$ is the dissolved solute concentration in the stream water, $c_{h_a}^\star$ is the adsorbed solute concentration in the hyporheic zone, $c_{h_d}^\star$ is the dissolved solute concentration in the hyporheic zone, $A_m^\star$ is the cross-sectional area of the main channel, $Q_x^\star$ is the volumetric flow rate, $u_m^\star$ is the cross-sectional average velocity in the main channel, $x^\star$ is the longitudinal distance, $t^\star$ is time, $z^\star$ is the lateral co-ordinate, $D_m^\star$ is the dispersion coefficient in the main flow, $D_h^\star$ exchange diffusion coefficient in the hyporheic zone, ϵ is the porosity in the hyporheic zone (-), k_r is the ratio of the cross-sectional area of the hyporheic zone and the cross-sectional area of the main channel (-), $\hat{\lambda}_h^\star$ is the sorption rate coefficient in the hyporheic zone, $k_h (= \frac{c_{h_a}^\star}{c_{h_d}^\star})$ is the equilibrium distribution coefficient in the hyporheic zone and $P^\star$ is the wetted perimeter of the main channel.

Eq. (5.1) is obtained by linking the one-dimensional classical advection-dispersion equation for the main channel with a diffusive exchange between the main channel of stream and the hyporheic zone. Eq. (5.2) represents the one-dimensional diffusion equation for the dissolved solute concentration in the hyporheic zone with a first order kinetic reaction between the adsorbed and dissolved solute concentrations. Eq. (5.3) represents a first order linear relationship between the adsorbed and dissolved phases of solute concentration in the hyporheic zone.

5.2.2 General boundary and initial conditions

The upstream boundary condition due to the continuous injection of solutes in the main channel is given by

$$c_m^\star(x^\star = x_0^\star, t^\star) = c_u^\star(t^\star), \tag{5.4}$$

where $x_0^\star$ is the upstream boundary location, $c_u^\star(t^\star)$ is the solute concentration in the stream water at $x_0^\star$ at time $t^\star$. It is also assumed that Laplace transform of $c_u^\star(t^\star)$ exists and is bounded.

The other boundary condition at the downstream location is given as,

$$c_m^\star(x^\star \to \infty, t^\star) = 0 \text{ for all } t^\star, \tag{5.5}$$

Apart from this, the dissolved phase concentrations in the main channel and in the hyporheic zone are equal

$$c_{h_d}^\star(x^\star, z^\star = 0, t^\star \geq 0) = \epsilon\, c_{m_d}^\star(x^\star, t^\star \geq 0), \tag{5.6}$$

and the other boundary condition in the hyporheic zone is taken as,

$$c_{h_d}^\star(x^\star, z^\star \to \infty, t^\star) = 0 \text{ for } t^\star > 0, \tag{5.7}$$

The initial conditions in the main channel and in the hyporheic zone are

$$c_m^\star(x^\star, t^\star = 0) = c_{minit}^\star(x^\star), \tag{5.8}$$

$$c_{h_d}^\star(x^\star, z^\star, t^\star = 0) = c_{h_{dinit}}^\star(x^\star, z^\star), \tag{5.9}$$

$$c_{h_a}^\star(x^\star, z^\star, t^\star = 0) = c_{h_{ainit}}^\star(x^\star, z^\star). \tag{5.10}$$

where $c_{minit}^\star(x^\star)$, $c_{h_{dinit}}^\star(x^\star, z^\star)$ and $c_{h_{ainit}}^\star(x^\star, z^\star)$ are initial concentrations of solute in the main channel, in the dissolved and in the adsorbed phases of hyporheic zone respectively.

5.2.3 Dimensionless forms of governing equations, general boundary and initial conditions

The dimensionless forms of the governing equations, boundary and initial conditions (5.1)-(5.10) are given as

$$\frac{\partial c_m}{\partial t} + \frac{\phi}{(1+k_r)} c_m + \frac{1}{(1+k_r)} \frac{\partial c_m}{\partial x} = \frac{1}{Pe_m(1+k_r)} \frac{\partial^2 c_m}{\partial x^2} + \frac{\epsilon}{R_h Pe_h} \frac{\partial (c_{h_d}/\epsilon)}{\partial z}\Big|_{z=0}, \tag{5.11}$$

$$\frac{\partial c_{h_d}}{\partial t} = \frac{1}{Pe_h} \frac{\partial^2 c_{h_d}}{\partial z^2} - Da_{sh}(k_h c_{h_d} - c_{h_a}), \tag{5.12}$$

$$\frac{\partial c_{h_a}}{\partial t} = Da_{sh}(k_h c_{h_d} - c_{h_a}), \tag{5.13}$$

$$c_m(x_0, t) = c_u(t), \tag{5.14}$$

$$c_m(x \to \infty, t) = 0 \text{ for all } t, \tag{5.15}$$

$$c_{h_d}(z = 0, t) = \epsilon \; c_{m_d}(x, t), \tag{5.16}$$

$$c_{h_d}(z \to \infty, t) = 0 \text{ for } t > 0, \tag{5.17}$$

$$c_m(x, t = 0) = c_{minit}(x), \tag{5.18}$$

$$c_{h_d}(x, z, t = 0) = c_{h_{dinit}}(x, z), \tag{5.19}$$

$$c_{h_a}(x, z, t = 0) = c_{h_{ainit}}(x, z), \tag{5.20}$$

where $x \left(= \frac{x^\star}{l^\star}\right)$ is the distance in the longitudinal direction, $l^\star (\approx \sqrt{2.5A_m^\star})$ is the characteristic length, $t \left(= \frac{u_m^\star t^\star}{l^\star}\right)$ is the time, $u_m^\star (= \frac{Q_1^\star}{A_m^\star})$ is a constant quantity, $Q_1^\star$ is the volumetric flow rate at the sampling location, $c_m \left(= \frac{c_m^\star}{c_0^\star}\right)$ is the concentration in the main channel of the stream, $c_0^\star$ is the plateau concentration at the head of the tracer experiment, $c_h \left(= \frac{c_h^\star}{c_0^\star}\right)$ is the concentration in the hyporheic zone, $c_{h_d} \left(= \frac{c_{h_d}^\star}{c_0^\star}\right)$ is the concentration in dissolved form in hyporheic zone, $c_{h_a} \left(= \frac{c_{h_a}^\star}{c_0^\star}\right)$ is the concentration in adsorbed form in hyporheic zone, $c_{minit}(x) \left(= \frac{c_{minit}^\star(x^\star)}{c_0^\star}\right)$ is the initial concentration in the main channel, $c_{h_{dinit}}(z) \left(= \frac{c_{h_{dinit}}^\star(z^\star)}{c_0^\star}\right)$ is initial concentration in dissolved form in hyporheic zone, $c_{h_{ainit}}(z) \left(= \frac{c_{h_{ainit}}^\star(z^\star)}{c_0^\star}\right)$ is initial concentration in adsorbed form in hyporheic zone, $c_u(t) \left(= \frac{c_u^\star(t)}{c_0^\star}\right)$ is the upstream concentration, $Pe_m \left(= \frac{u_m^\star l^\star}{D_m^\star}\right)$ is the Péclet number in the main channel, $Pe_h \left(= \frac{u_m^\star l^\star}{D_h^\star}\right)$ is the Péclet number in the hyporheic zone, $Da_{sh} \left(= \frac{\hat{\lambda}_h^\star l^\star}{u_m^\star}\right)$ is the sorption Damköhler number in the hyporheic zone and $\phi \left(= \frac{l^\star}{u_m^\star A_m^\star} \frac{dQ_x^\star}{dx^\star}\right)$ is the dilution factor.

5.3 Analytical solution for diffusive diffusive transfer of reactive solutes with hyporheic zone

The analytical solutions of (5.11)-(5.20) are obtained by using Laplace transform.

Using the given initial conditions (5.19) and (5.20) in the transformed forms of Eqs. (5.12) and (5.3), we get

$$\frac{1}{Pe_h}\frac{d^2\bar{c}_{h_d}}{dz^2} - A_1\bar{c}_{h_d} = -c_{h_{dinit}}(x,z) - \frac{Da_{sh}c_{hainit}(x,z)}{s+Da_{sh}}, \tag{5.21}$$

$$\bar{c}_{h_a} = \frac{c_{h_{ainit}}(x,z) + k_h Da_{sh}\bar{c}_{h_d}}{s+Da_{sh}}, \tag{5.22}$$

where $A_1 = s + k_h Da_{sh} - \frac{k_h Da_{sh}^2}{s+Da_{sh}}$, $\bar{c}_{h_d}$ and $\bar{c}_{h_a}$ are Laplace transforms of c_{h_d} and c_{h_a} respectively.

Using the boundary conditions (5.16) and (5.17) in the solution of Eq. (5.21), we obtain,

$$\begin{aligned}\bar{c}_{h_d}(x,z,s) &= e^{-z\sqrt{Pe_h A_1}}\left[\frac{\epsilon\bar{c}_m}{1+k_d} + \frac{\sqrt{Pe_h}}{2\sqrt{A_1}}\left\{\int_0^{+\infty} -A_2(x,-1,z^{'})dz^{'}\right.\right. \\ &+ \left.\left.\int_0^{z} A_2(x,+1,z^{'})dz^{'}\right\}\right] + \frac{\sqrt{Pe_h}\ e^{z\sqrt{Pe_h A_1}}}{2\sqrt{A_1}}\int_z^{+\infty} A_2(x,-1,z^{'})dz^{'},\end{aligned} \tag{5.23}$$

where $\bar{c}_m$ is Laplace transform of c_m and

$$A_2(x,si,z^{'}) = \left(c_{h_{dinit}}(x,z^{'}) + \frac{Da_{sh}c_{hainit}(x,z^{'})}{s+Da_{sh}}\right)e^{si\ z^{'}\sqrt{Pe_h A_1}}$$

On applying Laplace transform to Eq. (5.11), using Eqs. (5.18) and (5.23), we obtain a non-homogeneous differential equation as,

$$\frac{1}{Pe_m(1+k_r)}\frac{d^2\bar{c}_m}{dx^2} - \frac{1}{1+k_r}\frac{d\bar{c}_m}{dx} - A_3\bar{c}_m = -c_{minit}(x) - \frac{1}{R_h}\int_0^{+\infty} A_2(x,-1,z^{'})dz^{'} \tag{5.24}$$

where $A_3 = \left(s + \frac{\phi}{1+k_r} + a_1\sqrt{A_1}\right)$ and $a_1 = \frac{\epsilon}{R_h(1+k_d)\sqrt{Pe_h}}$.

Using the boundary conditions (5.14) and (5.15) in the solution of Eq. (5.24), we obtain

$$\begin{aligned}\bar{c}_m(x,s) &= \bar{c}_u(s)e^{m_1 x} + \frac{Pe_m(1+k_r)}{(m_2-m_1)}\left[-e^{m_1 x}\int_0^{+\infty} A_4(x^{'})e^{-m_2 x^{'}}dx^{'}\right. \\ &+ \left. e^{m_1 x}\int_0^{x} A_4(x^{'})e^{-m_1 x^{'}}dx^{'} + e^{m_2 x}\int_x^{+\infty} A_4(x^{'})e^{-m_2 x^{'}}dx^{'}\right],\end{aligned} \tag{5.25}$$

where $\bar{c}_u(s)$ is the Laplace transform of $c_u(t)$ and $m_{1,2} = \frac{Pe_m}{2} \mp \sqrt{Pe_m(1+k_r)}\sqrt{\frac{Pe_m}{4(1+k_r)} + A_3}$ and $A_4(x^{'}) = c_{minit}(x^{'}) + \frac{1}{R_h}\int_0^{+\infty} A_2(x^{'}, -1, z^{'})dz^{'}$

With the help of convolution theorem (given in Prudnikov et al. [27], Sneddon [36]), inverse Laplace transform of Eq. (5.25) gives,

$$\begin{aligned} c_m(x,t) &= \int_0^t c_u(\eta) f_1(x, t-\eta) d\eta \\ &+ \int_0^{+\infty} c_{minit}(x^{'}) \Big(f_2(x-x^{'}, -1, t) - e^{Pe_m x} f_2(x+x^{'}, +1, t) \Big) dx^{'} \\ &+ \frac{1}{R_h} \int_0^{+\infty} \int_0^{+\infty} c_{h_{dinit}}(z^{'}) \Big(f_3(x-x^{'}, -1, t) - e^{Pe_m x} f_3(x+x^{'}, +1, t) \Big) dz^{'} dx^{'} \\ &+ \frac{Da_{sh}}{R_h} \int_0^{+\infty} \int_0^{+\infty} c_{h_{ainit}}(z^{'}) \Big(f_4(x-x^{'}, -1, t) - e^{Pe_m x} f_4(x+x^{'}, +1, t) \Big) dz^{'} dx^{'}, \end{aligned} \tag{5.26}$$

$$\begin{aligned} f_1(x,t) &= \int_0^t c_0(x,\gamma) \Big[c_1(a_1\gamma, t-\gamma) e^{-k_h Da_{sh}(t-\gamma)} \\ &+ Da_{sh} \int_0^{t-\gamma} c_1(a_1\gamma, \mu) e^{-a_2-a_3} \sqrt{\frac{a_2}{a_3}} I_1(2\sqrt{a_2 a_3}) d\mu \Big] d\gamma, \end{aligned} \tag{5.27}$$

$$\begin{aligned} f_2(x, si, t) &= \int_0^t c_2(x, si, \gamma) \Big[c_1(a_1\gamma, t-\gamma) e^{-k_h Da_{sh}(t-\gamma)} \\ &+ Da_{sh} \int_0^{t-\gamma} c_1(a_1\gamma, \mu) e^{-a_2-a_3} \sqrt{\frac{a_2}{a_3}} I_1(2\sqrt{a_2 a_3}) d\mu \Big] d\gamma, \end{aligned} \tag{5.28}$$

$$\begin{aligned} f_3(x, si, t) &= \int_0^t c_2(x, si, \gamma) \Big[c_1(a_1\gamma + z^{'}\sqrt{Pe_h}, t-\gamma) e^{-k_h Da_{sh}(t-\gamma)} \\ &+ Da_{sh} \int_0^{t-\gamma} c_1(a_1\gamma + z^{'}\sqrt{Pe_h}, \mu) e^{-a_2-a_3} \sqrt{\frac{a_2}{a_3}} I_1(2\sqrt{a_2 a_3}) d\mu \Big] d\gamma, \end{aligned} \tag{5.29}$$

$$f_4(x, si, t) = \int_0^t c_2(x, si, \gamma) \Big[\int_0^{t-\gamma} c_1(a_1\gamma + z^{'}\sqrt{Pe_h}, \mu) e^{-a_2-a_3} I_0(2\sqrt{a_2 a_3}) d\mu \Big] d\gamma, \tag{5.30}$$

where $a_2 = k_h Da_{sh}\mu$, $a_3 = Da_{sh}(t-\gamma-\mu)$,

$$c_0(x,t) = \frac{x\sqrt{Pe_m(1+k_r)}}{2\sqrt{\pi t^3}} \exp\left(- \frac{Pe_m(x(1+k_r)-t)^2}{4(1+k_r)t} - \frac{\phi t}{1+k_r}\right), \tag{5.31}$$

$$c_1(a_1\tau_1,\tau_2) = \frac{a_1\tau_1}{2\sqrt{\pi {\tau_2}^3}} \exp\left(- \frac{(a_1\tau_1)^2}{4\tau_2}\right), \tag{5.32}$$

$$c_2(x,si,t) = \frac{\sqrt{Pe_m(1+k_r)}}{2\sqrt{\pi t}} \exp\left(- \frac{Pe_m(x(1+k_r)+si\ t)^2}{4(1+k_r)t} - \frac{\phi t}{1+k_r}\right), \tag{5.33}$$

The analytical solution for the hyporheic zone solute concentration is obtained by substituting Eq. (5.25) into Eq. (5.23) and applying inverse Laplace transform as,

$$\begin{aligned} c_h(x,z,t) &= \frac{\epsilon(1+k_h)}{1+k_d}\Bigg[\int_0^t c_u(\eta) f_5(x,t-\eta)d\eta \\ &+ \int_0^{+\infty} c_{minit}(x^{'})\Big(f_6(x-x^{'},-1,t) - e^{Pe_m x} f_6(x+x^{'},+1,t)\Big)dx^{'} \\ &+ \frac{1}{R_h}\int_0^{+\infty}\int_0^{+\infty}(c_{h_{dinit}}(x^{'},z^{'})\Big(f_7(x-x^{'},-1,t) - e^{Pe_m x} f_7(x+x^{'},+1,t)\Big)dx^{'}dz^{'} \\ &+ \frac{Da_{sh}}{R_h}\int_0^{+\infty}\int_0^{+\infty} c_{h_{ainit}}(x^{'},z^{'})\Big(f_8(x-x^{'},-1,t) - e^{Pe_m x} f_8(x+x^{'},+1,t)\Big) \\ &\times dx^{'}dz^{'}\Bigg] + (1+k_h)\int_0^{+\infty} c_{h_{dinit}}(x,z^{'})(f_9(z+z^{'},t) - f_9(z-z^{'},t))dz^{'} \\ &+ Da_{sh}\int_0^{+\infty} c_{h_{ainit}}(x,z^{'})(f_{10}(z+z^{'},t) - f_{10}(z-z^{'},t))dz^{'}, \end{aligned} \tag{5.34}$$

$$\begin{aligned} f_5(x,t) &= \int_0^t c_0(x,\gamma)\Bigg[c_1(a_1\gamma + z\sqrt{Pe_h}, t-\gamma)e^{-k_h Da_{sh}(t-\gamma)} \\ &+ Da_{sh}\int_0^{t-\gamma} c_1(a_1\gamma + z\sqrt{Pe_h},\mu)e^{-a_2-a_3}\sqrt{\frac{a_2}{a_3}}I_1(2\sqrt{a_2 a_3})d\mu\Bigg]d\gamma, \end{aligned} \tag{5.35}$$

$$\begin{aligned} f_6(x,si,t) &= \int_0^t c_2(x,si,\gamma)\Bigg[c_1(a_1\gamma + z\sqrt{Pe_h}, t-\gamma)e^{-k_h Da_{sh}(t-\gamma)} \\ &+ Da_{sh}\int_0^{t-\gamma} c_1(a_1\gamma + z\sqrt{Pe_h},\mu)e^{-a_2-a_3}\sqrt{\frac{a_2}{a_3}}I_1(2\sqrt{a_2 a_3})d\mu\Bigg]d\gamma, \end{aligned} \tag{5.36}$$

$$f_7(x,si,t) = \int_0^t c_2(x,si,\gamma)\Bigg[c_1(a_1\gamma + z\sqrt{Pe_h}, t-\gamma)e^{-k_h Da_{sh}(t-\gamma)} + Da_{sh}\int_0^{t-\gamma} c_1(a_1\gamma + z\sqrt{Pe_h},\mu)e^{-a_2-a_3}\sqrt{\frac{a_2}{a_3}}I_1(2\sqrt{a_2a_3})d\mu\Bigg]d\gamma, \tag{5.37}$$

$$f_8(x,si,t) = \int_0^t c_2(x,si,\gamma)\Bigg[\int_0^{t-\gamma} c_1(a_1\gamma + (z+z')\sqrt{Pe_h},\mu)e^{-a_2-a_3}I_0(2\sqrt{a_2a_3})d\mu\Bigg]d\gamma, \tag{5.38}$$

$$f_9(z,t) = c_3(z,t)e^{-k_h Da_{sh}t} + Da_{sh}\int_0^t c_3(z,\gamma)e^{-a_4-a_5}\sqrt{\frac{a_4}{a_5}}I_1(2\sqrt{a_4a_5})d\gamma, \tag{5.39}$$

$$f_{10}(z,t) = \int_0^t c_3(z,\gamma)e^{-a_4-a_5}I_0(2\sqrt{a_4a_5})d\gamma, \tag{5.40}$$

$a_4 = k_h Da_{sh}\gamma$, $a_5 = Da_{sh}(t-\gamma)$

$$c_3(z,t) = \frac{\sqrt{Pe_h}e^{-\frac{z^2 Pe_h}{4t}}}{2\sqrt{\pi t}}, \tag{5.41}$$

It is verified that Eqs. (5.26) and (5.34) satisfy the initial-boundary problem (5.11)-(5.20). This assures the analytical expressions given in Eqs. (5.26) and (5.34) are the exact analytical solutions of Eqs. (5.11)-(5.13).

5.4 Results and Discussion

Effects of dilution factor, Péclet number, porosity, sorption Damköhler number and equilibrium distribution coefficient in the hyporheic zone on the concentration-time curves in the main channel are studied for a hypothetical situation. A sensitivity analysis is presented in order to obtain the critical parameters for reactive solute. $u_m^\star$ is calculated in the similar way as described in the section 4.4.

x	M	Pe_m	Pe_h	k_r	ϵ	ϕ	R_h	k_h
500	500	0.4275	1.0443×10^{3}	0.112	0.6761	2.2×10^{-4}	1.3341	$2.0\times10^{+4}$

Table 5.1: *Parameter values for the analysis of results of reactive solute for diffusive transfer model.*

5.4.1 Hypothetical Experiment

In order to discuss the effects of dilution factor (ϕ), Péclet number in the hyporheic zone (Pe_h), porosity in the hyporheic zone (ϵ), sorption Damköhler number in the hyporheic zone (Da_{sh}) and equilibrium distribution coefficient in the hyporheic zone (k_h) on the main channel solute concentration, a hypothetical situation is considered and the parameters values are chosen from the Table 5.1.

An instantaneous injection ($\frac{M^\star}{Q_0^\star}\delta(t^\star)$) serves as upstream boundary at the injection location, so the upstream boundary condition in the dimensionless form will be,

$$c_m(x_0 = 0, t) = c_u(t) = M\delta(t). \tag{5.42}$$

where $M\left(= \frac{M^\star u_m^\star}{Q_0^\star l^\star c^\star{}_0} \right)$ is the dimensionless mass, $M^\star$ is the injected mass and $Q_0^\star$ is the volumetric flow rate at the injection location.

The analytical solution for the main channel is obtained from the Eq. (5.26), using the upstream boundary condition given in Eq. (5.42), as

$$c_m(x, t) = Mf_1(x, t), \tag{5.43}$$

where f_1 is given by Eq. (5.27).

The solute concentration profiles for the main channel is calculated at 500 unit downstream from the injection location $x_0 = 0$ using the time step $\Delta t = 0.05$.

Effects of dilution factor (ϕ)

In order to discuss the effects of dilution factor, the concentration-time curves are presented in Fig. 5.2. The increase in the dilution factor decreases the peak value of

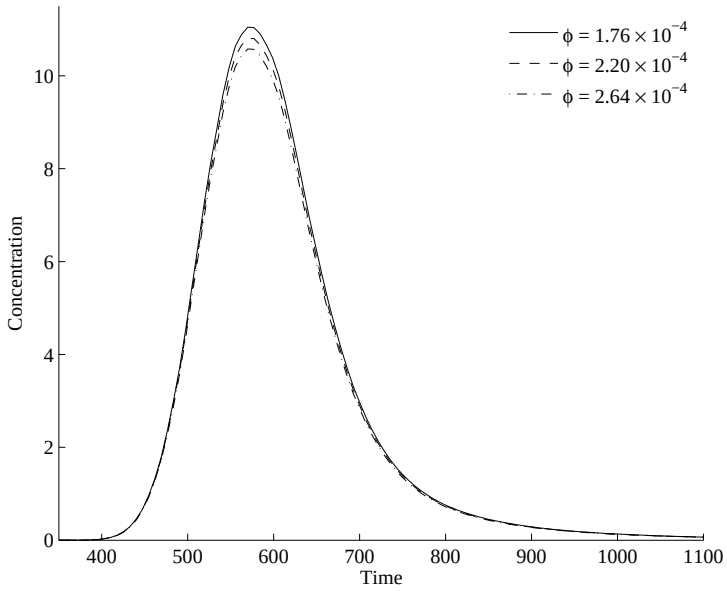

Figure 5.2: *Effects of dilution factor on concentration-time curve at* 500 *unit downstream from the injection location.*

the concentration-time curve in the main channel at downstream locations and the overall solute concentration also gets diluted (which can be seen from Fig. 5.2).

Effects of Péclet number in hyporheic zone (Pe_h)

Results are obtained at 500 unit downstream from the injection location for different values of $Pe_h (= 1.20\times10^3,\ 1.04\times10^3$ and $0.63\times10^3)$ and the concentration-time curves are presented in Fig. 5.3. It shows that with the decrease in the value of Pe_h, the concentrations of the front shoulder of the concentration-time curve decreases. Difference between any two curves for different Péclet numbers increases with time and reaches its maximum at the peak. As time elapses the difference become insignificant. Fig. 5.3 also depicts that the peak concentration decreases with the decrease in the value of Pe_h. The main cause for these effects on the concentration-time curves could be the diffusive exchange between the main channel and the hyporheic zone.

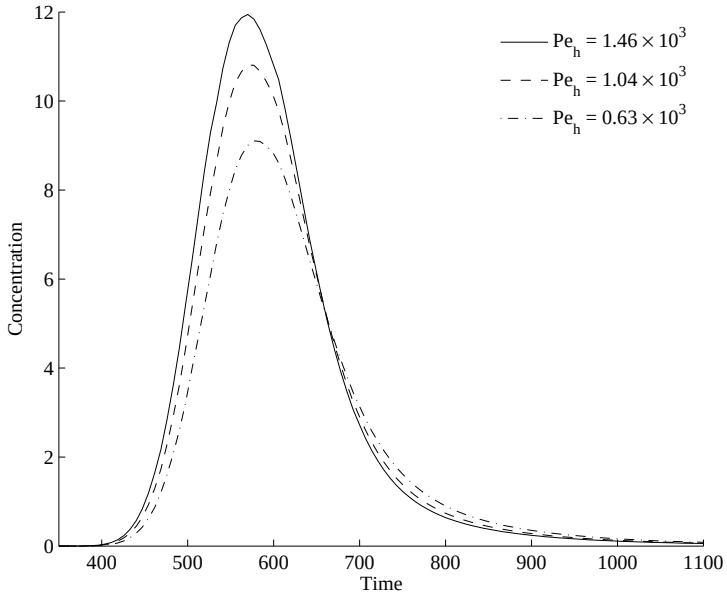

Figure 5.3: *Effects of Péclet number in the hyporheic zone on concentration-time curve at* 500 *unit downstream from the injection location.*

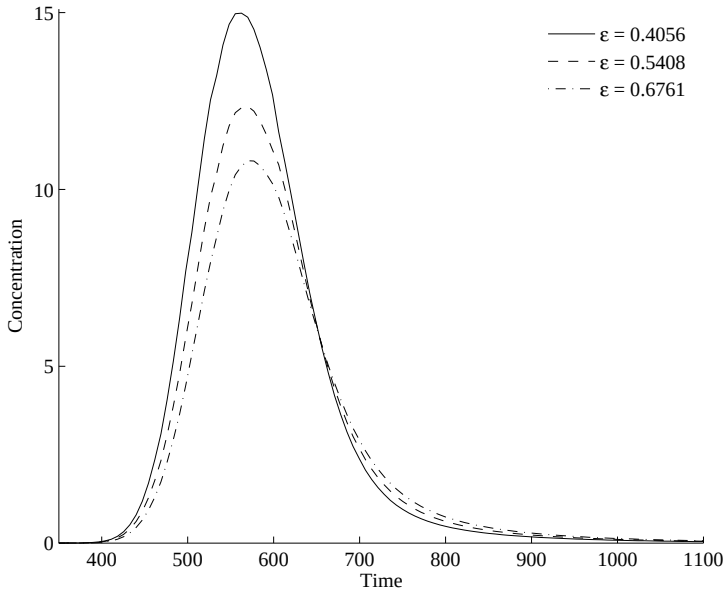

Figure 5.4: *Effects of porosity on concentration-time curve at* 500 *unit downstream from the injection location.*

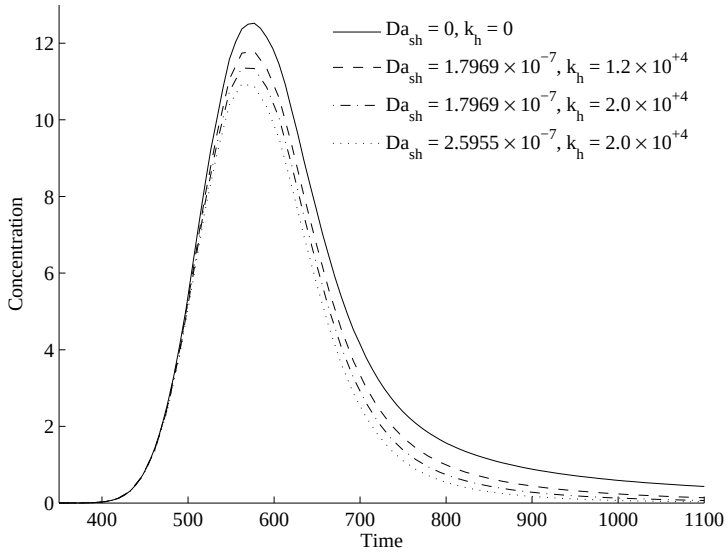

Figure 5.5: *Effects of sorption Damköhler number in the hyporheic zone and equilibrium distribution coefficient in the hyporheic zone on the concentration-time curve at* 500 *unit downstream from the injection location.*

Effects of porosity in the hyporheic zone (ϵ)

In order to study the effects of porosity (ϵ) on the concentration-time curves in the main channel of stream, different values of ϵ are chosen and results are presented in Fig. 5.4. It shows that the peak value of the concentration-time curve decreases with the increase in the value of ϵ. It is seen that the concentration graph moves towards right with decrease in ϵ. This effect is mainly because of more solute particles enter into the hyporheic zone but reside there for the lesser period of time.

Effects of the sorption Damköhler number and equilibrium distribution coefficient in the hyporheic zone

In order to discuss the effects of the sorption Damköher number (Da_{sh}) and equilibrium distribution coefficient (k_h), the resulting concentration-time curves based on the analytical solution are presented in Fig. 5.5. Due to increase in the value of Da_{sh} and k_h, the value of concentration decreases after passing the front edge of the

p_j	dc_{min}	dc_{max}	$dc_{max} - dc_{min}$
Pe_m	-7.27	9.95	17.21
k_r	-67.33	41.58	108.91
Pe_h	-5.18 $\times 10^{-4}$	0.0036	0.0041
ϵ	-11.18	1.60	12.78
R_h	-0.81	5.67	6.48
Da_{sh}	-6.16 $\times 10^{9}$	0.0	6.16 $\times 10^{9}$

Table 5.2: *Diffusive transfer model for reactive solute: minimum (dc_{min}) and maximum (dc_{max}) values of sensitivity of solute concentration in the main channel to the parameter p_j respectively.*

concentration-time curves. Normally, the solute particles enter into the hyporheic zone due to the diffusive transfer between the main channel and the hyporheic zone. These particles reside for a longer time in the hyporheic zone due to slow kinetic transfer of solute between the adsorbed and dissolved phases of the solute in the hyporheic zone.

Sensitivity Analysis

Sensitivity analysis is performed to elucidate the most sensitive parameters on the main channel concentrations. Sensitivities of different parameters (i.e. Péclet numbers, (Pe_m, Pe_h); ratio of cross-sectional areas, (k_r) ; hydraulic radius, (R_h) ; porosity, (ϵ); sorption Damköhler number in the hyporheic zone (Da_{sh})) are calculated at 500 unit downstream from the injection location. Results for the sensitivities of the solute concentration to different parameters are presented in Figs. 5.6-5.8 and Table 5.2. From the table and figures, it is clear that Da_{sh} is the most sensitive and Pe_h is the least sensitive parameters. Among rest of the parameters, k_r is relatively more sensitive.

5.5 Conclusions

In this chapter, general analytical solutions for the continuous injection of reactive solute are presented. A hypothetical situation is considered to study the effects of

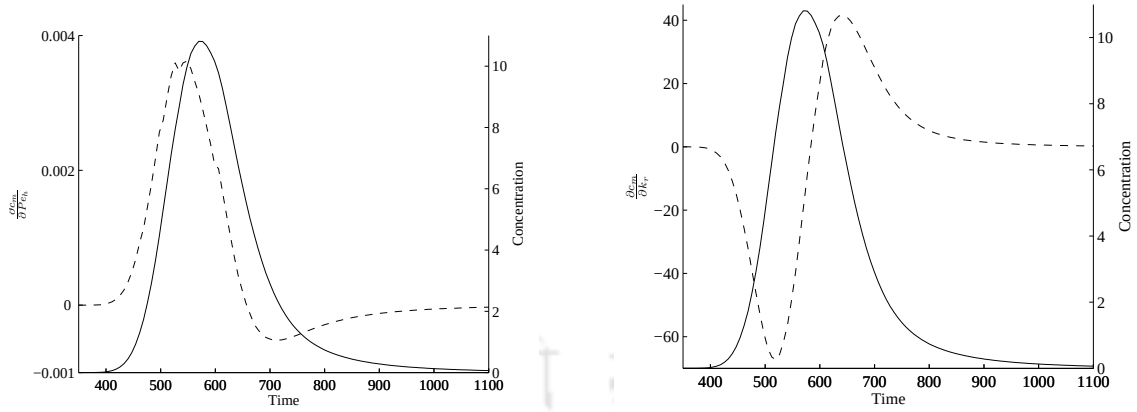

(a) *sensitivity (dashed line) to hyporheic Péclet number*

(b) *sensitivity (dashed line) to ratio of cross-sectional areas*

Figure 5.6: *Sensitivity of Péclet number in the hyporheic zone and ratio of cross-sectional areas on the concentration-time curve (solid line) calculated with the analytical solution given by Eq.* (5.43) *at* 500 *unit downstream from the injection location.*

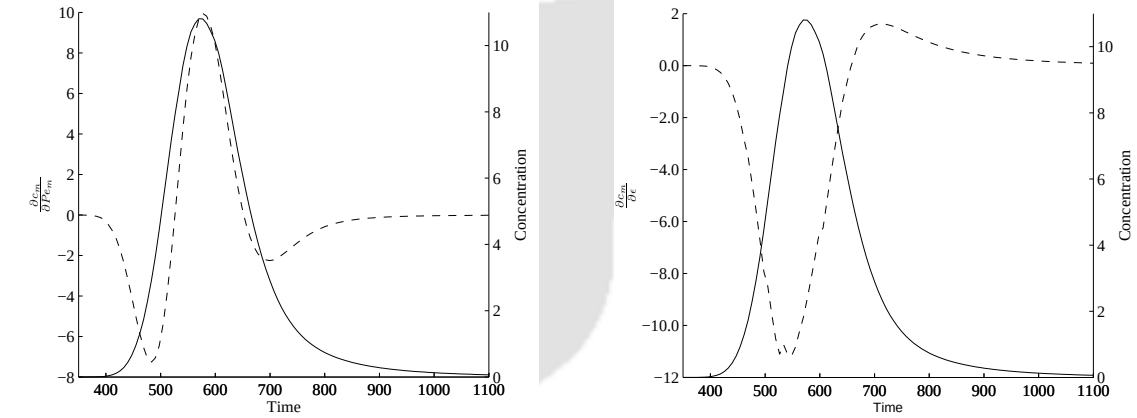

(a) *sensitivity (dashed line) to main channel Péclet number*

(b) *sensitivity (dashed line) to ratio of cross-sectional areas*

Figure 5.7: *Sensitivity of Péclet number in the main channel and porosity in the hyporheic zone on the concentration-time curve (solid line) calculated with the analytical solution given by Eq.* (5.43) *at* 500 *unit downstream from the injection location.*

dilution factor, Péclet number, porosity, sorption Damköhler number and equilibrium distribution coefficient in the hyporheic zone on the concentration-time curves in the main channel. A sensitivity analysis is presented in order to find the critical parameters on the solute concentration in the main channel. Results are presented

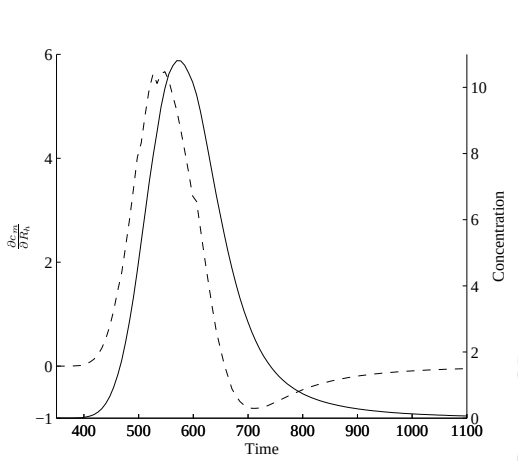

(a) *sensitivity (dashed line) to hydraulic radius*

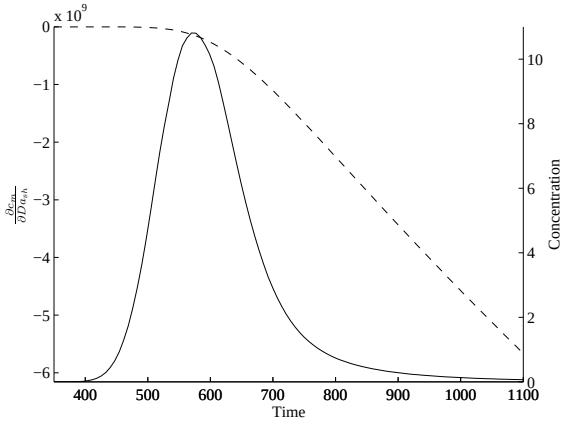

(b) *sensitivity (dashed line) to sorption Damköhler number in the hyporheic zone*

Figure 5.8: *Sensitivity of hydraulic radius and sorption Damköhler number in the hyporheic zone on the concentration-time curve (solid line) calculated with the analytical solution given by Eq.* (5.43) *at* 500 *unit downstream from the injection location.*

for the instantaneous injection of solute.

Present analytical solutions reveal that the solute concentration gets diluted because of the dilution factor, as expected. With the increase in the value of porosity (ϵ), the solute concentration in the main channel decreases. With the decrease in the value of Péclet number in the hyporheic zone (Pe_h), the overall solute concentration in the main channel decreases. Due to increase in the value of the sorption rate coefficient in the hyporheic zone, solute particles once enter into the hyporheic zone, reside for a longer time in the hyporheic zone. Sensitivity analysis shows that the Damköhler number in the hyporheic zone is the most sensitive parameter among all the parameters.

Chapter 6

Conclusions

6.1 Observations and Remarks

This thesis focuses on the derivation of analytical solutions of the transient storage models. To analyze the different properties (e.g. hydrological, geochemical) of the solute transport in streams, new analytical solutions are derived for conservative as well as for reactive solutes for a general situation, in which initial concentrations are not constant. These solutions are derived with the help of Laplace transform. Analytical solutions for conservative solute are compared with the existing experimental data of the Uvas Creek tracer experiment for chloride concentration. A sensitivity analysis is performed in order to find the critical parameters on solute concentrations for the transient storage models. Also, effects of different parameters, that represent physical, chemical and hydrological processes are studied. A step concentration-time profile is used as an upstream boundary condition for conservative solute, whereas an instantaneous injection of solute is used as an upstream boundary condition for reactive solute.

Analytical solution for the conservative solutes in streams with lateral inflow and transient storage is derived. The analytical solution for the case of no storage zone can easily be obtained from the present analytical solution. Analytical solution for the main channel of stream is applied for the analysis of the Uvas Creek tracer experiment. The analytical results are found to be in good agreement with the observed data

of the Uvas Creek tracer experiment. Sensitivity analysis shows that the exchange Damköhler number in the main channel (Da_{em}) and lateral inflow rate (q_L) are much more sensitive compared to the Péclet number in the main channel (Pe_m) and ratio of cross-sectional areas (k_r). Due to the presence of lateral inflow rate, solute mass gets diluted at downstream locations. Due to the the exchange Damköhler number also, the solute mass gets reduced but the long tail appears in the downstream edge of the concentration profile.

Analytical solutions of the reactive solutes by including the effects of decay and reaction are also derived for a general situation in which initial concentrations are function of space, lateral inflow concentration and the storage zone equilibrium concentration are both the function of time and space. Results are presented for instantaneous release of the solute for a hypothetical situation. Effects of background concentration can be realized through the solutions in the case of RSTM without decay, by simply adding the background concentration. It is observed that the peak values of the concentration-time curves decrease with the increase in the decay Damköhler numbers. Delaying of the solute concentration profiles with the increase in the reaction Damköhler number in the main channel is also noticed by our analytical solutions. The dilution of solute concentration takes place when the effect of lateral inflow is included. Present analytical solutions clearly reveal the effects of decay, reaction Damköhler numbers and lateral inflow. Sensitivity analysis shows that the decay Damköhler number in the main channel is more sensitive compared to that in the storage zone in the case of RSTM without sorption and lateral inflow, whereas in the case of RSTM without decay and lateral inflow, the reaction Damköhler number in the storage zone is more sensitive compared to that in the main channel.

Analytical solutions of the diffusive transfer model are derived for conservative solute for a general situation in which the initial concentrations are not constant. The analytical solution of the classical advection-dispersion equation can be obtained

from the general analytical solution of the main channel, when the Péclet number in the hyporheic zone tends to infinity in the absence of dilution factor. Solutions are used to analyze the parameters of the model for the Uvas Creek tracer experiment for chloride concentration. The analytical results are found to be in good agreement with the observed data of the Uvas Creek tracer experiment. It is observed that the diffusive transfer model is computationally more efficient and realistic compared to the TSM. Sensitivity analysis shows that the ratio of the cross-sectional areas (k_r) is much more sensitive compared to the other parameters Péclet numbers (Pe_m, Pe_h), hydraulic radius (R_h) and porosity (ϵ) and Pe_h is less sensitive. Present analytical solutions reveal that the solute concentration becomes diluted because of the dilution factor, which is similar to the expected results. Results depict that the long tail gradually becomes prominent with the increase in the Péclet number in the hyporheic zone. Increased porosity accounts for decrease in the peak concentration and also for clipping of the shoulders of the leading edges at downstream locations in the main channel.

New analytical solutions for the reactive solutes by including the effects of sorption in the hyporheic zone are derived for a general situation in which initial concentrations are not constant. Present analytical solutions reveal that with the decrease in the value of Pe_h, the overall solute concentration in the main channel decreases. Due to increase in the value of the sorption rate coefficient in the hyporheic zone, solute particles once enter into the hyporheic zone, reside for a longer time in the hyporheic zone. Sensitivity analysis shows that the Damköhler number in the hyporheic zone is the most sensitive parameter.

The analytical solutions derived in this thesis are useful in several situations.

1. Models describe the different properties (e.g. hydrological, geochemical) of the solute transport in streams. These models also describe the exchange processes between the main channel and the storage/hyporheic zone. Similar type of

equations are generally used in the study of soil dynamics, heat transfer and porous media. Thus, it can be concluded that solutions can be reliably applied to these kind of studies.

2. Analytical solutions play an important role in the testing of models evaluated by numerical methods. These analytical solutions can be used as tools to verify the numerical schemes used in the transport problems and the accuracy of their solutions.

3. The solutions can also be used as tools to verify the complex models for solute transport problems.

4. The examination of the sensitivity of each parameter (hydrological or chemical) to the behavior of the transport process is easy to perform, when the analytical solutions are available.

5. The closed form analytical solutions are obtained based on the fact that the volumetric flow rate varies linearly and exponentially between the injection location and downstream sampling location for the two different transport models. It is noticed that the closed form analytical solutions are in good agreement with the observed results. So, it can be concluded that the present analytical solutions can be reliably applied for the analysis of processes involved in tracer experiments.

6.2 Scope for future work

The work also opens up a host of interesting research possibilities, the major ones of which are listed below.

1. As mentioned earlier, we have derived general analytical solutions for the transient storage models in the case of stagnant water zones (where advection and

dispersion are absent) and hyporheic zone (where only diffusion processes are taking place). This opens up the possibility to derive the analytical solutions in which advection and dispersion processes are included in the hyporheic zone also.

2. All the analytical solutions derived in this work are obtained by considering the medium to be homogeneous. This opens up the possibility to derive the analytical solutions for more complex models involving nonlinearities and heterogeneity.

3. The analytical solutions for the diffusive transfer model are found in which the first order kinetic reaction is considered in the hyporheic zone only. This opens up the possibility to derive the analytical solutions for the model in which the first order kinetic reaction can be assumed in the main channel as well.

Appendix A

Outline to find inverse Laplace transform

The purpose of this appendix is to give an outline to find inverse Laplace transform with the help of the generalized convolution theorem of the Laplace transform given in Sneddon [36].

Eq. (3.20) is written as,

$$\begin{aligned}\overline{c}_m(x,s) &= \overline{c}_u(s)e^{m_1 x} - \frac{Pe_m e^{m_1 x}}{(m_2-m_1)}\int_0^{+\infty} R_2(x^{'})e^{-m_2 x^{'}}dx^{'} \\ &+ \frac{Pe_m e^{m_1 x}}{(m_2-m_1)}\int_0^{x} R_2(x^{'})e^{-m_1 x^{'}}dx^{'} + \frac{Pe_m e^{m_2 x}}{(m_2-m_1)}\int_x^{+\infty} R_2(x^{'})e^{-m_2 x^{'}}dx^{'},\end{aligned} \tag{A.1}$$

where

$$m_{1,2} = \frac{Pe_m}{2} \mp \sqrt{Pe_m}\sqrt{\frac{Pe_m}{4} + R_1(s)},$$

$$R_1(s) = \left(s + q_L + Da_{dm} + Da_{em} + \rho k_d Da_{rm} - \frac{Da_{em}^2}{k_r\left(s + \frac{Da_{em}}{k_r} + Da_{rs} + Da_{ds}\right)} - \frac{\rho k_d Da_{rm}^2}{s + Da_{rm}}\right),$$

$$R_2(x) = c_{minit}(x) + \frac{Da_{em}(c_{sinit}(x) + Da_{rs}\overline{\hat{c}}_s(x,s))}{s + \frac{Da_{em}}{k_r} + Da_{rs} + Da_{ds}} + \frac{\rho Da_{rm} c_{sedinit}(x)}{s + Da_{rm}} + q_L\overline{c}_L(x,s),$$

$\overline{c}_L(x,s)$ and $\overline{c}_u(s)$ are the Laplace transforms of $c_L(x,t)$ and $c_u(t)$ respectively.

The following procedure is used to find the inverse Laplace transform of the first term on the right hand side of the Eq. (A.1), which is

$$\overline{c}_u(s)e^{\frac{Pe_m x}{2}-x\sqrt{Pe_m}\sqrt{\frac{Pe_m}{4}+R_1(s)}}.$$

This term is the product of two individual functions: the first function is $\overline{c}_u(s)$ and the second one is $e^{\frac{Pe_m x}{2}-x\sqrt{Pe_m}\sqrt{\frac{Pe_m}{4}+R_1(s)}}$. Inverse Laplace transform of first function $\overline{c}_u(s)$ is $c_u(t)$. In order to find inverse Laplace transform of the second function, we consider

$$L[f_1(x,t)] = \overline{f}_1(x,s) = e^{\frac{Pe_m x}{2}-x\sqrt{Pe_m}\sqrt{\frac{Pe_m}{4}+R_1(s)}}, \tag{A.2}$$

To obtain inverse Laplace transform of Eq. (A.2), we make use of the generalized convolution theorem of the Laplace transform given in Sneddon [36] as

$$L\left[\int_0^t f(\gamma, t-\gamma)d\gamma; t\to s\right] = L\{L[f(t_1,t_2); t_2\to s]; t_1\to s\} \tag{A.3}$$

Inverse Laplace transform is performed in two steps by considering two different indices of Laplace variable such as $s_1 = s_2 = s$. So, the Eq. (A.2) can be written as

$$\overline{f}_1(x,s_1,s_2) = e^{\frac{Pe_m x}{2}-x\sqrt{Pe_m}\sqrt{\frac{Pe_m}{4}+R_1(s_1,s_2)}}, \tag{A.4}$$

where

$$\begin{aligned} R_1(s_1,s_2) &= \left(s_1 + q_L + Da_{dm} + Da_{em} + \rho k_d Da_{rm} - \frac{Da_{em}^2}{k_r\left(s_2 + \frac{Da_{em}}{k_r} + Da_{rs} + Da_{ds}\right)}\right. \\ &- \left.\frac{\rho k_d Da_{rm}^2}{s_2 + Da_{rm}}\right). \end{aligned}$$

The inverse Laplace transform of Eq. (A.4) with respect to s_1 gives

$$L[f_1(x,t_1,t_2); t_2\to s_2] = e^{\frac{Pe_m x}{2}}\frac{x\sqrt{Pe_m}}{2\sqrt{\pi t_1^3}}e^{-\frac{x^2 Pe_m}{4t_1}}e^{-R_1'(s_2)t_1}, \tag{A.5}$$

where

$$R_1'(s_2) = \frac{Pe_m}{4} + q_L + Da_{dm} + Da_{em} + \rho k_d Da_{rm} - \frac{Da_{em}^2}{k_r\left(s_2 + \frac{Da_{em}}{k_r} + Da_{rs} + Da_{ds}\right)} - \frac{\rho k_d Da_{rm}^2}{s_2 + Da_{rm}}$$

Eq. (A.5) can be rewritten as

$$L[f_1(x,t_1,t_2);t_2\rightarrow s_2]=c_0(x,t_1)e^{-(Da_{em}+\rho k_d Da_{rm})t_1}e^{R_2^{'}(s_2)t_1}e^{R_3^{'}(s_2)t_1}, \tag{A.6}$$

where

$$c_0(x,t_1)=\frac{x\sqrt{Pe_m}}{2\sqrt{\pi {t_1}^3}}e^{-\frac{Pe_m(x-t_1)^2}{4t_1}-(Da_{dm}+q_L)t_1},$$

$$R_2^{'}(s_2)=\frac{Da_{em}^2}{k_r\left(s_2+\frac{Da_{em}}{k_r}+Da_{rs}+Da_{ds}\right)} \quad \text{and} \quad R_3^{'}(s_2)=\frac{\rho k_d Da_{rm}^2}{s_2+Da_{rm}}.$$

Inverse Laplace transform of $e^{R_2^{'}(s_2)t_1}$ and $e^{R_3^{'}(s_2)t_1}$ with respect to s_2 ([27]) gives,

$$L_{s_2}^{-1}[e^{R_2^{'}(s_2)t_1}]=e^{-(\frac{Da_{em}}{k_r}+Da_{rs}+Da_{ds})t_2}\left\{\delta(t_2)+Da_{em}\sqrt{\frac{t_1}{k_r t_2}}I_1\left(2\sqrt{\frac{Da_{em}^2}{k_r}t_1t_2}\right)\right\}, \tag{A.7}$$

I_1 is the modified Bessel function of first kind, and of order one,

$$L_{s_2}^{-1}[e^{R_3^{'}(s_2)t_1}]=e^{-Da_{rm}t_2}\left\{\delta(t_2)+Da_{rm}\sqrt{\frac{\rho k_d t_1}{t_2}}I_1\left(2\sqrt{\rho Da_{rm}^2 k_d t_1 t_2}\right)\right\} \tag{A.8}$$

The standard convolution theorem of the Laplace transform given in Sneddon [36] as

$$L^{-1}[f(s)g(s)]=\int_0^t f(t)g(t-\mu)d\mu \tag{A.9}$$

In view of Eqs. (A.7)-(A.9), the inverse Laplace transform of $e^{R_2^{'}(s_2)t_1}e^{R_3^{'}(s_2)t_1}$ with respect to s_2 gives,

$$\begin{aligned}L_{s_2}^{-1}[e^{R_2^{'}(s_2)t_1}e^{R_3^{'}(s_2)t_1}] &= \int_0^{t_2} e^{-(\frac{Da_{em}}{k_r}+Da_{rs}+Da_{ds})\mu}\left\{\delta(\mu)+Da_{em}\sqrt{\frac{t_1}{k_r\mu}}\right.\\ &\times \left. I_1\left(2\sqrt{\frac{Da_{em}^2}{k_r}t_1\mu}\right)\right\}e^{-Da_{rm}(t_2-\mu)}\left\{\delta(t_2-\mu)+Da_{rm}\sqrt{\frac{\rho k_d t_1}{t_2-\mu}}\right.\\ &\times \left. I_1\left(2\sqrt{\rho Da_{rm}^2 k_d t_1(t_2-\mu)}\right)\right\}d\mu. \end{aligned}\tag{A.10}$$

Now, Eq. (A.6) can be rewritten as

$$\begin{aligned}f_1(x,t_1,t_2) &= c_0(x,t_1)e^{-(Da_{em}+\rho k_d Da_{rm})t_1}\int_0^{t_2} e^{-(\frac{Da_{em}}{k_r}+Da_{rs}+Da_{ds})\mu}\left\{\delta(\mu)\right.\\ &+ \left. Da_{em}\sqrt{\frac{t_1}{k_r\mu}}I_1\left(2\sqrt{\frac{Da_{em}^2}{k_r}t_1\mu}\right)\right\}e^{-Da_{rm}(t_2-\mu)}\left\{\delta(t_2-\mu)\right.\\ &+ \left. Da_{rm}\sqrt{\frac{\rho k_d t_1}{t_2-\mu}}I_1\left(2\sqrt{\rho Da_{rm}^2 k_d t_1(t_2-\mu)}\right)\right\}d\mu. \end{aligned}\tag{A.11}$$

In view of Eqs. (A.2) and (A.3), Eq. (A.11) yields

$$\begin{aligned} f_1(x,t) &= \int_0^t c_0(x,\gamma) e^{-(Da_{em}+\rho k_d Da_{rm})\gamma} \int_0^{t-\gamma} e^{-(\frac{Da_{em}}{k_r}+Da_{rs}+Da_{ds})\mu} \Bigg\{ \delta(\mu) \\ &+ Da_{em}\sqrt{\frac{\gamma}{k_r\mu}} I_1\left(2\sqrt{\frac{Da_{em}^2}{k_r}\gamma\mu}\right)\Bigg\} e^{-Da_{rm}(t-\gamma-\mu)} \Bigg\{ \delta(t-\gamma-\mu) \\ &+ Da_{rm}\sqrt{\frac{\rho k_d \gamma}{t-\gamma-\mu}} I_1\left(2\sqrt{\rho Da_{rm}^2 k_d \gamma(t-\gamma-\mu)}\right)\Bigg\} d\mu d\gamma, \end{aligned} \tag{A.12}$$

Using the property of Dirac delta function in the Eq. (A.12), we get

$$\begin{aligned} f_1(x,t) &= c_0(x,t) e^{-(Da_{em}+\rho k_d Da_{rm})t} \\ &+ \frac{Da_{em}}{k_r}\int_0^t c_0(x,\gamma) e^{-a-b-p-r}\sqrt{\frac{a}{b}}\, I_1(2\sqrt{ab}) d\gamma \\ &+ Da_{rm}\int_0^t c_0(x,\gamma) e^{-a-p-q}\sqrt{\frac{p}{q}}\, I_1(2\sqrt{pq}) d\gamma \\ &+ \frac{Da_{em}Da_{rm}}{k_r}\int_0^t c_0(x,\gamma)\int_0^{t-\gamma} e^{-a-b_1-p-q_1-r_1}\sqrt{\frac{ap}{b_1 q_1}} I_1(2\sqrt{ab_1}) \\ &\times I_1(2\sqrt{pq_1}) d\mu d\gamma, \end{aligned} \tag{A.13}$$

where

$$a = Da_{em}\gamma, \quad b = \frac{Da_{em}}{k_r}(t-\gamma), \quad p = \rho k_d Da_{rm}\gamma, \quad q = Da_{rm}(t-\gamma),$$

$$b_1 = \frac{Da_{em}}{k_r}\mu, \quad r_1 = (Da_{ds}+Da_{rs})\mu, \quad q_1 = Da_{rm}(t-\gamma-\mu),$$

and

$$c_0(x,t) = \frac{x\sqrt{Pe_m}}{2\sqrt{\pi t^3}} e^{-\frac{Pe_m(x-t)^2}{4t} - (Da_{dm}+q_L)t}, \tag{A.14}$$

Inverse Laplace transform of $\bar{c}_u(s) e^{\frac{Pe_m x}{2} - x\sqrt{Pe_m}\sqrt{\frac{Pe_m}{4}+R_1(s)}}$ is now obtained by means of Eq. (A.9) and is expressed as

$$\int_0^t c_u(\gamma) f_1(x, t-\gamma) d\gamma, \tag{A.15}$$

In the similar way, we can find inverse Laplace transform of other terms present in the right hand side of the Eq. (A.1). Hence, the complete analytical solution of Eq. (A.1) can be written as:

$$\begin{aligned}
c_m(x,t) &= \int_0^t c_u(\eta) f_1(x, t-\eta) d\eta \\
&+ \int_0^{+\infty} \Big[c_{minit}(x^{'})(f_2(x-x^{'}, -1, t) - e^{Pe_m x} f_2(x+x^{'}, +1, t)) \\
&+ Da_{em} c_{sinit}(x^{'})(f_3(x-x^{'}, -1, t) - e^{Pe_m x} f_3(x+x^{'}, +1, t)) \\
&+ \rho Da_{rm} c_{sedinit}(x^{'})(f_4(x-x^{'}, -1, t) - e^{Pe_m x} f_4(x+x^{'}, +1, t)) \\
&+ \int_0^t \{ q_L c_L(x^{'}, \eta)(f_2(x-x^{'}, -1, t-\eta) - e^{Pe_m x} f_2(x+x^{'}, +1, t-\eta)) \\
&+ Da_{em} Da_{rs} \hat{c}_s(x^{'}, t)(f_3(x-x^{'}, -1, t-\eta) - e^{Pe_m x} \\
&\times f_3(x+x^{'}, +1, t-\eta)) \} d\eta \Big] dx^{'},
\end{aligned} \tag{A.16}$$

where

$$\begin{aligned}
f_2(x, si, t) &= c_1(x, si, t) e^{-(Da_{em} + \rho k_d Da_{rm})t} \\
&+ \frac{Da_{em}}{k_r} \int_0^t c_1(x, si, \gamma) e^{-a-b-p-r} \sqrt{\frac{a}{b}}\, I_1(2\sqrt{ab}) d\gamma \\
&+ Da_{rm} \int_0^t c_1(x, si, \gamma) e^{-a-p-q} \sqrt{\frac{p}{q}}\, I_1(2\sqrt{pq}) d\gamma \\
&+ \frac{Da_{em} Da_{rm}}{k_r} \int_0^t c_1(x, si, \gamma) \int_0^{t-\gamma} e^{-a-b_1-p-q_1-r_1} \sqrt{\frac{ap}{b_1 q_1}} I_1(2\sqrt{ab_1}) \\
&\times I_1(2\sqrt{pq_1}) d\mu d\gamma,
\end{aligned} \tag{A.17}$$

$$
\begin{aligned}
f_3(x,si,t) &= \int_0^t c_1(x,si,\gamma)e^{-a-b-p-r}\ I_0(2\sqrt{ab})d\gamma \\
&+ Da_{rm}\int_0^t c_1(x,si,\gamma)\int_0^{t-\gamma} e^{-a-b_1-p-q_1-r_1}\sqrt{\frac{p}{q_1}}I_0(2\sqrt{ab_1}) \\
&\times I_1(2\sqrt{pq_1})d\mu d\gamma, \qquad \text{(A.18)}
\end{aligned}
$$

I_0 is the modified Bessel function of first kind, and of order zero,

$$
\begin{aligned}
f_4(x,si,t) &= \int_0^t c_1(x,si,\gamma)e^{-a-p-q}\ I_0(2\sqrt{pq})d\gamma \\
&+ \frac{Da_{em}}{k_r}\int_0^t c_1(x,si,\gamma)\int_0^{t-\gamma} e^{-a-b_1-p-q_1-r_1}\sqrt{\frac{a}{b_1}}I_1(2\sqrt{ab_1}) \\
&\times I_0(2\sqrt{pq_1})d\mu d\gamma, \qquad \text{(A.19)}
\end{aligned}
$$

$r = (Da_{ds} + Da_{rs})(t-\gamma)$,

and

$$
c_1(x,si,t) = \frac{\sqrt{Pe_m}}{2\sqrt{\pi t}}\exp\left(-\frac{Pe_m(x+si\ t)^2}{4t} - (q_L + Da_{dm})t\right), \qquad \text{(A.20)}
$$

Eq. (A.16), which is the inverse Laplace transform of Eq. (3.20), is presented as Eq. (3.21) in the chapter 3.

Bibliography

[1] Avanzino RJ, Zellweger GW, Kennedy VC, Zand SM, Bencala KE, 1984. Results of a solute transport experiment at Uvas Creek, september 1972, California. *US Geological Survey.*

[2] Bencala KE, Walters RA, 1983. Simulation of solute transport in a mountain pool-and-riffle stream: a transient storage model. *Water Resources Research* **19**(3), 718-724.

[3] Bencala KE, 1983. Simulation of solute transport in a mountain pool-and-riffle stream with a kinetic mass-transfer model for sorption. *Water Resources Research* **19**(3), 723-738.

[4] Bencala KE, McKnight DM, Zellweger GW, 1990. Characterizetion of transport in an acidic and metal-rich moutain stream based on a lithium tracer injection and simulations of transient storage. *Water Resources Research* **26**(5), 989-1000.

[5] Broshears RE, Runkel RL, Kimball BA, Mcknight, Bencala KE, 1996. Reactive solute transport in an acidic stream: experimental pH increase and simulation of controls on pH, aluminum and iron. *Environmental Science and Technology*, **30**(10), 3016-3024.

[6] Carslaw HS, Jaeger JC, 1959. *Conduction of Heat in Solids.* Oxford University Press.

[7] Choi J, Harvey JW, Conklin MH, 2000. Characterizing multiple timescales of stream and storage zone interaction that affect solute fate and transport in streams. *Water Resources Research* **36**(6), 1511-1518.

[8] Coleman TF, Li Y, 1994. On the convergence of reflexive Newton methodes for large-scale nonlinear minimization subject to bounds. *Mathematical Programming* **2**, 189-224.

[9] Coleman TF, Li Y, 1996 . An interior trust region approach for nonlinear minimization subject to bounds. *SIAM Journal on Optimization* **6**, 418-445.

[10] Davis PM, Atkinson TC, Wigley TML, 2000. Longitudinal dispersion in natural channels: 2. The roles of shear flow dispersion and dead zones in the River Severn, UK. *Hydrology and Earth System Sciences* **4**(3), 355-371.

[11] De Smedt F, Brevis W, Debels P, 2005. Analytical solution for solute transport resulting from instantaneous injection in streams with transient storage. *Journal of Hydrology* **315**(1), 25-39.

[12] De Smedt F, 2006. Analytical solutions for transport of decaying solutes in rivers with transient storage. *Journal of Hydrology* **330**(3), 672-680.

[13] De Smedt F, 2007. Analytical solution and analysis of solute transport in rivers affected by diffusive transfer in the hyporheic zone. *Journal of Hydrology* **239**(4), 29-38.

[14] Fischer HB, List EJ, Koh RCY, Imberger J, Brooks NH, 1979. *Mixing in Inland and Coastal Waters*. Academic Press, Inc.

[15] Fernald, AG, Wigington Jr, PJ, Landers DH, 2001. Transient storage and hyporheic flow along the Willamette River, Oregon: field measurements and model estimates. *Water Resources Research* **37**(6), 1681-1694.

[16] Gooseff MN, Bencala KE, Scott DT, Runkel RL, McKnight DM, 2005. Sensitivity analysis of conservative and reactive stream transient storage models applied to field data from multiple-reach experiments. *Advance in Water Resources* **28**(6), 479-492.

[17] Hart DR, 1995. Parameter estimation and stochastic interpretation of the transient storage model for solute transport in streams. *Water Resources Research* **31**, 323-328.

[18] Harvey JW, Wagner BJ, Bencala KE, 1996. Evaluating the reliability of the stream traces approach to characterize stream subsurface water exchange. *Water Resources Research* **32**(8), 2441-2451.

[19] Hays JR, Krenkel PA, Schnelle KB, 1966. Mass transport mechanisms in open-channel flow. Sanitary and Water Resources Engineering **Technical Report** No. **8**, Vanderbilt University, Nashville, Tennessee.

[20] Holley ER, Jirka G, 1986. Mixing in rivers. US Army Engineer Waterways Experiment Station, **Technical reports**, Vicksburg, Miss.

[21] Jackman AP, Walters RA, Kennedy VC, 1984. Transport and concentration controls for chloride, strontium, potassium and lead in Uvas Creek, a small cobble-bed stream in Santa Clara Country, California, USA: 2. Mathematical modeling. *Journal of Hydrology* **75**, 111-141.

[22] Jonsson K, 2003. Effect of hyporheic exchange on conservative and reactive solute transport in streams. **Ph.D. Thesis** Acta Universitatics Upsaliensis Uppsala.

[23] Jonsson K, Johansson H, Wörman A, 2003. Hyporheic exchange of reactive and conservative solutes in streamstracer methodology and model interpretation. *Journal of Hydrology* **278**, 153-171.

[24] Keefe, SH, Barber BL, Runkel RL, Ryan JN, McKnight D M, Wass RD, 2004. Conservative and reactive solute transport in constructed wetlands. *Water Resources Research* **40**(6), 1-12.

[25] Kimball BA, Bencala KE, McKnight, 1988. Research on metals in acid mine drainage in the Leadville, Colorado, area, USGS Toxic Substances Hydrology Program, Proceedings, Phoenix, AZ, September 26-30. *US Geological Survey.*

[26] Maloszewski P, Zuber A, 1990. Mathematical modeling of tracer Behavior in short-term experiments in fissured rocks. *Water Resources Research* **26**(7), 1517-1528.

[27] Prudnikov AP, Bryckhkov Yu A, Marichev AY, 1992. *Integral and Series: Inverse Laplace Transform.* vol **5**, CRC Press LLC.

[28] Rowiński PM, Dysarz T, Napiórkowski JJ, 2004. Estimation of longitudinal dispersion and storage zone parameters. *River Flow*, Greco, Carravetta Della Morte, 1201-1210.

[29] Runkel RL, Chapra SC, 1993. An efficient numerical solution of the transient storage equations for solute transport in small streams. *Water Resources Research* **29**(1), 211-215.

[30] Runkel RL, Chapra SC, 1994. Reply. *Water Resources Research* **30**(10), 2863-2865.

[31] Runkel RL, 1998. One-dimensional transport with inflow and storage (OTIS): a solute transport model of streams and rivers. U.S. Geological Survey Water-Resources **Investigation Report** 98-4018.

[32] Rutherford JC, 1994. *River mixing.* John Wiley and Sons.

[33] Schmid BH, 1997. Analytical solution of the transient storage equations accounting for solute decay. *Proc. 27th Congress of the Int. Assoc. for Hydraulic Research, Water Resources Engineering Division* August 10-15, San Francisco, CA, USA, ASCE **B**, 15-20.

[34] Schmid BH, 2003. Temporal moments routing in streams and rivers with transient storage. *Advances in Water Resources* **26**, 1021-1027.

[35] Scott DL, Gooseff MN, Bencala KE, Runkel RL, 2003. Automated calibration of a stream solute transport model: implications for interpretation of biogeochemical parameters. *Journal of North American Benthological Society* **22**(4), 492-510.

[36] Sneddon IN, 1972. *The Use of Integral Transforms*. Tata McGraw- Hill Publ. Co. Ltd., New Delhi.

[37] Stream Solute Workshop, 1990. Concepts and Methods for Assessing Solute Dynamics in Stream Ecosystems. *Journal of North American Benthological Society* **9**(2), 95-119.

[38] Thackston EL, Schnelle KB, 1970. Predicting effects of dead zones on stream mixing. *Proc. ASCE, Journal of Sanitary Engineering Division* **96**(2), 319-331.

[39] Wagner BJ, Harvey JW, 1997. Experimental design for estimating parameters of rate-limited mass transfer: analysis of stream tracer studies. *Water Resources Research* **33**(7), 1731-1741.

[40] Wörman A, 1998. Analytical solution and timescale for transport of reacting solutes in rivers and streams. *Water Resources Research* **34**(10), 2703-2716.

[41] Wörman A, Forsman J, Johansson H, 1998. Modeling retention of sorbing solutes in streams based on tracer experiment using 51 Cr. *Journal of Environmental Engineering* **124**(2), 122-130.

[42] Wörman A, 2000. Comparison of models for transient storage of solute in small streams. *Water Resources Research* **36**(2), 455-468.

[43] Yan Ge, Boufadel MC, 2006. Solute transport in multiple-reach experiments: Evaluation of parameters and reliability of prediction. *Journal of Hydrology* **323**(1), 106-119.

List of papers published/communicated from the thesis

1. Kumar A, Dalal DC, 2008. Analytical solution for continuous injection of solute in rivers with diffusive transfer in the hyporheic zone. *Proc.* 11^{th} *International Conference on Wetland Systems for Water Pollution Control*, November 1-7, Ujjain, Indore, India, IWA **II**, 862-867.

2. Kumar A, Dalal DC, 2008. Anaytical solution for instantaneous injection of conservative solutes in rivers with hyporheic zone. *Proc.* II^{nd} *World Aqua Congress*, November 26-28, New Delhi, India, 533-539.

3. Kumar A, Dalal DC. Analysis of solute transport in rivers with transient storage and lateral inflow: An analytical study (*Under Revision in Acta Geophysica*).

4. Kumar A, Dalal DC. Analytical solution and analysis for solute transport in streams with diffusive transfer in the hyporheic zone (*Communicated to Journal*).